IFAC

INTERNATIONAL FEDERATION OF AUTOMATIC CONTROL

WARSZAWA 1969

Power Systems

Heat Exchangers

Fourth Congress of the International Federation of Automatic Control
Warszawa 16–21 June 1969

TECHNICAL SESSION

47

Organized by
Naczelna Organizacja Techniczna w Polsce

INTERNATIONAL FEDERATION OF AUTOMATIC CONTROL

Power Systems

Heat Exchangers

TECHNICAL SESSION No 47

FOURTH CONGRESS OF THE INTERNATIONAL FEDERATION OF AUTOMATIC CONTROL
WARSZAWA 16 – 21 JUNE 1969

Organized by
Naczelna Organizacja Techniczna w Polsce

Contents

Wydawnictwa Czasopism Technicznych NOT - Polska

Zakład Poligraficzny WCT NOT. Zam. 103/69.

DETERMINATION OF THE SPATIAL STABILITY OF THE AXIAL FLUX SHAPE OF RE-ENTRANT FLOW GAS-COOLED POWER REACTORS WITH AUTOMATIC POWER CONTROL

By: R.L. Carstairs
B.H. Bickers
Atomic Power Constructions Limited,
Sutton,
England.

INTRODUCTION

Conventional automatic control of steady-state power level in gas-cooled power reactors operates to maintain constant outlet gas temperature. The axial neutron flux shape is not controlled, and its spatial stability depends on the balance between neutron leakage and destabilising factors such as positive reactivity-temperature coefficients and xenon 135 burn-out. The spatial stability also depends on the control arrangements, and is affected both by the amount of automatic control rod group penetration and by the amount of penetration of coarse control rod groups. The axial spatial stability problem is an example of a type of auxiliary control problem which can put constraints such as limited rod movement, for example, on what is otherwise a straightforward reactor power control loop problem.

For cores having a single coolant flow direction the effects on axial stability of neutron flux shape and automatic or coarse control rod group penetration are well understood[1]. For re-entrant flow systems with coolant flow in both directions the interactions between parameters are more complicated, and the spatial stability margin depends in addition to the features already mentioned on the re-entrant to forward flow ratio and the heat transfer between the flow paths.

This paper describes an approximate method for the determination of axial flux shape stability margins in conventionally controlled re-entrant flow advanced gas-cooled nuclear reactors. Simplified equations are developed and various methods of solution suggested based on a trajectory method which is suitable for both analogue and digital computation. Results for a typical advanced gas-cooled reactor are presented and discussed, and compared with more detailed transient solutions.

DESCRIPTION OF REACTOR

Fig. 1 shows a schematic section of a single fuel channel, showing the re-entrant cooling flow arrangement. Part of the coolant flow carries heat from the moderator and mixes with the by-pass flow at the bottom of the core. The total flow then passes upward through the main coolant channel, taking heat from the inner sleeve and fuel.

Fig. 2 shows typical neutron flux distributions. The spatial distribution of the flux depends on the local neutron leakage and multiplication effects. Any local flux disturbance is naturally stable due to the resultant change in local neutron leakage, but if the disturbance gives rise to an increase in local multiplication sufficient to offset the extra leakage, then instability could result.

Changes in local multiplication or reactivity are due to temperature effects of fuel and moderator, changes in the concentration of xenon 135 nuclei, and local effects due to control rod movement. The temperature coefficient of the fuel is usually negative and therefore stabilising, but that of the moderator is often positive and destabilising. The xenon reactivity coefficient is always negative, but the time constants of the various processes involved in the production, burn-out, and decay of xenon may result in a divergent long-period oscillation when combined with the temperature effects. The overall effect of xenon is destabilising.

In considering flux shape instability, it is useful to consider the flux distribution as an expansion in harmonics. The fundamental mode is controlled by the total power control operating on outlet gas temperature, and flux shape instability can only arise if one or more harmonics are present and are unstable. Since the first harmonic is the least stable, the condition for flux shape stability is that a first harmonic perturbation should be stable, both intrinsically and in the presence of fundamental mode control response.

A physical explanation of the occurence of first harmonic instability is given in Fig. 3. Assume that a reactivity increment near the top of the core causes a first harmonic flux disturbance as shown. The diagrams below show the resulting moderator and coolant temperature perturbations and the corresponding reactivity increments due to a positive moderator coefficient. The first harmonic component from both sleeve and moderator in destabilising, but the fundamental components result in control rod movement which could either suppress or aggravate the initial disturbance depending on the rod position and the relative magnitudes of moderator and sleeve components.

It should be noted that the effect of the moderator temperature changes on the coolant are considerably diluted by the by-pass flow, and thus the sleeve effects dominate with the result that the tendency to instability is greatest with the rods at the top of the core.

The steady-state flux shape, re-entrant flow fraction, amount of intersleeve heat transfer and the proportion of the moderator coefficient due to the sleeve have been found to affect very strongly the balance of the various effects, and hence the stability. Some typical results are discussed later in this paper.

EQUATION DEVELOPMENT

It is first assumed that reactor spatial behaviour in the axial and radial-azumithal directions can be considered separately, and that the axial behaviour can be described by considering conditions in a single representative fuel channel. A multivariable transient distributed parameter representation[2] of considerable complexity still remains, however, and considerable simplification is required if parameter survey work is to be carried out with convenience and reasonable economy.

Suitable simplified equations describing the system are developed in the Appendix. It is assumed that small disturbances are being studied, so that a linear perturbation representation can be used, and that the heat production in the fuel and moderator is proportional to the neutron flux.

It is further assumed that the time behaviour of disturbances in practice is dominated by the xenon and iodine equation time constants which are measurable in hours. The remaining time constants are therefore neglected in comparison.

Equations (1) to (11) now form a set of 9 algebraic and 2 first-order differential equations which may be solved for a series of axial points with the spatial differentials expressed as finite differences. The quantities expressed are in general axially variant.

This solution of the equations may be obtained by analogue or digital computation[2], but is expensive and time consuming for initial studies or parameter survey work.

The approach described in this paper overcomes these disadvantages. It is assumed that all variables have an exponential time behaviour, $e^{\omega t}$, ω being in general complex. The iodine and xenon equations are then combined to give the xenon parameter Q and the resulting equation used as a characteristic equation in ω to give the value Q_o of Q for which the real part of ω is zero. Q_o is the maximum value of Q for which the system will be stable.

The problem is now reduced to finding a value of some adjustable parameter such as the moderator coefficient a_g for which a first harmonic disturbance can exist. This value, usually expressed as a margin a_g' above the expected reactor equilibrium value, can be regarded as a stability margin.

It is shown in the Appendix that the heat transfer equations can be combined to express all the variables in terms of a mixed coolant temperature, the normalized power, and the intersleeve heat transfer variable A. This arrangement obviates the necessity for integrating against a coolant flow, which can cause numerical instability in the solution.

The resulting equations (14), (19), (20), (21) can be solved to find the value of a_g as an eigenvalue for which the boundary conditions are satisfied. Conditions (22), (23), (26) are apparent from Fig. 2, and (24), (25) follow from the assumption that the control system is perfect and acts to keep the outlet gas temperature constant. The coolant inlet temperature is also assumed constant.

The control reactivity δ is assumed to be represented by a step function over a narrow bandwidth 2θ. The bandwidth value is not sensitive, and the amplitude of δ is unimportant, because δ is the only isolated term in the equations, and so acts only as a scaling factor on the solution amplitude, without affecting the eigenvalue.

METHOD OF SOLUTION

Various approximate methods[2] have been attempted for the solution of the equations but these do not take into account generalized variations in initial flux shape, or allow for intersleeve heat transfer or axial parameter variation.

A trajectory method has been found most satisfactory for the solution of the equations, and may be used equally well on analogue or digital computers.

Both methods employ integration from the bottom of the active core with iterative methods to determine both the starting values of the variables, and an eigenvalue which will enable the three boundary conditions at the top of the core to be satisfied.

The analogue trajectory technique has been used for representations without intersleeve heat transfer, using an X-Y plotter. The calculation is terminated after a fixed time (equivalent to the time taken to integrate along the active core length), the final values of the variables noted, and the process repeated with new initial values until convergence to the boundary conditions is obtained. The iterations can be performed simply, guided by parameter-error plots, or may be done automatically by means of a variable gain control which sets new initial conditions based on the preceding final conditions.

The latest digital computer program uses a 4th-order Runge-Kutta integration procedure, and for a given eigenvalue estimate performs four integrations with two values each of A_o and v_o. The values of these quantities to satisfy (24) and (25) may now be readily found as the values of t_c and A at the top of the core are linearly dependent on the starting values of A and v. The process is repeated for each eigenvalue estimate.

The problem is now to find an eigenvalue (which may be either Q or a_g and which may have more than one value), to satisfy (26). A typical plot of the convergence parameter $-(\frac{p}{\lambda e} + v)$ vs a_g' is shown in Fig. 6., and the points at which this crosses the axis are the eigenvalues required for the solution of the equations. In practice the lowest value is usually of greatest interest but in some cases this could be associated with a higher harmonic than the first.

The procedure for finding the zeros of (26) is to carry out a search, increasing a_g' until three points are found which indicate that the condition is satisfied in their vicinity. The next value of a_g' to be attempted then depends on the pattern of the convergence parameter shown by the preceding values. If the patterns suggests convergence, then a zero is indicated in the immediate vicinity, and an iterative sequence based on quadratic fitting is employed to find the exact value of a_g' to satisfy (26).

Thus the margin in [illegible]derator coefficient for first harmonic instability to be possible is known, and the axial shapes associated with the harmonic of any of the variables may be plotted.

DISCUSSION

Figs. 4, 7 & 8 show the results of a parameter survey for a typical re-entrant AGR. Fig. 4 shows that in general flux distortion away from the control rod position is de-stabilising. The rods are working in a position of low flux and therefore have reduced effect, while the reactivity changes in the flux peak region are accentuated. Thus the reactivity distribution due to the moderator becomes nearer to a first harmonic shape with a corresponding reduction in the stabilising fundamental.

Increased inner sleeve reactivity-temperature coefficient and the inclusion of intersleeve heat transfer representation have been shown to affect the harmonic very similarly to flux distortion, reducing the stability with control at the top of the core and increasing it with control at the bottom.

Fig. 5 shows the results of a check with an analogue transient solution[2]. Intersleeve heat transfer was not included in the transient solutions, and a comparable representation was used for the trajectory solution. Good agreement was obtained.

The double roots occurring in Fig. 4, and marked A & B in the typical case shown in Fig. 7 may be explained by a consideration of the corresponding flux shapes, also shown in Fig. 7. Case B has been analyzed and found to have a negative fundamental component (a positive second sine mode component ensures no resultant power change) which gives a destabilising influence from the sleeve. Increasing a'_g further from the threshold value of 68 mN/°C tends to change the balance between control and temperature reactivity effects. The shape of the first harmonic shape changes such that for Case A, also analyzed, a positive fundamental component appears and the stabilising effect of the moderator becomes dominant. Further increases of a'_g then result in increasing stability.

The effect of varying the re-entrant flow with the control rods at the top of the core is shown in Fig. 8. It may be seen that with low flux distortion the increased moderator temperature is stabilising at low re-entrant flows, but with high distortion the moderator reactivity is predominantly first harmonic and becomes destabilising.

CONCLUSIONS

First harmonic flux instability in a nuclear reactor may be initiated by control movements under certain circumstances. For a re-entrant flow reactor the conditions under which this can occur are seen to depend on a fine balance between the opposing effects of different moderating components. This leads to unexpected results, such as an increase of stability with moderator reactivity-temperature coefficient, and the rapid changes of margin with flux shape change, which occur in some conditions.

Effective automatic control using rods with tips very near the top of the core is very unlikely in practice, and current designs of advanced gas-cooled reactors have a large margin of axial stability in all practical conditions.

It is however important in design work to be able to determine conveniently the axial stability for a wide range of parameters, and the method discussed in this paper has been found useful for this purpose.

ACKNOWLEDGEMENTS

Axial stability calculations for once-through reactor cores using trajectory methods were first carried out by B.E. Roberts, J.B. Pollard, and R.I. Vaughan, then at the UKAEA. The re-entrant core combined coolant temperature form was suggested by Mr. W.M. MacInnes, whilst at APC.

REFERENCES

1. A.J. Hitchcock, Nuclear Reactor Stability, Nuclear Engineering Monographs, Temple Press, 1960.

2. B. Wilson, J.R. Enselmoz, A.J. Hartley. Axial Stability Calculations for AGR Systems. UKAEA TRG Report 1138(R), December 1965.

NOMENCLATURE

a_g	moderator temperature-reactivity coefficient
a_u	fuel temperature-reactivity coefficient
a_x	xenon reactivity coefficient
A	intersleeve heat transfer term
C	coolant specific heat
E	heat production term
f	re-entrant flow fraction
h	convective heat transfer coefficient
i	iodine concentration
k	effective total conductance term
k_∞	neutron multiplication factor
L_e	extrapolated core height
p	normalised power term
Q	xenon parameter
r	radiative heat transfer coefficient
t	temperature
v	axial power gradient
W	coolant mass flow
x	xenon concentration
z	axial co-ordinate
z_r	automatic control rod tip position
δ	control reactivity term
λ	fraction of a_g attributable to component
λ_i	iodine decay constant
λ_x	xenon decay constant
λ_e	extrapolation distance
σ_x	xenon absorption cross-section
2θ	control term bandwidth
Φ	neutron flux
ω	time constant

SUBSCRIPTS

c1	main coolant
c2	re-entrant coolant
g1	inner sleeve
g2	outer sleeve
m	main moderator
r	automatic control rod tip position
s	can
u	fuel
o	steady state, or value at bottom of core

APPENDIX

EQUATION DEVELOPMENT

The one-energy-group neutron diffusion equation is used to describe the distribution in space and time of neutron flux in the reactor. In its axial perturbation form it may be approximated for slowly varying conditions as

$$M_z^2 \frac{\partial^2 p}{\partial z^2} + (k_{\infty o}-1)p + \Delta k_{\infty} p_o = 0 \qquad (1)$$

The perturbation in neutron multiplication is a summation of various effects as follows,

$$\Delta k_{\infty} = a_u t_u + a_g(\lambda_1 t_{g1} + \lambda_2 t_{g2} + \lambda_m t_m) + a_x x + \delta \qquad (2)$$

The perturbation form of the heat transfer equations (see Fig.2) may be approximated for slowly varying conditions as

$$0 = E_u p - k_{us}(t_u - t_s) \qquad (3)$$

$$0 = k_{us}(t_u - t_s) - h_{sc1}(t_s - t_{c1}) + r_{g1}t_{g1} - r_s t_s \qquad (4)$$

$$(WC)_1 \frac{\partial t_{c1}}{\partial z} = h_{sc1}(t_s - t_{c1}) + h_{g1c1}(t_{g1} - t_{c1}) \qquad (5)$$

$$0 = E_{g1}p - h_{g1c1}(t_{g1} - t_{c1}) - k_1 t_{g1} + k_2 t_{g2} + r_s t_s - r_{g1}t_{g1} \qquad (6)$$

$$0 = E_{g2}p - h_{g2c2}(t_{g2} - t_{c2}) + k_1 t_{g1} - k_2 t_{g2} + r_m t_m - r_{g2}t_{g2} \qquad (7)$$

$$-f(WC)_1 \frac{\partial t_{c2}}{\partial z} = h_{g2c2}(t_{g2} - t_{c2}) + h_{mc2}(t_m - t_{c2}) \qquad (8)$$

$$0 = E_m p - h_{mc2}(t_m - t_{c2}) - r_m t_m + r_{g2}t_{g2} \qquad (9)$$

The xenon and iodine equations are as follows,

$$\frac{\partial i}{\partial t} = \sigma_x p \Phi_o - \lambda_i i \qquad (10)$$

$$\frac{\partial x}{\partial t} = \lambda_i i - \sigma_x p_o \Phi_o x - \sigma_x p \Phi_o x_o - \lambda_x x \qquad (11)$$

A modal time behaviour of the form $x = x'e^{\omega t}$ is assumed and (10) and (11) combined to give

$$Q = \frac{a_x x'}{p'} = a_x \frac{\left(\frac{\lambda_i \sigma_x \Phi_o}{\lambda_i + \omega} - \sigma_x \Phi_o x_o \right)}{(\omega + \sigma_x p_o \Phi_o + \lambda_x)} \qquad (12)$$

Equation (12) is treated as a characteristic equation for ω, and solved to give a threshold value Q_o for Q below which the real part of ω is less than zero[1], thus indicating stability. Then

$$Q_o = \frac{-a_x \sigma_x \Phi_o p_o x_o}{\sigma_x \Phi_o p_o + \lambda_i + \lambda_x} \qquad (13)$$

Adding equations (3) - (9) and introducing a combined coolant temperature $t_c = t_{c1} - f\, t_{c2}$,

$$(WC)_1 \frac{\partial t_c}{\partial z} = \Sigma E_p \qquad (14)$$

A further variable A is introduced to describe the heat transfer between the sleeves, and is conveniently expressed as

$$A = \frac{1}{(WC)_1} \left[\int_o^z h_{12} dz - \int_o^{L_e} h_{12} dz \right] \qquad (15)$$

where $h_{12} = k_{g1} t_{g1} - k_{g2} t_{g2}$ (16)

All component temperatures may now be expressed in terms of p, t_c and A by algebraic manipulations of the equations. The separate coolant temperatures are related to the combined coolant temperature as follows,

$$t_{c1} = \frac{E_u + E_{g1}}{\Sigma E} t_c - A \qquad (17)$$

$$t_{c2} = \left(\frac{E_{g2} + E_m}{f \Sigma E} \right) t_c - \frac{A}{f} \qquad (18)$$

Equations (1) and (2) may then be written as

$$\frac{\partial v}{\partial z} = \left[- \frac{(k_{\infty o} - 1)}{M_z^2} - \frac{p_o}{M_z^2} \left\{ a_u A_1 + a_g H + Q_o \right\} \right] p - \frac{p_o}{M_z^2} \left\{ a_u + a_g G_1 \right\}$$

$$\left\{ e_1 t_c - A \right\} + \frac{p_o}{M_z^2} \left[a_g G_2 \right] \left\{ e_2 t_c + \frac{A}{f} \right\} - \frac{p_o}{M_z^2} \delta \qquad (19)$$

$$\frac{\partial p}{\partial z} = v \qquad (20)$$

A, G, H, e's are constants comprising heat transfer coefficients, heat production terms etc.

Equation (15) may be expressed as a first order differential equation as follows,

$$\frac{\partial A}{\partial z} = \frac{1}{(WC)_1} h_{12} \qquad (21)$$

Equations (14), (19), (20), (21) form a set of non-linear first order differential équations. All the quantities can be z-variant. The boundary conditions as described in the text may be summarised as follows,

$z = \lambda_{e1}$, $t_c = 0$ (22) $\qquad z = L_e - \lambda_{e2}$, $t_c = 0$ (24)

$p = \lambda_e v$ (23) $\qquad A = 0$ (25)

$p = -\lambda_e v$ (26)

The control term takes the value δ for $(z_r - \theta) < z < (z_r + \theta)$, and is zero elsewhere.

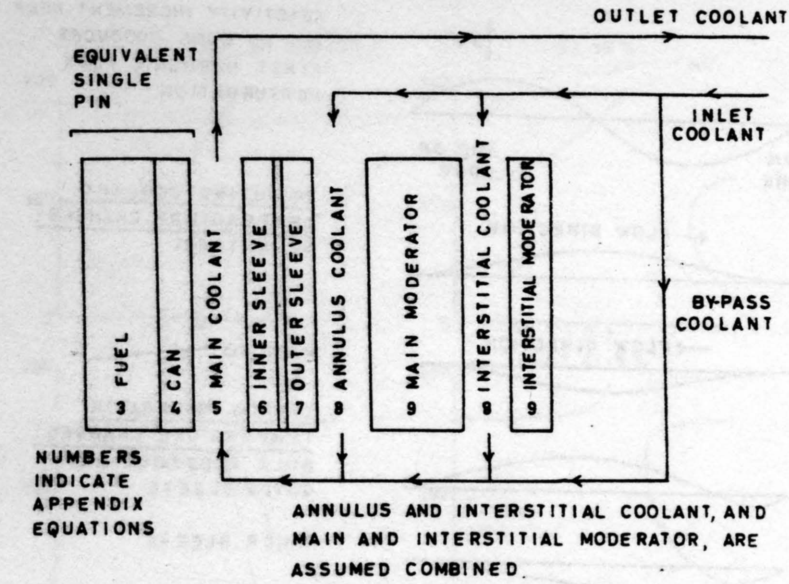

FIG.1 SCHEMATIC FUEL CHANNEL SECTION.

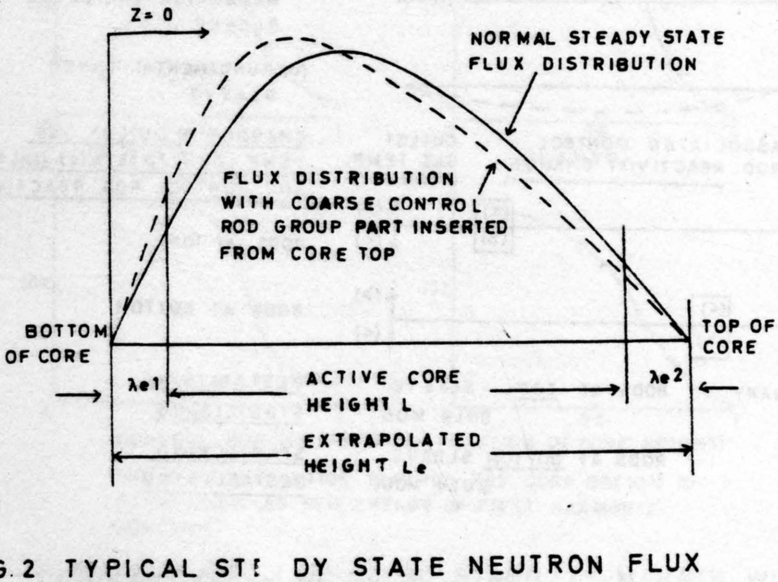

FIG.2 TYPICAL ST! DY STATE NEUTRON FLUX DISTRIBUTIONS.

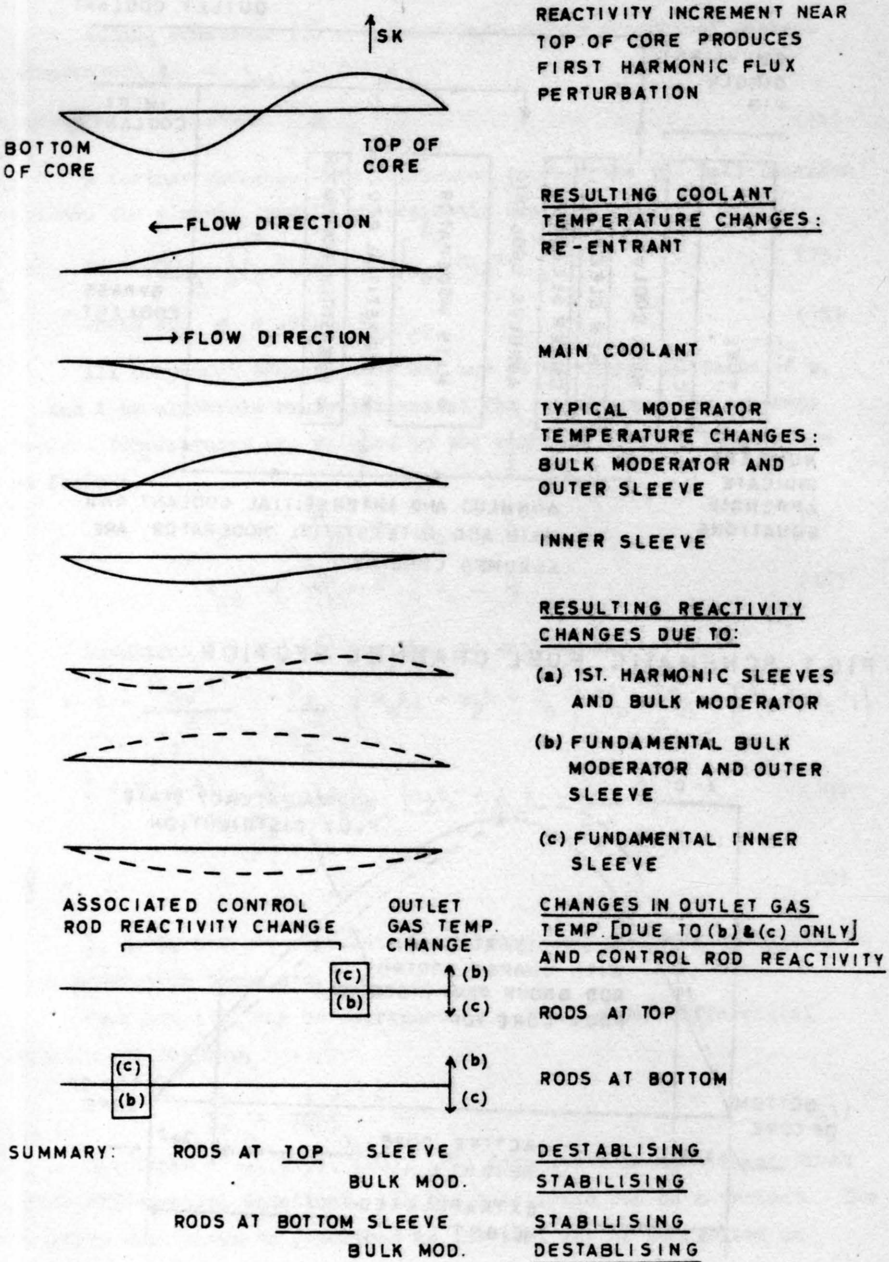

FIG. 3 PHYSICAL EXPLANATION OF FIRST HARMONIC AXIAL INSTABILITY FOR RE-ENTRANT FLOW SYSTEMS.

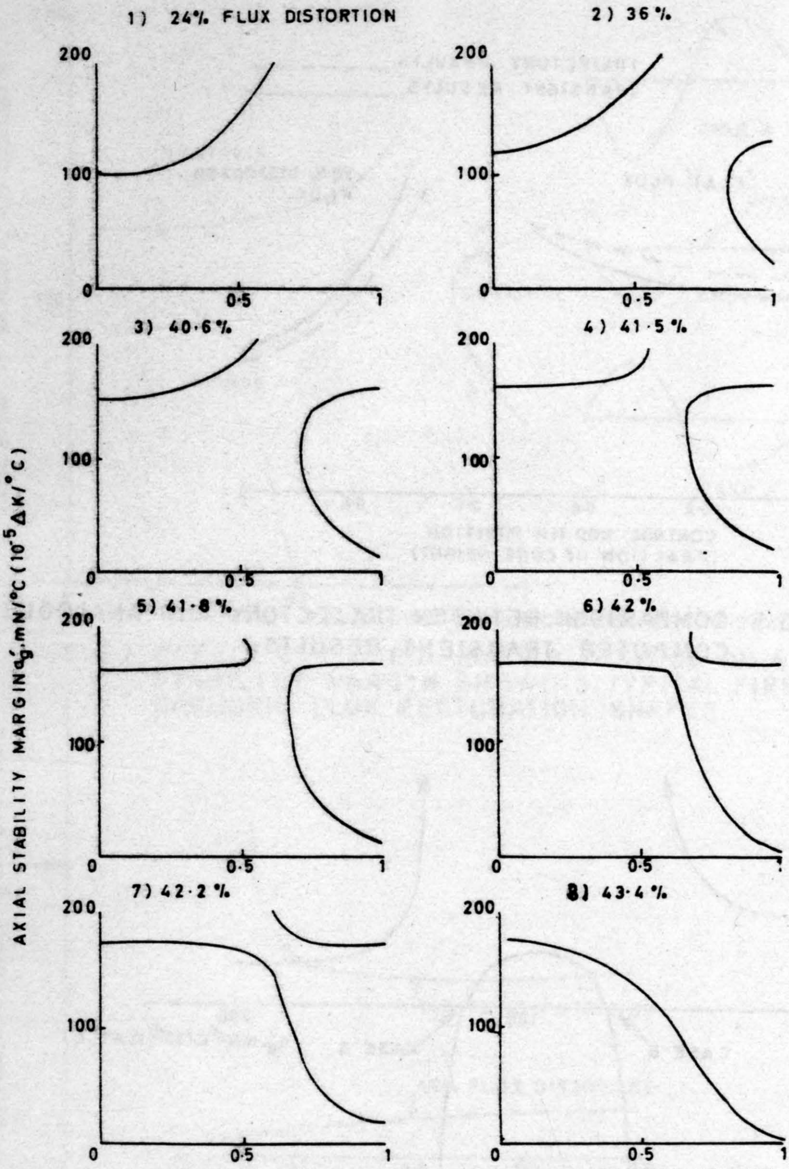

THE FLUX DISTORTION TOWARDS THE CORE BOTTOM IS EXPRESSED AS PERCENTAGE OF FIRST HARMONIC CONTENT.

FIG.4 VARIATI N OF AXIAL STABILITY MARGIN WITH AUTOMA IC CONTROL ROD TIP POSITION FOR VARIOUS FLUX DISTORTIONS

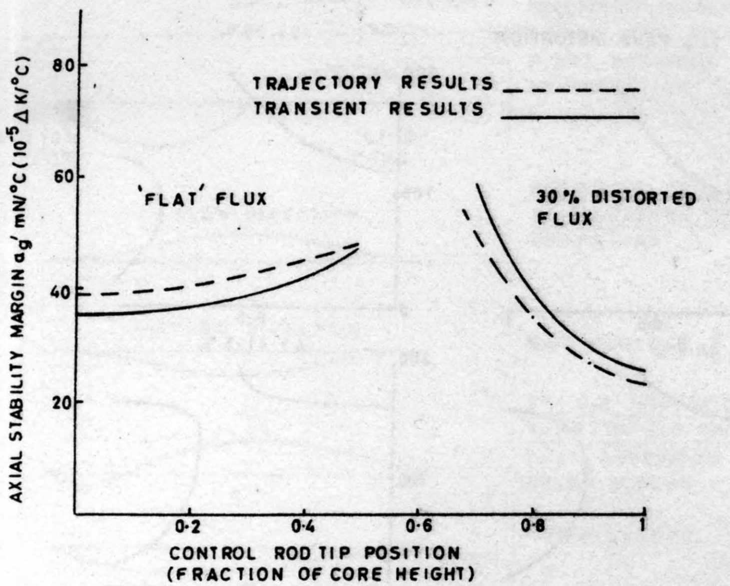

FIG. 5 COMPARISON BETWEEN TRAJECTORY AND ANALOGUE COMPUTER TRANSIENT RESULTS.

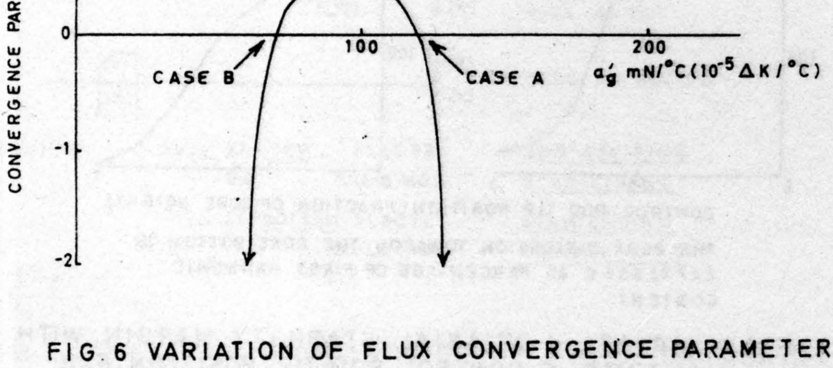

FIG. 6 VARIATION OF FLUX CONVERGENCE PARAMETER WITH MODERATOR COEFFICIENT MARGIN a_g'

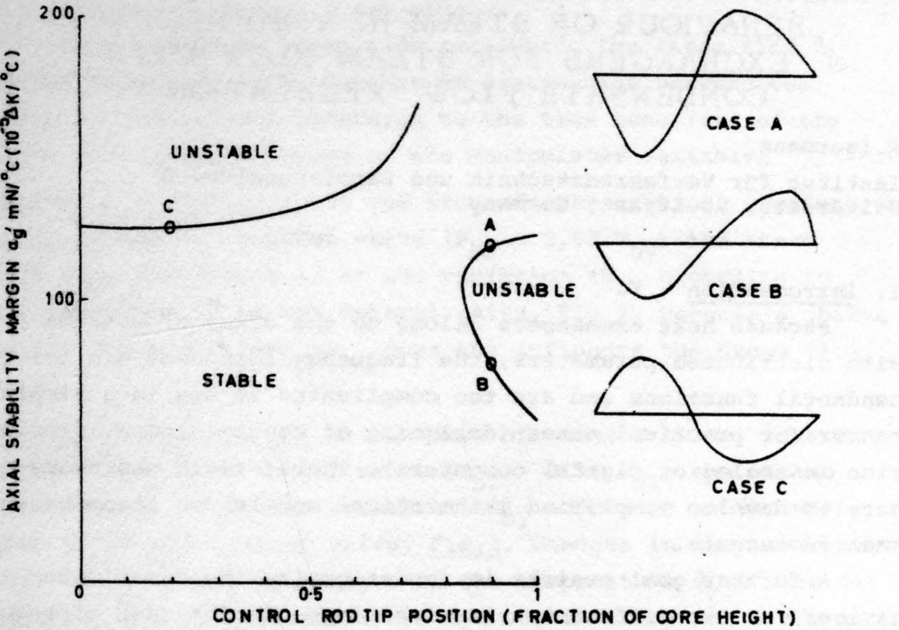

FIG. 7 EFFECT OF CONTROL ROD TIP POSITION ON AXIAL STABILITY MARGIN SHOWING TYPICAL FIRST HARMONIC FLUX PERTUBATION SHAPES

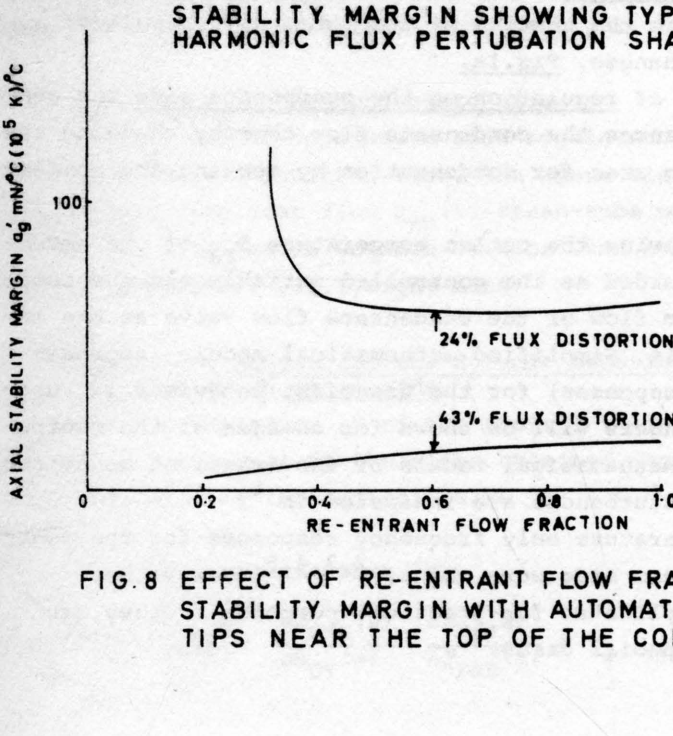

FIG. 8 EFFECT OF RE-ENTRANT FLOW FRACTION ON AXIAL STABILITY MARGIN WITH AUTOMATIC CONTROL ROD TIPS NEAR THE TOP OF THE CORE.

MATHEMATICAL MODELS FOR THE DYNAMIC BEHAVIOUR OF STEAM HEATED HEAT EXCHANGERS FOR STEAM FLOW OR CONDENSATE FLOW REGULATION

R.Isermann

Institut für Verfahrenstechnik und Dampfkesselwesen
Universität Stuttgart, Germany

1. Introduction

Because heat exchangers belong to the class of systems with distributed parameters, the frequency responses are transcendental functions and are too complicated to use in a simple manner for practical cases (designing of control loops, simulation on analog or digital computers). Therefore it was necessary to develop simplified mathematical models for steam heated heat exchangers.

A further goal exsists in investigating the dynamic behaviour for two different valve locations. In the case of regulation on the steam side the control valve influences the steam flow and therefore the heating of the tubes as a result of steam pressure changes, Fig.1a.

In the case of regulation on the condensate side the control valve influences the condensate flow thereby changing the effective heating area for condensation by storing the condensate, Fig.1b.

In the following the outlet temperature ϑ_{Fa} of the secondary flow is regarded as the controlled variable and the position of the steam flow or the condensate flow valve as the manipulated variable. Simplified mathematical models (approximate frequency responses) for the transient behaviour in tube-shell heat exchangers will be shown for changes of the manipulated variable. Mathematical models of the transient behaviour for different disturbances are indicated in [1].

In past literature only frequency responses for the regulation on the steam side were shown, [2,3,4,5], but either they are too complicated for practical purposes or they are only valid for special cases.

1.1. Regulation on the steam side

In the case of steam side regulation the steam flow $\dot{M}_D$ is the regulated flow. One has to distinguish between two operating conditions according to the time behaviour of the steam flow after a change of the manipulated variable:

Operating condition 1: In the case of over critical pressure ratio across the control valve ($P_{Di} < 0,58\ P_{DV}$) the steam flow does not change after the variation $\Delta\dot{M}_{DY}$ according to the variation ΔY of the control valve, Fig.2, because a change in the steam pressure ΔP_{Di} does not influence the steam flow rate.

Operating condition 2: In the case of under critical pressure ratio across the control valve ($P_{Di} > 0,58\ P_{DV}$) the steam flow changes after the variation $\Delta\dot{M}_{DY}$ according to the variation ΔY of the control valve, Fig.3. Changes in the steam pressure ΔP_{Di}, caused by changes of the temperature ϑ_F of the secondary flow $\dot{M}_F$ then influence the steam flow and therefore the heating of the tubes.

Thus the left hand classification, Fig.4, is obtained.

1.2. Regulation on the condensate side

In the case of condensate side regulation the condensate flow $\dot{M}_K$ is the manipulated flow. The steam flow $\dot{M}_D$ changes according to the heat flow $\dot{q}_{WD}(t)$ steam-tube wall.

One has to distinguish between vertical and horizontal position of the tubes, Fig.4, right hand.

2. Mathematical models for the dynamic behaviour in the case of regulation on steam side

After a variation ΔY of the control valve the steam flow changes proportional to the slope obtained from the operating characteristic of the control valve

$$\Delta\dot{M}_{DY} = c_v \cdot \Delta Y, \tag{1}$$

The frequency response then is

$$F_Y(s) = \frac{\Delta\dot{M}_{DY}(s)}{\Delta Y(s)} \cdot \frac{\Delta\vartheta_{FaR}(s)}{\Delta\dot{M}_{DY}(s)} \cdot \frac{\Delta\vartheta_{Fa}(s)}{\Delta\vartheta_{FaR}(s)} = c_v . F_{MD}(s) . F_{AK}(s). \tag{2}$$

In the following first the frequency response of the tubes

$$F_{MD}(s) = \Delta\vartheta_{FaR}(s) \big/ \Delta\dot{M}_{DY}(s) \qquad (3)$$

will be described and then the frequency response $F_{AK}(s)$ of the outlet header.

The influence of the heat storage in the shell on the dynamic behaviour of the outlet temperature ϑ_{FaR} of the secondary flow is negligible[1], if

$$\frac{b_a}{b_i} = \frac{\alpha_{WDa} D_3}{\alpha_{WDi} d_2 n} \leqq 0,25. \qquad (4)$$

That is applicable for heat exchangers with shell diameters $D_3 \geqq 0,2$ m.

The dynamic behaviour of the tube part of the heat exchanger can be described by the dynamic behaviour of one single tube of the length ℓ.

The parameters for the dynamic behaviour of a heated tube are [1]:

$\varkappa_F = \dfrac{4\alpha_{WF}\ell}{d_1 \rho_F c_F w_F}$	(fluid parameter)	(5)
$T_{WF} = \dfrac{(d_2^2-d_1^2)\ \rho_W c_W}{4\alpha_{WF} d_1}$	(time constant of the wall inner side)	(6)
$T_t = \dfrac{\ell}{w_F}$	(dead time constant)	(7)
$z = \dfrac{\alpha_{WD} d_2}{\alpha_{WF} d_1}$	(heating factor)	(8)
$T_F = \dfrac{T_t}{\varkappa_F} = \dfrac{d_1 \rho_F c_F}{4\alpha_{WF}}$	(fluid time constant)	(9)
$T_{WD} = \dfrac{T_{WF}}{z} = \dfrac{(d_2^2-d_1^2)\ \rho_W c_W}{4\alpha_{WD} d_2}$	(time constant of the wall outer side)	(10)

2.1. Operating condition 1: constant steam flow

In the case of over critical pressure ratio across the control valve the magnitude of the steam flow rate and therefore the heating of the tubes is independent of the inside pressure P_{Di} respectively of the tube wall temperature θ_W ($z = 0$).

For a tube the exact frequency response is [6]

$$F_{MDS}(s) = \frac{\Delta \vartheta_{FaR}(s)}{\Delta \dot{M}'_{DY}(s)} = F_{MDS}(0)\ \frac{1}{T_1 s}\ \frac{1}{(1+T_2 s)} \underbrace{\left[1-e^{-\varkappa_F \frac{T_{WF}s}{T_{WF}s+1}} . e^{-T_t s} \right]}_{F'_3(s)} \qquad (11)$$

with

$$F_{MDS}(0) = \frac{i_{De}-i'}{\dot{M}'_F c_F} \qquad (12)$$

$$\left.\begin{aligned} T_1 &= \left(1 + \frac{T_{WF}}{T_F}\right) T_t \\ T_2 &= \frac{T_{WF}}{(1+\frac{T_{WF}}{T_F})} \end{aligned}\right\} \qquad (13)$$

Approximate frequency responses of the tube part: (compare Fig. 5)

a) For the transcendental part of the frequency response the approximation [8]

$$e^{-\varkappa_F \frac{T_{WF}s}{T_{WF}s+1}} \approx a + \frac{b_S}{1+T_{bS} \cdot s} \qquad (0 \leqq \varkappa_F \leqq 2) \qquad (14)$$

is valid with

$$a = e^{-\varkappa_F} \qquad (15)$$

$$b = b_S = 1 - a \qquad (16)$$

$$T_b = T_{bS} = \frac{1}{1-a}\ \varkappa_F T_{WF} \qquad (17)$$

As approximate frequency response for eq.(11) is

$$\tilde{F}_{MDS1}(s) = F_{MDS}(0) \cdot \frac{1}{T_1 s} \cdot \frac{1}{(1+T_2 s)} \left[1-(a+ \frac{b_S}{1+T_{bS} \cdot s}) e^{-T_t s} \right] \qquad (18)$$

$F_{MDS}(s)$ and $\tilde{F}_{MDS1}(s)$ agree very well, Fig.5.

b) For $b_S = 0$ one obtain

$$\tilde{F}_{MDS2}(s) = F_{MDS}(0)\ \frac{K_2}{1+T_1 s} \cdot \frac{1}{1+T_2 s} \left[1-a\ e^{-T_t s} \right] \qquad (19)$$

$$K_2 = \frac{1}{1-a} \qquad (20)$$

c) With $a = 1$ and $b_S = 0$

$$\tilde{F}_{MDS3}(s) = F_{MDS}(0)\ \frac{1}{T_t s} \cdot \frac{1}{(1+T_2 s)} \left[1-e^{-T_t s}\right] \tag{21}$$

d) Neglecting the heat capacity of the tube wall ($T_{WF} = 0$)

$$\tilde{F}_{MDS4}(s) = F_{MDS}(0) \cdot \frac{1}{T_t s} \left[1-e^{-T_t s}\right] \tag{22}$$

e) For $0{,}7 \leq \varkappa_F \leq 5{,}0$ the waves in the frequency response curves, arising from $F_3'(s)$, eq.(11), can be neglected*) and then reads, compare eq.(19)

$$\tilde{F}_{MDS5}(s) = F_{MDS}(0)\ \frac{1}{(1+T_1 s)} \cdot \frac{1}{(1+T_2 s)}. \tag{23}$$

The approximate frequency response $\tilde{F}_{MDS1}(s)$ and $\tilde{F}_{MDS5}(s)$ show the best agreement with the exact frequency response $F_{MDS}(s)$, Fig.5.

For the dynamic behaviour of the outlet header in the case of ideal mixing ($w_F > 0{,}5$ m/s) one obtains

$$F_{AK}(s) = \frac{\vartheta_{Fa}(s)}{\vartheta_{FaR}(s)} = \frac{1}{1+T_{AK}s} \tag{24}$$

with

$$T_{AK} = \frac{m_{FK}}{\dot{M}_F}. \tag{25}$$

The mathematical models for the dynamic behaviour of the outlet temperature ϑ_{Fa} of the heat exchanger are with $F_Y(s) = c_v \cdot F_{MD}(s) \cdot F_{AK}(s)$ ($P_{Di} < 0{,}58\ P_{DV}$):

For $0{,}7 \leq \varkappa_F \leq 5{,}0$: ($\tilde{F}_{MDS5}(s)$)

$$F_Y(s) = \frac{\Delta\vartheta_{Fa}(s)}{\Delta Y(s)} = c_v \cdot \frac{F_{MDS}(0)}{(1+T_1 s)} \cdot \frac{1}{(1+T_2 s)} \cdot \frac{1}{1+T_{AK}s} \tag{26}$$

For $\varkappa_F < 0{,}7$: ($\tilde{F}_{MDS1}(s)$)

$$F_Y(s) = \frac{\Delta\vartheta_{Fa}(s)}{\Delta Y(s)}$$

$$= c_v\ F_{MDS}(0) \cdot \frac{1}{T_1 s} \cdot \frac{1}{(1+T_2 s)} \left[1-\left(a+\frac{b_S}{1+T_{bS} \cdot s}\right) \cdot e^{-T_t s}\right] \frac{1}{1+T_{AK}s} \tag{27}$$

*) maximum error of the amplitude ratio about 30 - 45 %

For estimating one can use eq.(26) also in the case of $\varkappa_F < 0,7$.

2.2. Operating condition 2: Changeable steam flow

In the case of under critical pressure ratio across the control valve the steam flow rate and therefore the heating of the tubes depends on the inside pressure P_{Di} respectively on the tube wall temperature Θ_W. For a tube the exact frequency response is [6]

$$F_{MDK}(s) = \frac{\Delta \vartheta_{FaR}(s)}{\Delta \dot{M}_D(s)}$$

$$= G_{MD} \cdot \frac{1}{T_{WD}T_F s^2 + (T_F \frac{1+z}{z} + T_{WD})s + 1} \left[1 - e^{-\varkappa_F \frac{T_{WD}s+1}{T_{WD}s + \frac{1+z}{z}}} \cdot e^{-T_t s} \right] \quad (28)$$

with

$$G_{MD} = \frac{(i_{De} - i')}{\pi d_2 \ell} \cdot \frac{1}{\alpha_{WF}} \cdot \frac{d_2}{d_1} \cdot \frac{1}{z} \,. \quad (29)$$

<u>Approximate frequency responses of the tube part:</u>

a) For the transcendental part of the frequency response the approximation [8]

$$e^{-\varkappa_F \frac{T_{WD}s+1}{T_{WD}s+\frac{1+z}{z}}} \approx a + \frac{b_K}{1+T_{bK} \cdot s} \qquad (0 \leq \varkappa_F \leq 2) \quad (30)$$

$$a = e^{-\varkappa_F} \quad (15)$$

$$b = b_K = e^{-\varkappa_F \frac{z}{1+z}} - a \quad (31)$$

$$T_b = T_{bK} = \frac{b_K}{(1-a)^2} \varkappa_F T_{WF}. \quad (32)$$

The approximate frequency response for eq.(28) then is:

$$\tilde{F}_{MDK1}(s) = G_{MD} \frac{1}{T_{WD}T_F s^2 + (T_F \frac{1+z}{z} + T_{WD})s + 1} \left[1 - (a + \frac{b_K}{1+T_{bK}s}) e^{-T_t s} \right] \quad (33)$$

For the operating condition 2 as well as for the operating condition 1 several approximate frequency responses, <u>Fig.6</u>, were investigated:

b) $$\tilde{F}_{MDK2}(s) = G_{MD} \frac{1}{(1+T_F s)\cdot(1+T_{WD}s)} \left[1-(a+\frac{b_K}{1+T_{bK}s}).e^{-T_t s} \right] \quad (34)$$

c) $$\tilde{F}_{MDK3}(s) = G_{MD} \frac{1}{(1+T_F s)\cdot(1+T_{WD}s)} \left[1-(a+b_K)\cdot e^{-T_t s} \right] \quad (35)$$

d) $$\tilde{F}_{MDK4}(s) = G_{MD} \frac{1}{1+T_F s} \left[1-(a+b_K)\, e^{-T_t s} \right] \quad \text{comp.}^4 \quad (36)$$

e) $$\tilde{F}_{MDK5}(s) = F_{MDK}(0) \frac{1}{(1+T_3 s)} \cdot \frac{1}{(1+T_4 s)} \quad (37)$$

The best agreement with $F_{MDK}(s)$ are $\tilde{F}_{MDK1}(s)$ and $\tilde{F}_{MDK5}(s)$.

Therefore the mathematical models for the dynamic behaviour of the outlet temperature ϑ_{Fa} of the heat exchanger are ($P_{Di} > 0{,}58\ P_{DV}$):

For $0{,}7 \leq \varkappa_F \leq 5{,}0$: ($\tilde{F}_{MDK5}(s)$)

$$F_Y(s) = \frac{\Delta\vartheta_{Fa}(s)}{\Delta Y(s)} = c_v \cdot \frac{F_{MDK}(0)}{(1+T_3 s)} \cdot \frac{1}{(1+T_4 s)} \cdot \frac{1}{(1+T_{AK}s)} \; {}^{*)} \quad (38)$$

with

$$F_{MDK}(0) = \frac{(i_{De}-i')}{\pi d_2 \ell} \cdot \frac{1}{\alpha_{WF}} \cdot \frac{d_2}{d_1} \cdot \frac{1}{z} \;(1-\psi) \quad (39)$$

$T_F \geq T_{WD}$:

$$T_{WD} < T_{31} = T_F\,(1-\psi) \longrightarrow \begin{cases} T_3 = T_{31} \\ T_4 = T_{WD} \end{cases} \quad (40)$$

$$T_{WD} \geq T_{31} = T_F\,(1-\psi) \longrightarrow \begin{cases} T_3 = T_{41} \\ T_4 = T_{41} \end{cases} \quad (41)$$

$T_F < T_{WD}$: see [1]

$$\psi = e^{-\varkappa_F \frac{z}{1+z}} \quad (42)$$

$$T_{41} = \sqrt{T_F\, T_{WD}\ (1-\psi)} \quad (43)$$

For $\varkappa_F < 0{,}7$: ($\tilde{F}_{MDK1}(s)$)

$$F_Y(s) = \frac{\Delta\vartheta_{Fa}(s)}{\Delta Y(s)}$$

$$= c_v \cdot G_{MD} \cdot \frac{1}{T_{WD}T_F s^2 + (T_F \frac{1+z}{z} + T_{WD})s + 1} \left[1-(a+\frac{b_K}{1+T_{bK}s}).e^{-T_t s} \right] \cdot \frac{1}{1+T_{AK}s} \quad (44)$$

*) maximum error of the amplitude ratio about 30 - 45 %

For estimating purposes one can use eq.(28) for the case of $\varkappa_F < 0{,}7$.

2.3. Dependence of the dynamic behaviour on the load in the case of steam side regulation

In regarding the secondary flow $\dot{M}_F$ as the load by constant temperature difference ($\vartheta_{Fa} - \vartheta_{Fe}$) one obtains different curves for the gains $F_{MDS}(O)$ (over critical pressure ratio) and $F_{MDK}(O)$ (under critical pressure ratio) of the frequency response $F_{MD}(s)$ (changes of manipulated variable) as shown in Fig.7. Crossing the critical pressure ratio while reducing the load, the gain rises from a small value $F_{MDK}(O)$ to a greater value $F_{MDS}(O)$. In general, therefore it is not possible, to obtain a good quality of control across the whole load region with only one single adjustment of the controller. For low load $\dot{M}_F$ the control loop can be instable because $F_{MDS}(O) \sim 1/\dot{M}_F$. However a part of the load dependence can be compensated using a control valve with equal percentage characteristic. Fig.8 shows transient curves in dependence on the load $\dot{M}_F$.

3. Mathematical models for the dynamic behaviour in the case of regulation on condensate side

3.1. Vertical heat exchanger

For the condensate flow valve

$$\Delta\dot{M}_K = c_v . \Delta Y$$

and therefore the frequency response for the manipulated variable becomes

$$F_Y(s) = \frac{\Delta\dot{M}_K(s)}{\Delta Y(s)} \cdot \frac{\Delta\vartheta_{FaR}(s)}{\Delta\dot{M}_K(s)} \cdot \frac{\Delta\vartheta_{Fa}(s)}{\Delta\vartheta_{FaR}(s)} = c_v . F_{MK}(s) . F_{AK}(s). \quad (45)$$

From the mass balance of the stored condensate one obtains for the vertical heat exchanger [1]

$$\boxed{F_Y(s) = \frac{\Delta\vartheta_{Fa}(s)}{\Delta Y} = c_v \cdot \frac{F_{MKS}(O)}{1+T_{MKS}s} \cdot e^{-T_t(\ell-H)} \cdot \frac{1}{1+T_{AK}.s}} \quad (46)$$

with

$$F_{MKS}(O) = \frac{r}{\dot{M}_F' c_F} \quad (47)$$

$$T_{MKS} = \frac{\rho_K . r}{\dot{q}_{WD}} \cdot \beta \cdot \frac{1}{\psi} \qquad (\rho_K \text{ condensate density}) \quad (48)$$

$$T_{t\ (\ell-H)} = \frac{\ell-H}{w_F} \qquad \text{(H condensate level)} \qquad (49)$$

$$\beta = \frac{A_H}{\pi d_2} = \frac{A_H \cdot \Delta H}{\pi d_2 \Delta H} = \frac{\text{stored condensate volume}}{\text{change of heating area}} \qquad (50)$$

β is called condensate volume number.

For a tube part with steam at the outside of the tubes

$$\beta = \frac{d_2}{4n} \left[\left(\frac{D_3}{d_2}\right)^2 - n \right]. \qquad (51)$$

The value of the time constant T_{MKS} is influenced mainly from the value of the condensate volume number β. To obtain a small time constant T_{MKS}, β has to be small, which means, with constructive arangements the condensate storage volume must be as little as possible.

3.2. Dependence of the dynamic behaviour on the load in the case of condensate side regulation

Also in the case of condensate side regulation the gain $F_{MKS}(0) \sim 1/\dot{M}_F$ increases with reduced secondary flow. Because the time constant too increases, one obtains a great dependence of the transient curves on the secondary flow, Fig.9.

A part of the dependence of the gain on the load can be compensated by using a control valve with equal percentage characteristic. Due to the large time constante T_{MKS} in the case of small secondary flow one obtains a very slow reacting transient behaviour at low loads.

4. Comparison of the dynamic behaviour for both steam side and condensate side regulation

For a heat exchanger with the data

D_3 = 0,2 m; d_1 = 0,021 m; d_2 = 0,025 m; ℓ= 5 m; n = 37;
A_R = 14,4 m^2; ϑ_{Fe} = 70°C; ϑ_{Fa} = 90°C; ϑ_{De} = 130°C; w_F = 2 m/s;
the transient curves of the tube part are shown in Fig.10.
In the case of steam side regulation the equalization time is T_G = 2,3 s. In the case of condensate side regulation the time constant is T_{MKS} = 91 s. Thus this value is about 40 time greater than the equalization time T_G in the case of steam side regulation. In the case of condensate side regulation the dominant time constant is always much greater than in the case of steam side regulation.

In Fig.11 the schematic curves for the gains and for the time constants of the transient curve in changing the manipulated variable are shown in dependence on the load for both steam side and condensate side regulation. Both the secondary flow $\dot{M}_F$ in the case of constant temperature difference ($\vartheta_{Fa} - \vartheta_{Fe}$) and the temperature difference ($\vartheta_{Fa} - \vartheta_{Fe}$) in the case of constant secondary flow is regarded as load.

When the secondary flow is regarded as load, the gain and the time constants for both cases show a similar trend. In both cases there is danger of instability for low load, because the gain goes to infinity for $\dot{M}_F \rightarrow 0$.

When the temperature difference is the load, the time constants change little with load, but in the case of steam side regulation the gain becomes very small. Within the low loads region one can obtain a better quality of control with condensate side regulation, because the gain is nearly independent on load.

5. Conclusions about the control of steam heated heat exchangers

The principal differences of steam side and condensate side regulation is the value of the dominant time constant of the transient curve for changes of the manipulated variable. In the case of steam side regulation the equalization time is relatively small ($T_G \approx 1 \ . \ . \ . \ 30$ s). However in the case of condensate side regulation the equalization time constant is 30 to 100 time greater than in the case of steam side regulation. But the time constants for changes in the disturbance $\Delta\dot{M}_F$ and $\Delta\vartheta_{Fe}$ in both cases are nearly equal.

If the velocity of the disturbances is small, one can obtain a sufficient quality of control, when the secondary flow is not too small. But if the velocity of disturbances is great, the steam side regulation is to prefer.

6. Literature

1 Isermann, R.: Das regeldynamische Verhalten dampfbeheizter Wärmeübertrager. Will be published shortly.

2 Hempel, Arvid: On the Dynamics of Steam Liquid Heat Exchangers. Transactions of the ASME, (1961), June, S.244-251.

3 Stermole, F.J., and Larson, M.A.: Dynamic Response of Heat Exchangers to Flow Rate Changes. Industr. Eng.Chem.(Fundamentals) (1963), 2, S.62-67.

4 Stainthorp, F.P., and Axon, A.G.: The Dynamic Behaviour of a Multipass steam-heated Exchanger. Chemical Engineering Science (1965), Vol.20, S.107-119.

5 Sieler, W.: Dynamische Modelle von Wärmeaustauschern. Tagung des NAMUR-Unterausschusses "Regelungstechnik" am 11./12.11.1965.

6 Isermann, R.: Das regeldynamische Verhalten von Überhitzern. Fortschritt-Bericht VDI-Zeitschrift, Reihe 6, Nr.4 (1965).

7 Isermann, R.: Messung und Berechnung des regeldynamischen Verhaltens eines Überhitzers. Fortschritt-Bericht VDI-Zeitschrift, Reihe 6, Nr.9 (1965).

8 Isermann, R.: Vorausbestimmung der Regelgüte der Dampftemperatur-Regelung von Trommelkesseln mit dem Analogrechner. Regelungstechnik 14 (1966) Nr.10, Teil I, S.469-475, Teil II, S.519-522.

7. Nomenclature

A_H	surface of condensate level (for one tube) ($A_H = A_{Hges/n}$)
c_F	specific heat of the fluid
c_W	specific heat of the tube wall
d_1	inner diameter of a tube
d_2	outer diameter of a tube
D_3	inner diameter of the shell
i'	specific enthalpy of the condensate
i_{De}	specific enthalpy of the steam before steam valve
ℓ	heated length of tube
m_{FK}	mass of the fluid in a header
$\dot{M}_D$	steam mass flow rate
$\dot{M}_F$	secondary mass flow rate
$\dot{M}_K$	condensate mass flow rate
$\dot{M}'$	mass flow rate referring to one tube
n	number of tubes
p_{Di}	steam pressure in the heat exchanger
p_{DV}	steam pressure before the steam valve
q_{WD}	heat flux steam - tube wall
r	specific heat for evaporization
s	complex variable $s = i\omega$
w_F	velocity of the secondary flow in a tube
Y	manipulated variable
$\alpha_{WD}=\alpha_{WDi}$	heat transfer coefficient steam- tube wall
α_{WDa}	heat transfer coefficient steam-shell wall
α_{WF}	heat transfer coefficient tube wall - fluid
ϑ_{De}	steam temperature before steam valve
ϑ_F	temperature of the fluid
ϑ_{Fa}	outlet temperature of the secondary flow of the heat exchanger
ϑ_{Fe}	inlet temperature of the secondary flow of the heat exchanger
ϑ_{FaR}	outlet temperature of the secondary flow of the tube part
ϑ_{FeR}	inlet temperature of the secondary flow of the tube part
θ_W	temperature of the tube wall
ρ_F	fluid density
ρ_W	tube wall density
ψ	$\psi = e^{-\varkappa_F \frac{z}{1+z}}$
ω	frequency

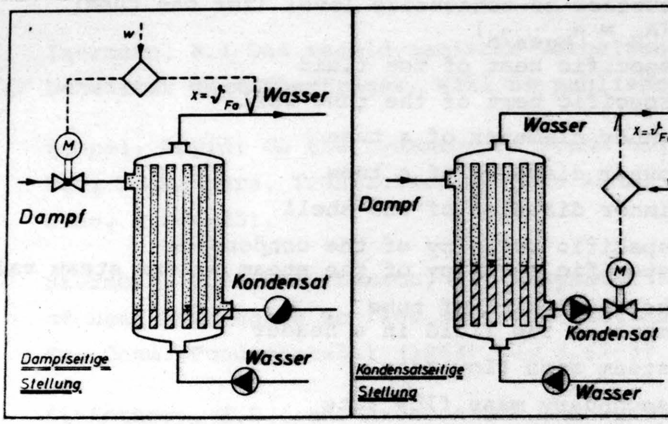

a) Regulation in steam flow   b) Regulation in condensate flow

Fig.1. Control loops for the outlet temperature of the secondary flow of steam heated heat exchangers.

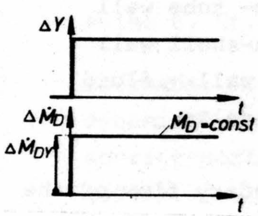

Fig.2. Steam flow after a change ΔY of the control valve under over critical pressure ratio

(operating condition 1)

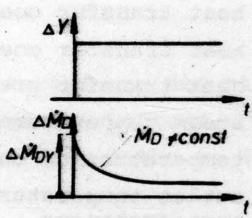

Fig.3. Steam flow after a change ΔY of the control valve under under critical pressure ratio

(operating condition 2)

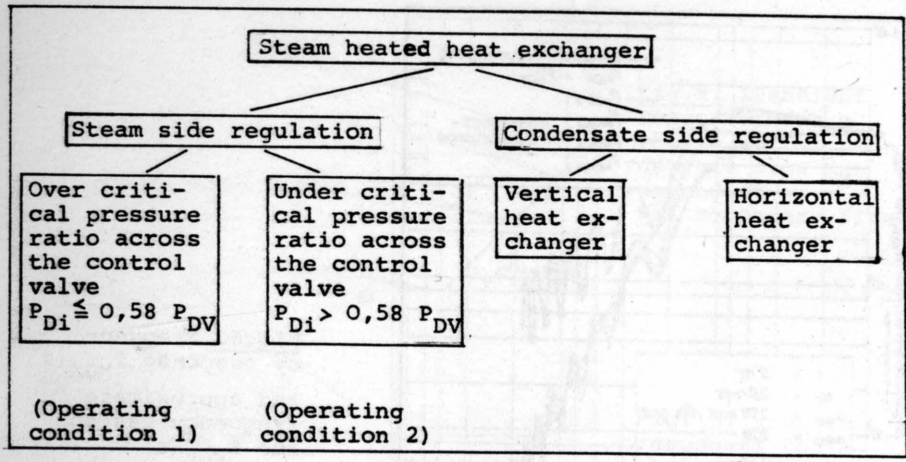

Fig.4. Classification to investigate the dynamic behaviour of steam heated heat exchangers.

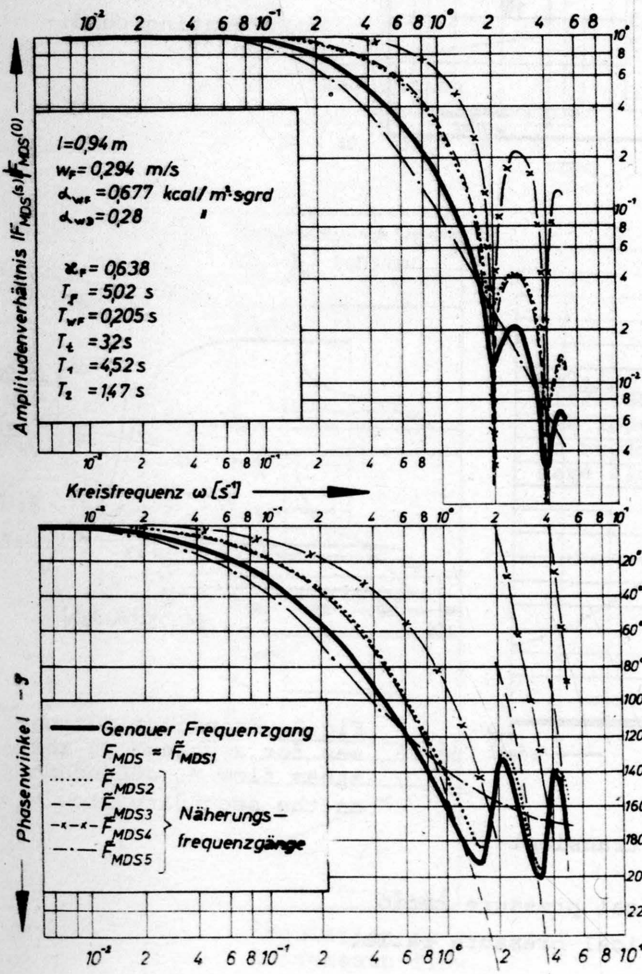

Fig.5. Frequency response $F_{MDS}(s)$ and approximate frequency responses $\tilde{F}_{MDS}(s)$ (operating condition 1)

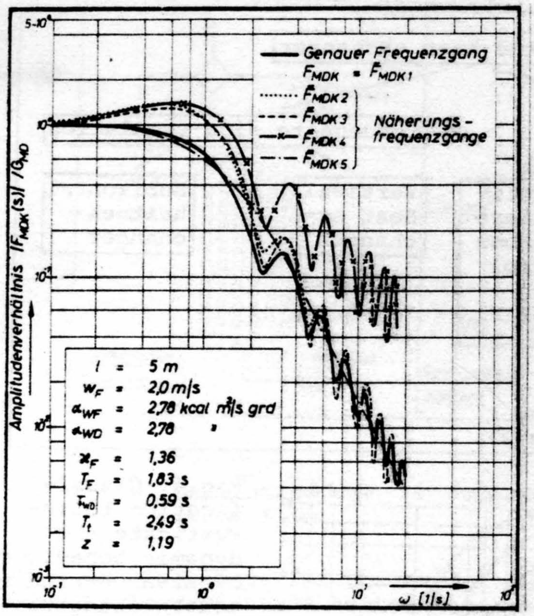

Fig.6. Frequency response $F_{MDK}(s)$ and approximate frequency responses $\tilde{F}_{MDK}(s)$

(operating condition 2)

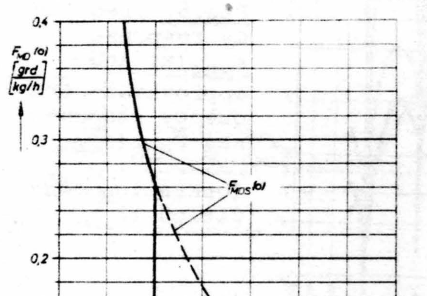

Fig.7. Gain of the transient behaviour.

$F_{MDS}(0)$: over critical pressure ratio

$F_{MDK}(0)$: under critical pressure ratio.

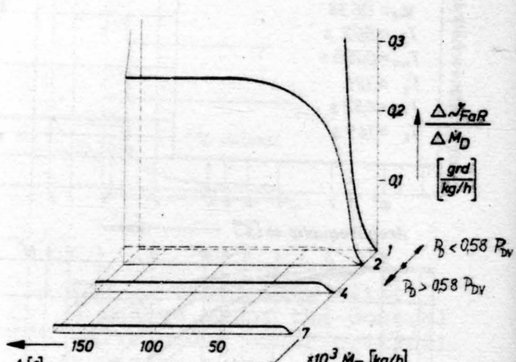

Fig.8. Transient responses for a change in the steam flow $\dot{M}_D$ dependent on the secondary flow $\dot{M}_F$

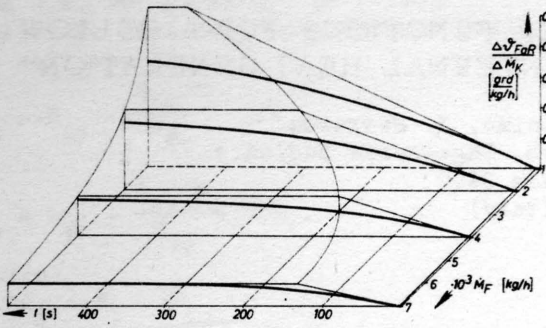

Fig.9. Transient responses for a change in the condensate flow $\dot{M}_K$ dependent on the secondary flow $\dot{M}_F$.

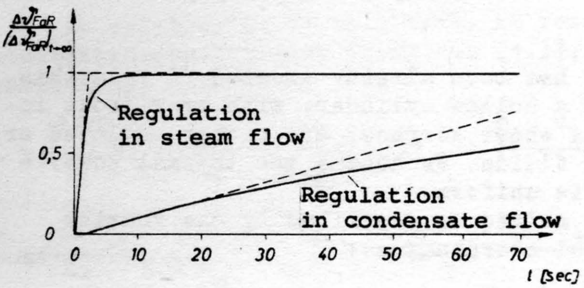

Fig.10. Transient responses for a change in the steam flow and condensate flow.

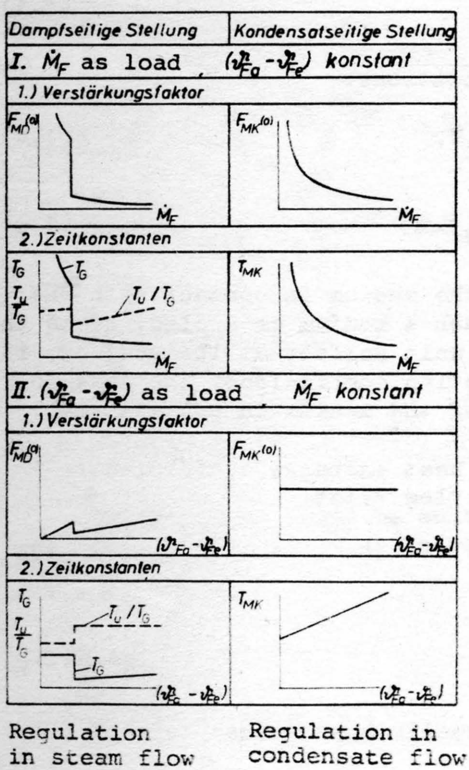

Regulation in steam flow — Regulation in condensate flow

Fig.11. Dependence of different parameters on the load for both changes in steam flow or condensate flow.

THERMAL TRANSFER FUNCTIONS FOR A HOLLOW CYLINDER WITH INTERNAL HEAT GENERATION

by E. Cosimo, S. Petrarca
C.N.E.N. - Lab. Ingegneria Nucleare
Casella Postale 2400
00100 Rome (Italy)

1. Problem formulation

We solve the problem of radial heat transmission in a cylinder, assuming its conductivity and diffusity are constant:
k = const.,
$\alpha = k/\rho c$ = const.

The full cylinder has been already treated [1,2]; in this work we will deal with a hollow cylinder, with or without internal heat generation, whose surfaces are either isolated or in contact with moving fluids. We assume the thermal power density, if there is, is uniform.

The problem to be solved is described by the Fourier equation (in cylindrical coordinates):

$$\frac{\partial^2 T_c}{\partial r^2} + \frac{1}{r}\frac{\partial T_c}{\partial r} - \frac{1}{\alpha}\frac{\partial T_c}{\partial t} = -\frac{p}{k} \tag{1.1}$$

with the following boundary conditions:

$$-k\left(\frac{\partial T_c}{\partial r}\right)_{r=R_i} = h_i\,(T_i - T_{ci}), \tag{1.2}$$

$$-k\left(\frac{\partial T_c}{\partial r}\right)_{r=R_e} = h_e\,(T_{ce} - T_e). \tag{1.3}$$

T_i is the temperature of the medium in contact with the cylinder's inner surface. If such a medium is a clad, h_i is the inverse thermal resistance per unit surface at the contact; if it is a fluid, h_i is the convection coefficient. The same is valid for T_e, the temperature of the medium in contact with the outer surface, and for h_e.

In the general case, both heat exchange coefficients depend on fractional powers of flow rates:

$$h_i = h_{io}\left(\frac{W_i}{W_{io}}\right)^{m_i}, \tag{1.4}$$

$$h_e = h_{eo}\left(\frac{W_e}{W_{eo}}\right)^{m_e}. \tag{1.5}$$

The exponents m_i and m_e usually have values between 0.4

and 0,8. The index "$_o$" in (1.4) and (1.5) refers to steady state. We just take into account small variations of flow rates, so we linearize:

$$h_i = h_{io} + \frac{h_{io}\, m_i}{W_{io}} \Delta W_i, \qquad (1.6)$$

$$h_e = h_{eo} + \frac{h_{eo}\, m_e}{W_{eo}} \Delta W_e, \qquad (1.7)$$

where:

$$\Delta W_i = W_i - W_{io},$$
$$\Delta W_e = W_e - W_{eo}.$$

As equation (1.1) is linear, it remains unchanged when considering variations; (1.2) and (1.3), written in terms of variations, turn into:

$$-k\left(\frac{\partial \Delta T_c}{\partial r}\right)_{r=R_i} = h_{io}(\Delta T_i - \Delta T_{ci}) + \frac{h_{io}\, m_i (T_{io} - T_{cio})}{W_{io}} \Delta W_i, \qquad (1.8)$$

$$-k\left(\frac{\partial \Delta T_c}{\partial r}\right)_{r=R_e} = h_{eo}(\Delta T_{ce} - \Delta T_e) + \frac{h_{eo}\, m_e (T_{ceo} - T_{eo})}{W_{eo}} \Delta W_e, \qquad (1.9)$$

if terms including products of variations are neglected.

It is very useful to rewrite the above equations as follows:

$$-\left(r\frac{\partial \Delta T_c}{\partial r}\right)_{r=R_i} = \frac{R_i\, h_{io}}{k}(\Delta T_i - \Delta T_{ci}) + b_i \,\Delta W_i, \qquad (1.10)$$

$$-\left(r\frac{\partial \Delta T_c}{\partial r}\right)_{r=R_e} = \frac{R_e\, h_{eo}}{k}(\Delta T_{ce} - \Delta T_e) - b_e \,\Delta W_e, \qquad (1.11)$$

with

$$b_i = \frac{m_i\,(T_{io} - T_{cio})}{W_{io}}, \qquad (1.12)$$

$$b_e = \frac{m_e\,(T_{eo} - T_{ceo})}{W_{eo}}. \qquad (1.13)$$

Equation (1.1) may be solved by Laplace transform. For the sake of generality we introduce two dimensionless variables:

$$a = i\, R_e \sqrt{s/\alpha}\,, \qquad (1.14)$$

$$x = \frac{a}{R_e}\, r\,, \qquad (1.15)$$

and three dimensionless parameters:

$$M = \frac{R_e h_{eo}}{k} , \qquad (1.16)$$

$$R = \frac{R_i}{R_e} , \qquad (1.17)$$

$$H = \frac{h_{io}}{h_{eo}} . \qquad (1.18)$$

By means of these notations, equation (1.1) and boundary conditions are rewritten as follows (from now on, symbols we introduced above for physical variables will be used to designated Laplace transform of variations: T_c stands for $\mathcal{L}[\Delta T_c]$, etc):

$$\frac{d^2T_c}{dx^2} + \frac{1}{x}\frac{dT_c}{dx} + T_c = - \frac{R_e^2}{a^2k} p , \qquad (1.19)$$

$$-(x \frac{dT_c}{dx})_{x = Ra} = RHM \left[(T_i - T_{ci}) + b_i W_i\right] , \qquad (1.20)$$

$$-(x \frac{dT_c}{dx})_{x = a} = M \left[(T_{ce} - T_e) - b_e W_e\right] . \qquad (1.21)$$

So we put the problem in terms of dimensionless variables: x, including both space and time-dependence, and a, which contains the time-dependence only; furthermore, we have just to deal with three dimensionless parameters, M, R and H, whose meaning is quite evident.

2. Exact solution

The homogeneous equation associated to (1.19) is the zero-order Bessel equation, whose general solution is:

$$T_1 = A\, J_0(x) + B\, N_0(x),$$

while a particular solution of complete equation is:

$$T_2 = - \frac{R_e^2}{a^2k} p .$$

Thus complete solution of (1.19) is:

$$T_c(x) = T_1 + T_2 = AJ_0(x) + BN_0(x) - \frac{R_e^2}{a^2k} p , \qquad (2.1)$$

with A and B to be deduced by imposing boundary conditions. Before we do that, it is suitable to introduce simpler symbols for several functions recurring in the equations we will write. We use simple symbols, without specifying arguments, to designate Bessel functions calculated for $x = a$ (i.e. $r = R_e$):

$$J_0 = J_0(a)\ ,\ J_1 = J_1(a)\ ,\ N_0 = N_0(a)\ ,\ N_1 = N_1(a)\ ; \tag{2.2}$$

instead, to designate the same functions calculated for $x = Ra$ (i.e. $r = R_i$), we use the symbols:

$$J_{0R} = J_0(Ra),\ J_{1R} = J_1(Ra),\ N_{0R} = N_0(Ra),\ N_{1R} = N_1(Ra)\ . \tag{2.2a}$$

Since:

$$\frac{dJ_0(x)}{dx} = -J_1(x), \qquad \frac{dN_0(x)}{dx} = -N_1(x)\ , \tag{2.3}$$

from (2.1) we deduce:

$$-x\frac{dT_c}{dx} = x\left[AJ_1(x) + BN_1(x)\right].$$

Thus (1.20) and (1.21) are written:

$$Ra(AJ_{1R}+BN_{1R}) = RHM\left[T_i - AJ_{0R} - BN_{0R} + \frac{R_e^2}{a^2k} + b_i\ W_i\right],$$

$$a(AJ_1+BN_1) = M\left[AJ_0+BN_0 - T_e - \frac{R_e^2}{a^2k}\ p - b_e\ W_e\right]\ ,$$

and from that we obtain:

$$A = \frac{HM(MN_0 - aN_1)\ F_i - M\ (HM\ N_{0R} + aN_{1R})\ F_e}{D(a)}\ ,$$

$$B = \frac{-\ HM(MJ_0 - aJ_1)\ F_i + M(HM\ J_{0R} + aJ_{1R})\ F_e}{D(a)},$$

where:

$$F_i = T_i + \frac{R_e^2}{a^2k}\ p + b_i\ W_i\ , \tag{2.4}$$

$$F_e = T_e + \frac{R_e^2}{a^2k}\ p + b_e\ W_e\ , \tag{2.5}$$

$$D(a) = (HMJ_{0R}+aJ_{1R})(MN_0-aN_1)-(HMN_{0R}+aN_{1R})(MJ_0-aJ_1)\ . \tag{2.6}$$

Substituting A and B into (2.1) we finally get:

$$T_c(x) = C_i(x)\ F_i + C_e(x)\ F_e - \frac{R_e^2}{a^2 k}\ p\ , \qquad (2.7)$$

where:

$$C_i(x) = \frac{HM\left[(MN_0 - aN_1)J_0(x) - (MJ_0 - aJ_1)N_0(x)\right]}{D(a)}\ , \qquad (2.8)$$

$$C_e(x) = \frac{M\left[-(HMN_{0R} + aN_{1R})\ J_0(x) + (HMJ_{0R} - aJ_{1R})N_0(x)\right]}{D(a)}\ . \qquad (2.9)$$

The above equations ((2.4) through (2.9)) allow us to obtain transfer functions from inner and outer temperatures and flow rates (T_i, W_i, T_e, W_e) and from power density, p, to the temperature at any point of the cylinder; in particular we get transfer functions to the outer surface temperature, T_{ce} (by putting x = a), and to inner surface temperature, T_{ci} (by putting x = Ra).

For the average temperature we have:

$$\overline{T}_c = \frac{2\ \pi}{\pi(R_e^2 - R_i^2)}\int_{R_i}^{R_e} r\ T_c(r)\ dr = \frac{2}{a^2(1-R^2)}\int_{aR}^{a} x\ T_c(x)\ dx \qquad (2.10)$$

To calculate this integral, remember that, for any integer n:

$$\int x^n\ J_{n-1}(x)\ dx = x^n\ J_n(x), \qquad (2.11)$$

$$\int x^n\ N_{n-1}(x)\ dx = x^n\ N_n(x). \qquad (2.12)$$

3. Transfer functions

The inner temperature, T_i, appears just in F_i (defined by (2.4)); then $C_i(x)$, in (2.8), is the transfer function from inner temperature to cylinder's temperature:

$$\frac{T_c(x)}{T_i(s)} = C_i(x). \qquad (3.1)$$

Similar considerations lead to establish the other transfer functions:

$$\frac{T_c(x)}{T_e(s)} = C_e(x)\ , \qquad (3.2)$$

$$\frac{T_c(x)}{W_i(s)} = b_i\ C_i(x)\ , \qquad (3.3)$$

$$\frac{T_c(x)}{W_e(s)} = b_e\, C_e(x)\,, \tag{3.4}$$

$$\frac{T_c(x)}{p(s)} = \frac{R_e^2}{a^2 k}\left[C_i(x) + C_e(x) - 1\right]. \tag{3.5}$$

Before deducing transfer functions to surface (T_{ci} and T_{ce}) and average ($\overline{T}_c$) temperatures, it is useful to recall a property of Bessel functions, we will use many times later on:

$$N_0(x)J_1(x) - N_1(x)J_0(x) = \frac{2}{\pi x}\,. \tag{3.6}$$

It is also useful to put:

$$\begin{aligned} L_1 &= N_{0R}\, J_1 - J_{0R} N_1\,, \\ L_2 &= N_0\, J_{1R} - J_0 N_{1R}\,, \\ L_3 &= N_{1R}\, J_1 - J_{1R} N_1\,, \\ L_4 &= N_0\, J_{0R} - J_0 N_{0R}\,. \end{aligned} \tag{3.7}$$

By these notations, equation (2.6) is rewritten:

$$D(a) = aHML_1 + aML_2 + a^2 L_3 + HM^2 L_4\,. \tag{3.8}$$

Calculating the integral in equation (2.10) and using (3.6) we get:

$$\overline{T}_c(a) = \bar{C}_i(a)F_i + \bar{C}_e(a)F_e - \frac{R_e^2}{a^2 k}\, p\,,$$

with:

$$\bar{C}_i(a) = \frac{\dfrac{2\,RHM}{a(1-R^2)}\left[\dfrac{2\,M}{\pi R\, a} - ML_2 - aL_3\right]}{D\,(a)} = \frac{\overline{T}_c(a)}{T_i(s)}\,, \tag{3.9}$$

$$\bar{C}_e(a) = \frac{\dfrac{2\,M}{a(1-R^2)}\left[\dfrac{2\,HM}{\pi\, a} - HML_1 - a\,L_3\right]}{D(a)}\,\frac{\overline{T}_c(a)}{T_e(s)} \tag{3.10}$$

Putting $x = Ra$ into (2.8) and (2.9), and using (3.7), we find:

$$\frac{T_{ci}(s)}{T_i(s)} = \frac{HM(ML_4 + a\,L_1)}{D(a)} = C_{ii}(a)\,, \tag{3.11}$$

$$\frac{T_{ci}(s)}{T_e(s)} = \frac{\frac{2M}{\pi R}}{D(a)} = C_{ei}(a) \; ; \tag{3.12}$$

and putting x = a:

$$\frac{T_{ce}(s)}{T_i(s)} = \frac{\frac{2HM}{\pi}}{D(a)} = C_{ie}(a) \; , \tag{3.13}$$

$$\frac{T_{ce}(s)}{T_e(s)} = \frac{M(HML_4+aL_2)}{D(a)} = C_{ee}(a) \; . \tag{3.14}$$

The other transfer functions may be obtained from equations (3.9) through (3.14) making use of general relations (3.3), (3.4) and (3.5).

In particular, we may also deduce transfer functions relating each to the other surface temperatures. The ratio of (3.13) to (3.11) yields:

$$\frac{T_{ce}(s)}{T_{ci}(s)} = \frac{2/\pi}{ML_4 + aL_1} \; ; \tag{3.15}$$

and the ratio of (3.12) to (3.14):

$$\frac{T_{ci}(s)}{T_{ce}(s)} = \frac{2/\pi R}{HML_4 + aL_2} \; . \tag{3.16}$$

4. <u>Expansion of transfer functions in Heaviside's series</u>

All transfer functions we deduced in the previous paragraph have the form:

$$G(a) = \frac{E(a)}{D(a)} \; . \tag{4.1}$$

The poles of G(a) are given by the equation:

$$D(a) = 0 \; , \tag{4.2}$$

which has infinite, all real, simple and symmetrical roots [2]. We order these roots as follows:

$$a_m > a_{m-1} \qquad (m = 1, 2, 3, \ldots) \; .$$

G(a) in (4.1) may be expanded in Heaviside's series:

$$G(s) = \sum_{1}^{\infty}{}_m \frac{G_m}{s - s_m} \; , \tag{4.3}$$

where, by virtue of (1.14):

$$s_m = -\frac{\alpha}{R_e^2} a_m^2 \; , \tag{4.4}$$

and G_m is the residue of $G(s)$ in s_m:

$$G_m = \left[\frac{E(a)}{\frac{d\,D(a)}{d\,s}} \right]_{s=s_m} \tag{4.5}$$

From (4.4):

$$\frac{d\,s}{d\,a} = - \frac{2\,\alpha a}{R_e^2}\,, \tag{4.6}$$

and then:

$$\frac{d\,D(a)}{d\,s} = - \frac{R_e^2}{2\,\alpha\,a} \frac{d\,D(a)}{d\,a} = - \frac{R_e^2}{2\,\alpha\,a} D'(a) \tag{4.7}$$

$$G_m = \frac{- \frac{2\,\alpha\,a_m}{R_e^2} E(a_m)}{\left[D'(a)\right]_{a=a_m}} \tag{4.8}$$

In order to calculate $D'(a)$ we must recall, besides equations (2.3), the following equations:

$$\frac{d\,J_1(x)}{dx} = J_0(x) - \frac{J_1(x)}{x}\;; \tag{4.9}$$

$$\frac{d\,N_1(x)}{dx} = N_0(x) - \frac{N_1(x)}{x}\;. \tag{4.10}$$

We may put $\left[D'(a)\right]_{a=a_m}$ into a very simple form if we notice that, when a is a root of equation (4.2), the following identity is true:

$$L(a) = \frac{a\,J_{1R} + HMJ_{OR}}{a\,J_1 - MJ_0} = \frac{a\,N_{1R} + HMN_{OR}}{a\,N_1 - MN_0}\;. \tag{4.11}$$

After all, we get:

$$\left[D'(a)\right]_{a=a_m} = - \frac{2}{\pi\,a_m} D^*(a_m)\,, \tag{4.12}$$

where:

$$D^*(a_m) = (a_m^2 + M^2)\,L(a_m) - \frac{a_m^2 + H^2M^2}{L(a_m)}\;. \tag{4.13}$$

Thus (4.8) becomes:

$$G_m = \frac{\pi \alpha}{R_e^2} \frac{a_m^2 E(a_m)}{D^*(a_m)} . \qquad (4.14)$$

Substituting numerators $E(a_m)$ of (3.9) through (3.14) into (4.14) and making use of (3.6) and (4.11) we get the following residues (first index refers to the fluid's or clad's temperature, second to cylinder's surface; e.g. $(G_{ie})_m$ is the residue, in the m-th pole, of the transfer function from T_i to T_{ce}):

$$(\bar{G}_i)_m = \frac{4\alpha H M^2}{R_e^2 (1-R^2)} \left[\frac{L(a_m) + H}{L(a_m) D^*(a_m)}\right] , \qquad (4.15)$$

$$(\bar{G}_e)_m = \frac{4M^2 \alpha}{R_e^2 (1-R^2)} \left[\frac{H+L(a_m)}{D^*(a_m)}\right] , \qquad (4.16)$$

$$(G_{ii})_m = \frac{2 \alpha H M}{R R_e^2} \left[\frac{a_m^2}{L(a_m) D^*(a_m)}\right] , \qquad (4.17)$$

$$(G_{ei})_m = \frac{2 \alpha M}{R R_e^2} \left[\frac{a_m^2}{D^*(a_m)}\right] , \qquad (4.18)$$

$$(G_{ie})_m = \frac{2 \alpha H M}{R_e^2} \left[\frac{a_m^2}{D^*(a_m)}\right] , \qquad (4.19)$$

$$(G_{ee})_m = \frac{2 \alpha M}{R_e^2} \left[\frac{a_m^2 L(a_m)}{D^*(a_m)}\right] . \qquad (4.20)$$

Equations (3.3) and (3.4) allow us to deduce immediately from previous equations (4.15) through (4.20) the residues of transfer functions from flow rates W_i and W_e.

As regards (3.5), we must notice that, if $E_i(x)$ and $E_e(x)$ are numerators of $C_i(x)$ and $C_e(x)$ respectively, we may write:

$$\frac{T_c(x)}{p(s)} = \frac{R_e^2}{a^2 k} \left[\frac{E_i(x)+E_e(x)-D(a)}{D(a)}\right] .$$

Thus, if P_m is the residue of the generical transfer function from thermal power density in the pole a_m, we have:

$$P_m = \frac{R_e^2}{a_m^2 k} \left[\frac{E_i(x) + E_e(x)}{\frac{d\, D(a)}{d\, s}}\right]_{a = a_m} ,$$

since $D(a_m) = 0$.

Ultimately we get:

$$P_m = \frac{R_e^2}{a_m^2 k} \left[(G_i)_m + (G_e)_m \right]. \qquad (4.21)$$

To summarize: if values of α and R_e and dimensionless parameters R, H and M are given, the knowledge of the roots of equation (4.2) is enough in order to calculate poles of all transfer functions, by means of (4.4). For the calculation of residues it is useful to employ function L(a), defined by (4.11), and function $D^*(a)$, defined by (4.13).

There are several important connections between the residues we are dealing with. For instance, the residues of transfer functions from outer temperature, T_e, are obtainable from corresponding residues referred to inner temperature, T_i, simply multiplying them by $L(a_m)/H$ (cfr. (4.15) through (4.20)):

$$\frac{(\bar{G}_e)_m}{(\bar{G}_i)_m} = \frac{(G_{ei})_m}{(G_{ii})_m} = \frac{(G_{ee})_m}{(G_{ie})_m} = \frac{L(a_m)}{H}. \qquad (4.22)$$

Another noticeable relation is the following:

$$\frac{(G_{ee})_m}{(G_{ei})_m} = \frac{(G_{ie})_m}{(G_{ii})_m} = R\, L(a_m). \qquad (4.23)$$

In order to calculate residues of transfer functions from power density, nothing but thermal conductivity k (constant) of cylinder must be besides specified.

Finally, residues of transfer functions from fluids' flow rates are simply proportional to those of fluids temperatures through b_i and b_e, defined by (1.12) and (1.13).

We carried out numerical programs for IBM 7094 computer, which calculate roots of equation (4.2) and corresponding residues and poles, and we obtained tables of the first 10 roots, for several values of M, R and H. These tables will be included in a report in preparation [3].

5. Approximation of transfer functions

Rewriting (4.3) in terms of time-constants we have:

$$G(s) = \sum_{1}^{\infty} \frac{G_m \tau_m}{1 + \tau_m s} \qquad (5.1)$$

where:

$$\tau_m = -\frac{1}{s_m} = \frac{R_e^2}{\alpha a_m^2} \qquad (5.2)$$

Notice that, as m increases (i.e. as τ_m decreases) the gain $G_m \tau_m$ decreases very rapidly, so that the first 4 ÷ 6 terms are enough to achieve a good approximation in practical cases.

If we hold in account just the first n terms of any series resumed in (5.1) we introduce errors in both the response to high frequencies and the steady state gain (the response to a step is initially slower and the final value is smaller). Let G_f be the steady gain of G(s); it is:

$$\sum_{1}^{n} G_m \tau_m = G_a \neq G_f.$$

The difference $G_f - G_a$ is the sum of steady gains of neglected poles, which all have time-constants smaller than the last held in account. It is then suitable to modify the gain and the time-constant of n-th pole, by compensating the steady error and slightly reducing its time-constant; $G_n \tau_n$ and τ_n are replaced by

$$(G_n \tau_n)^* = G_n \tau_n + (G_f - G_a),$$

$$\tau_n^* = \frac{G_f - G_a}{G_f} \tau_n.$$

This manipulation is logical and effectual for series whose terms are all positive. But some of series represented by (5.1) turn out to have terms of alternate sign; in these cases it is suitable to choose an even n and to modify gains and time-constants of the last two poles.

If values of $G_m \tau_m$, for $m > n$, are available, it is enough to add the sum of positive neglected gains to the gain of the last positive pole, and the sum of negative neglected gains to that of the last negative pole. Otherwise, the same end can be attained by making a diagram with s_m as abscissa and $G_m \tau_m$ as ordinate and then deducing remaining gains by extrapolation.

In the recent literature we found other methods of approximation, which - in our opinion - give results less accurate: see for example references 4 through 7.

List of symbols

a	defined by (1.14), non-dimensional variable
b_e, b_i	defined by (1.12) and (1.13), °C/(kg/sec)
c	specific heat, J/kg°C
$D(a)$	denominator of transfer functions, defined by (2.6) or (3.8)
$D^*(a_m)$	defined by (4.13)
F_e, F_i	defined by (2.4) and (2.5), °C
H	non-dimensional parameter, h_{io}/h_{eo}

h_e, (h_i)	heat exchange coefficient at the outer (inner) surface, W/m^2 °C
i	imaginary unit
J_o, J_1	Bessel's functions of first kind
k	thermal conductivity, W/ m °C
L(a)	defined by (4.11)
M	Biot's number for the outer surface, R_e h_{eo}/k
m_e, m_i	exponents of flow rates in convection coefficients (see (1.4) and (1.5)).
N_o, N_1	Bessel's functions of second kind
p	thermal power density, W/m^3
R	non-dimensional parameter, R_i/R_e
R_e, (R_i)	external (internal) radius of the cylinder, m
r	radial coordinate, m
s	Laplace's variable, sec^{-1}
T_c	cylinder's temperature, °C
T_{ce}, (T_{ci})	external (internal) surface temperature of the cylinder, °C
T_e, (T_i)	external (internal) fluid's or clad's temperature, °C
x	non-dimensional variable, a r/R_e
W_e, (W_i)	mass flow rate of external (internal) fluid, kg/sec
α	diffusivity, m^2/sec
ρ	density, Kg/m^3

References

1. P. GIORDANO, A. MATHIS, S. PETRARCA, "Critical comparison of different analog models for nuclear fuel rods", 4th International Analog Computation Meetings (Brighton, 14-18 Sept. 1964).

2. H.S. CARSLAW, J.C. JAEGER, "Conduction of heat in solids", 2nd ed., Oxford, Clarendon Press (1959).

3. S. PETRARCA, E. COSIMO, V. FEDELE, "Numerical programs for the thermal dynamics of a cylindrical nuclear fuel rod and of a heat exchanger tube", CNEN RT/ING(68) ... (number to be assigned).

4. J.M. GALLAGHER, D. HUNTER, "A study of complete loss of coolant flow in the Yankee Reactor", YAEC-83 (1958).

5. L. CALDAROLA, C. ZAFFIRO, "Transitori termici in simmetria cilindrica", Rendiconti A.E.I. 167 (1959).

6. M. IRIARTE, "An accurate transfer function for the dynamic analysis of temp ature and heat release in cylindrical fuel elements", Nucl. Sc. and Eng., 7, 26-32 (1960).

7. J.F. DE GREEF, "Cylindrical thermal equations for the analog computer", Proc. Int. Ass. Anal. Comput., vol. IX, 4, 195-197 (1967).

DETERMINING OF HEAT EXCHANGERS DYNAMICS BASING UPON THEIR STRUCTURAL CHARACTERISTICS

G. DAVOUST

Electricite de France

Directory of Studies and Research

Automation of Production Means Department

78 CHATOU - FRANCE

I - INTRODUCTION

Determining of a heat exchanger dynamics for pertubations with various origins needs mostly long and delicate experiments performed on the plant under different operation conditions. This identification problem, basing only upon the knowledge of the structural characteristics and static operation of the exchanger, has been treated by numerous authors [1, 2, 3, 4, 5, 6]. A majority of these researches are based on the theoretical method elaborated by Professor PROFOS [7, 8]. We propose here a study permitting to extend the domain of application and to make more easy the use of the above method.

II - HYPOTHESES

The method is not based on an accurate and complete mathematical model. It is designed to facilitate the control loops: setting, by a simple predetermining of proper dynamic characteristics of the exchanger. It can be applied to certain types of exchangers and is based on some simplyfying assumptions.

The exchangers under study are of parallel-tube, superheater or resuperheater type. Supposing that the steam flow and calorific flux are the same for all tubes, the overall exchanger's study reduces to one of the single-tube exchangers.

The perturbations arising in the system have low amplitudes and the system behavior in the vicinity of the operating point is supposed linear.

Heat transfer equations utilized are based on following assumptions:

1 - Metal conductance coefficient is infinite in transverse direction and is zero in axial direction.

2 - Steam conductance coefficent is infinite in axial direction and is zero in transverse direction.

3 - Metal-steam convection coefficient satisfies NUSSELT's law

4 - Steam variations do not affect the flue gases characteristics

5 - The specific heat and mass density of the steam are locally time-invariant, but vary along the exchanger.

6 - Geometric characteristics of the tubes and their nature as well are constant along the exchanger.

III - NOTATION

We'll denote. with the indices m, v, or f the following variables corresponding to metal, steam or flue-gases respectively:

- Cp - specific heat
- ρ - mass density
- S - cross section
- θ - temperature
- Q - mass flow

and

- π - tube interior perimeter
- h_{mv} - metal-steam convection coefficient

Qc - quantity of heat carried by flue gases /function of their flow and temperature/.

The index K indicates absolute temperatures, and the indices E, S - input, output respectively.

IV - PARTIAL DIFFERENTIAL EQUATION GOVERNING THE EXCHANGER DYNAMIC BEHAVIOR

Let us consider an elementary segment of the tube, having unit lenght and receiving a calorific flux q /fig.1/ in the unit time interval. This flux entering into the metal depends upon Q_c and θ_m

$$\frac{\Delta q}{q} = \frac{\Delta Q_c}{Q_c} - K \frac{\Delta \theta_m}{\theta_{mK}} \qquad /1/$$

On the basis of the assumptions presented above, various heat balances can be written:

- on the metal side:

$$q = C_{pm} \, \rho_m \, S_m \frac{\partial}{\partial t} /\theta_m/ + \pi h_{mv} /\theta_m - \theta_v/ \qquad /2/$$

- on the steam side:

$$\pi h_{mv} /\theta_m - \theta_v/ = S_v \frac{\partial}{\partial t} /C_{pv} \, \rho_v \, \theta_v/ + Q_v C_{pv} \frac{\partial}{\partial x} /\theta_v/ \qquad /3/$$

- the NUSSELT's law gives

$$\frac{\Delta h_{mv}}{h_{mv}} = m \frac{\Delta Q_v}{Q_v} \qquad /4/$$

After introduction of the parameters:

$$l = \frac{C_{pv} \, Q_v}{h_{mv} \, \pi} \qquad T_1 = \frac{C_{pv} \, \rho_v \, S_v}{\pi \, h_{mv}}$$

$$\alpha = \frac{C_{pm}\ \varrho_m\ S_m}{C_{pv}\ \varrho_v\ S_v} \qquad \varepsilon = \frac{K/\vartheta_m - \vartheta_v/}{\vartheta_{mK}}$$

and linearisation of the heat balance equations, the Laplace transform application when eliminating V_m leads to the equation:

$$\left[1 + \frac{l}{C_{pv}}\ \frac{\partial}{\partial x}/C_{pv}/ + p\,T_1 - \frac{1}{1+\varepsilon+p\alpha T_1}\right]\Delta\theta_v + l\frac{\partial}{\partial x}\ /\Delta\theta_v\ / =$$

$$\frac{1}{1+\varepsilon+p\alpha T_1} \cdot l\,\frac{\partial}{\partial x}\,/\theta_v/\left[\frac{\Delta Q_c}{Q_c} - /1 + /1-m/\varepsilon + /1-m/p\alpha\,T_1/\frac{\Delta Q_v}{Q_v}\right] \quad /5/$$

This partial differential equation, where derivatives are taken with respect to x and t, gives the steam temperature variation Q_v as a function of the steam flow and flue-gases heat variations, Q_v and Q_c respectively.

V - ANALYTIC INTEGRATION OF THE PARTIAL DIFFERENTIAL EQUATION

The purpose of the integration is to establish a formula for the exchanger output temperature variation as a function of the following principal quantities variations: steam temperature at the input, steam flow and the flue gases heat quantity. The formula:

$$\Delta\theta_s = F_{\theta_v}\ /p/\Delta\theta_E + F_{Qv}\ /p/\ \frac{\Delta Q_v}{Q_v} + F_{Qc}\ /p/\ \frac{\Delta Q_c}{Q_c} \qquad /6/$$

where $F_{\theta_v}\ /p/$, $F_{Qv}\ /p/$ and $F_{Qc}\ /p/$ represent three characteristic transfer functions of the exchanger.

The most widespread method of integration consists of integrating the first order equation with respect to x assuming in addition that:

- the quantity l is constant along the exchanger

- the terms containing the variable p are constant
- a tempe rature gradient $\frac{\partial\theta_v}{\partial x}$ is constant along the exchanger

By making use of these assumptions, the three transfer functions take forms:

$$F_{\theta_v}/p/ = e^{-f/p/}$$

$$F_{Qv}/p/ = g/p/\left[1 - F_{\theta_v}/p/\right] \qquad /7/$$

$$F_{Qc}/p/ = h/p/\left[1 - F_{\theta_v}/p/\right]$$

When the steam specific heat is practically constant /case of a resuperheater or of a small-lenght superheater/, the integration accuracy is conditioned on the last two assumptions only. This is not the case, however, when one considers a fragment of a superheater, which possesses a certain lenght and operates under pressure of 125 or 163 bars and temperature adjacent to 400 or 450^{o}C. The specific heat varies then in too large interval, as it is shown in fig.2, and so fails to satisfy the first of the last three assumptions.

Moreover, the experience shows that for such superheaters the static gain S of the transfer function $F_{Qv}/p/$ is often much higher than the unity. This implies the following: the explicit solutions proposed for the transfer functions $F_{Qv}/p/$ and F_{Qc} /p lead for these exchangers to a final decrease of the steam output temperature when the steam flow is decreased or when the quantity of the heat carried by flue-gases is increased, all oth factors remaining unchanged. This result does not conform to the actual experience, so one has to search for the cause in the assumptions relative to the integration and in the way the latter is accomplished.

The last assumption is out of the question. Indeed, a real exchanger analogy simulation based upon the initial differential equations has shown that the distribution along the exchanger of the heat flux q entering to the metal had only a minor effect on the exchanger responses to various perturbations. So, the first two assumptions remain only.

Certainly, it is possible to assume for C_{pv} a linear function of ϑ_v /hence it is function of x due to the third assumption/, on condition that the steam temperature increase $\Delta\vartheta_E^s$ between the input and the output is not too high. In this case, it is possible to accomplish a more rigorous integration, but the transfer functions obtained in this way are too complex, in contrary to our goal which is the simplicity of the consequent application.

Thus, the only way of integration that remains is a numerical one.

VI. - NUMERICAL INTEGRATION OF THE PARTIAL DIFFERENTIAL EQUATION

A. Method applied

An explicit method of integration i.e. the trapezoidal method[9] is applied. The integration is done by meshes, the /i,j/ node computation being done on the basis of the nodes /i-1,j/, /i-1,j-1/, /i,j-1/ and /i,j-2/ /fig.3/.

The derivatives are defined by the relations

$$\frac{\partial}{\partial t} s_{i,j} = \frac{s_{i,j} - s_{i,j-1}}{t_o}$$

$$\frac{\partial^2}{\partial t^2} s_{i,j} = \frac{s_{i,j} - 2s_{i,j-1} + s_{i,j-2}}{t_o^2}$$

$$\frac{\partial^2}{\partial x \, \partial t} s_{i,j} = \frac{s_{i,j} - s_{i,j-1} - s_{i-1,j} + s_{i-1,j-1}}{x_o \, t_o}$$

where x_o and t_o are x and t steps.

For convenience and for computation time economy, the integration has been first done in x, next in t.

Stability and acturacy studies have shown that the choice of 400 points in x and of 600 points in t /up to obtaining a steady state for step inputs/ is sufficient.

Partial differential equstion /5/ shows that the inputs Q_c and Q_v differs by the only term:

$$\left[1 + /1-m/\varepsilon + /1-m/ \, p \, \alpha \, T_1 \right]$$

Taking into account the low values of ε /approx. 0.02/ and of /1-m/ /ca 0.2/, when an additional impulse for step input is fed to Q_v, the time response is not modified in a significant manner. Hence, this term has been neglected, and the inputs Q_c and Q_v are no more distinguished /except sign, of course/.

The programming has been done on CDC 6600 computer. To obtain one time response, a time of 4.8 secs was necessary. The static gains were computed by an independent subroutine.

B. Method verification

In order to verify the partial differential equation validity, or the validity of the simplifying assumptions and integration method, series of experiments on the plant were performed with the superheaters of various characteristics and under various load conditions. The experimental responses have been plotted in BODE plane and have shown a good consistence of the theory and practice.

As an example, in figure 4 a shape of the frequency response of F_{Qv} /p/ for a superheater of 125 MW boiler turbine unit is shown. These results, as well as the study of a certain number of the exchangers have shown that the exchanger dynamics can be characterized mainly by the parameters:

$$\lambda' = \frac{L}{l/1+\mathcal{E}/}$$

called a reduced corrected lenght /where L is the exchanger lenght/

$$T'_m = \frac{\alpha T_1}{1+\mathcal{E}}$$

called a local corrected time constant.

Another more important parameters are:

- operating pressure
- steam mean temperature ϑ_1, equal to $\frac{\vartheta_{vE} + \vartheta_{vS}}{2}$
- steam temperature increase $\Delta\vartheta_E^S$ between the input and the output
- coefficient α, i.e. the ratio of metal - to steam calorific capacity by the lenght unit.

On account of application of the reduced parameters λ' and T'_m, the coefficient $\mathcal{E}$ does not affect the dynamics. On the contrary it preserves its influence on the transfer functions static gains, while the coefficient α is eliminated.

C. Systematic study

In view of fact that the steam characteristics variations along the exchanger have presented the main problem, three practical cases have been considered for french power plants, depending uniquely on the exchanger operating pressufe:

- 125 MW boiler-turbine unit's superheaters- pressure at the input = 125 bars
- 250 and 600 MW boiler-turbine unit's superheaters - pressure at the input = 163 bars
- the superheaters of all above units with the operating pressures varying from 10 to 40 bars, the range in which C_{pv} can be viewed as constant.

For the superheaters the law of the steam characteristics variations is based on the law of mean evolution of the pressure between the drum and the HP input, for a load close to 3/4 of the full load.

Mathematical relationships selected to represent C_{pv} and v are of type:

$$/\vartheta_v - \vartheta_{vo}/ \log Y = \text{const}$$

$$\text{or} \quad / x - x_o/ \log Y = \text{const}$$

due to the assumption concerning temperature gradient.

For each superheater we have selected 4 mean operating temperatures ϑ_i differing by 50 °C steps distributed uniformly between the saturation point and the final overheat temperature.

The exchangers segments under study correspond to the steam temperature increases $\Delta\theta_E^S$ equal to 50,100 and 150°C.

Selected time scale corresponds to a local time constant:

$T_m = \alpha T_1$ equal to 10 s.

The λ', α and ε parameters have been selected within their usual ranges:

- λ' from 3 to 20 with 10 values
- α from 5 to infinity with 9 values
- ε from 0,015 to 0,030 with 4 values.

The results required from the computer were:

- the static gain, computed by subroutine
- the exchanger dynamics characteristics for each input, computed by the main program.

For input temperature steps the response is aperiodic and well defined by an inflexion tangent and the time intervals T_u et T_a /fig.5/ that characterize a STREJC - type transfer transfer function:

$$\frac{S}{/1+T_p/^n} \qquad /8/$$

For the steps of the flue gases heat quantity , or of the steam flow, the time response has a unique form characterized by a maximal-slope tangent crossing the origin, and by a $\frac{TVA}{TVS}$ ratio /fig.6/.

VIII - <u>RESULTS</u>

As the principal goal was the simplicity of the method application, the graphical representation by nomograms has been provided. Hence, it has resulted in an a posteriori search of the laws relying various parameters of the exchanger and in their representation within accuracy of 1%. The goal has been achieved in all cases, and the accuracy with respect to the theoretical results calculated by the computer, mostly is best than 0.3%.

Turning to the global accuracy of the method with respect to the reality, the verification experiments undertaken on a 125 MW boiler-turbine unit guarantee an accuracy of 10% order of the dynamic product nT /order n multiplied by time constant T/ arising in a representation /8/.

A. Transfer functions static gain

For the transfer function F_{θ_v} /p/, the static gain can be represented by:

$$S = \frac{C_{pvE}}{C_{pvS}} e^{-\varepsilon\lambda'}$$

The term $e^{-\varepsilon\lambda'}$ is given directly by a nomogram.

For the transfer functions F_{Qc} /p/ and F_{Qv} /p/ of each of the three exchanger types, a nomogram has also been established. An example relative to 250 and 600 MW boiler-turbine unit is given in fig.7.

B. Transfer functions dynamics

1. Transfer function F_{θ_v} /p/.

The formula of STREJC /8/ has been preserved for this transfe function, the order n being non necessarily entire.

Such a representation is advantageous in the sense to enable the use of the records and nomograms already elaborated for the power plants control.

The results have shown that the steam characteristics had not any remarkable influence on this transfer function dynamics: two plots, valid for every exchanger type, give the reduced time constant T/T'_m and order n /fig.8/.

2. Transfer functions F_{Qc} /p/ and F_{Qv} /p/

The characteristic shape of the time response led us to an unique form:

$$F_{Qc,Qv} /p/ = \frac{G /1 + 0.2\ Tp/}{/1 + Tp/\ /1 + 0.5\ Tp/} \qquad /9/$$

This representation, temporarily satysfying, can also be done in the plane of BODE, as it is shown if fig.9.

Three nomograms, corresponding to each exchanger type, have been plotted, and supply the reduced time constant T/T'_m.

The figure 10 shows the nomogram for the exchangers of 125 MW boiler-turbine unit.

Remark

An examination of the nomograms representing the static gain and the transfer functions F_{Qc} /p/ and F_{Qv} /p/ dynamics shows that the assumptions on C_{pv} and ς_v steadiness, applicable to the resuperheaters, correspond only to the asymptotic solutions of plots established for the superheaters.

Thus, if a segment of superheater of 125 MW boiler-turbine-unit, with the following characteristics:

$\vartheta_1 = 430^oC$ $\quad \Delta\vartheta^S_E = 100$ degr. $\quad \lambda' = 8$ $\quad \alpha = 20$ $\quad \varepsilon = 0{,}0225$

is considered, then the exact solution yields:

$G = 115$ $\qquad T/T'_m = 5.37$

while the asymptotic solution /C_{pv} and $_v$ constant/ would give

$G = 89$ $\qquad T/T'_m = 4.27$

VIII. - PRACTICAL APPLICATION OF THE METHOD

The nomograms mentioned above were assembled into a document describing in detail the sequence of operations to obtain the exchanger transfer functions:

- collecting the structural and operating data of the exchanger /number of tubes, tube lenghts, diameters, metal kind, steam pressure, flow Q_V, ϑ_1, $\Delta\vartheta_E^S$ .../
- computing the characteristic parameters / λ', T'_m, α, ε /
- determining the transfer functions /their static and dynamic parameters/

To avoid any onerous intermediary stage, the exchanger parameters computations are facilitated due to the plots. One of them, established on the basis of a formula difficult to apply, is given as example in fig.11 and enables the computation of metal-steam exchange coefficient h_{mv}.

For example, the fig.12 represents a computed variation of the output temperature of 125 MW boiler-turbine unit's superheater due to a step change of steam flow, when the pressure controlled automatically.

IX - CONCLUSION

The present study has shown the influence of steam characteristics variations on the dynamics of modern power plant's superheaters.

Moreover, determining of the exchangers transfer functions has could be reduced to the use of a few plots. We think the simple representation of our study results will made more easy to set up the temperature control loops of the superheat and resuperheat, in existing plants as well as in the projected ones.

BIBLIOGRAPHY

1 - A. MARTIN - Etude de l'inertie thermique des échangeurs de chaleur Revue Universelle des Mines - june, 1959.

2 - J.FRENSCH - Dynamic Behaviour of stem superheaters. Proceedings of the IFAC Congress - Moscow 1960.

3 - ACKLIN et LAUBLI - Le calcul du comportement dynamique d'échangeurs de chaleur à l'aide de calculateurs analogiques - Revue Technique Sulzer - 4 - 1960

4 - BOSSUYT, COLASSIN et VAN KERCKHOVEN - Etude du comportement transitoire des échangeurs à surface dans les chaudières à vapeur
Revue A - IV - 2 - 1962

5 - F.J. - STERMOLE et M.A. - LARSON - The dynamics of flow forced distributed parameters heat exchangers. A.I.Ch. E.Journal sept. 1964

6 - R.ISERMANN - Le fonctionnement transitoire des surchauffers - Traduction EDF n° 1427 d'après Fortschriftberichte VDI Zeitschrift VI - 4, march, 1965

7 - P. PROFOS - La dynamique du réglage dans les surchauffeurs. Revue Technique Sulzer - 4 - 1958

8 - P. PROFOS - Die Regelung von Dampfanlagen - Springer Verlag - 1962

9 - M. SALVADORI et M. BARON - Numerical Methods in Engineering Pratice Hall Inc. 1961

10 - R. CHAUSSARD, J. GRAUVOGEL et G. DAVOUST - Mise en oeuvre rationnelle des régulations d'une centrale thermique - Proceedings of IFAC Congress, London 1966.

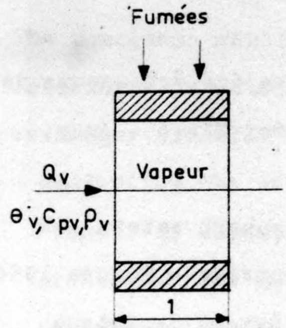

Figure 1

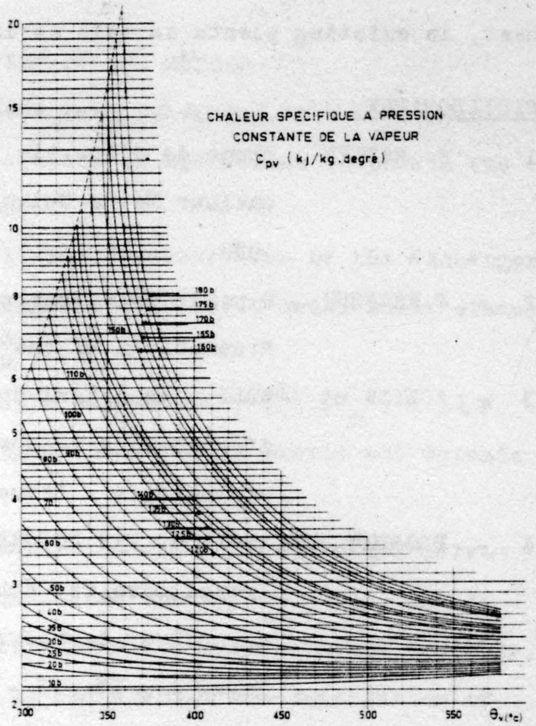

Figure 2

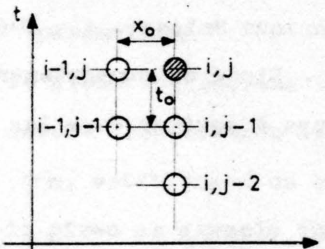

Figure 3

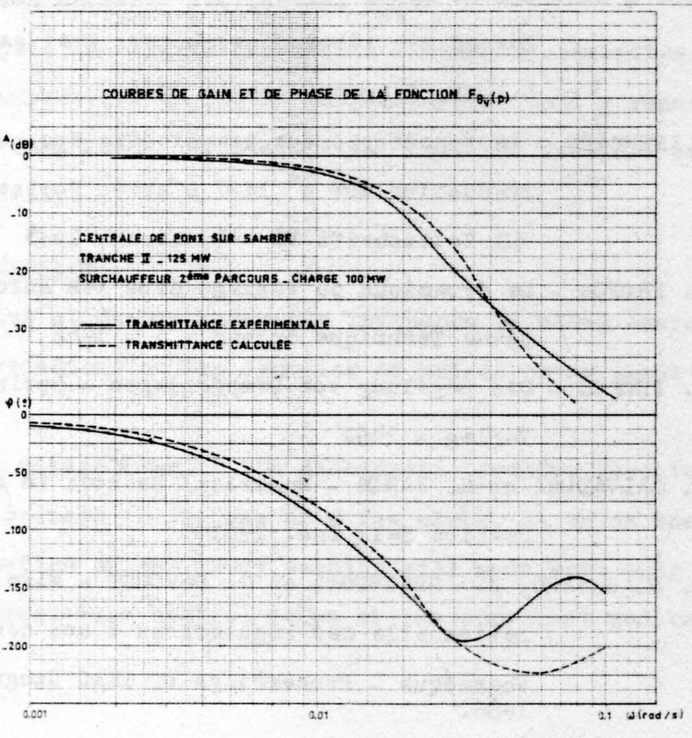

Figure 4

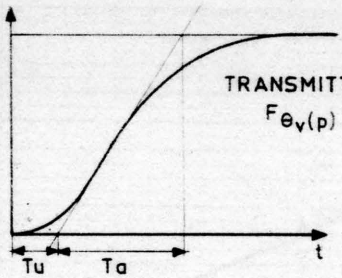

Figure 5

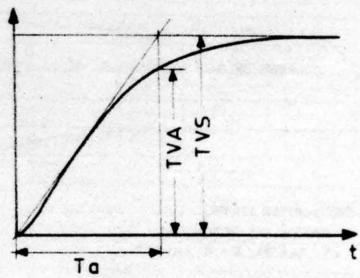

Figure 6

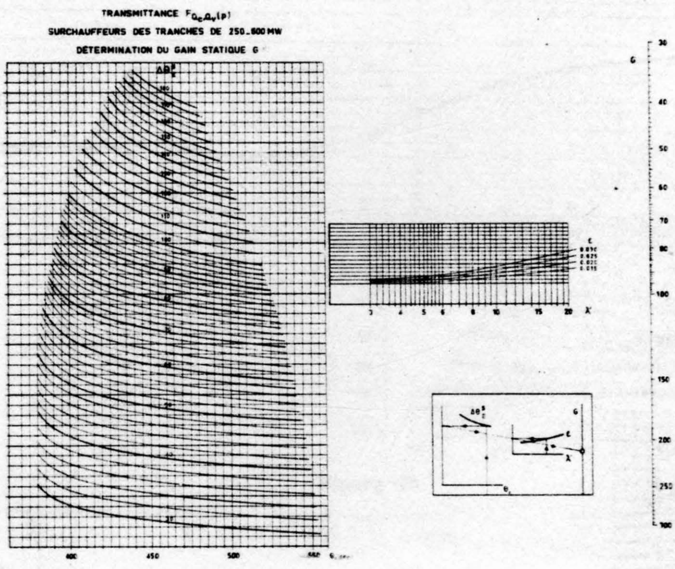

Figure 7

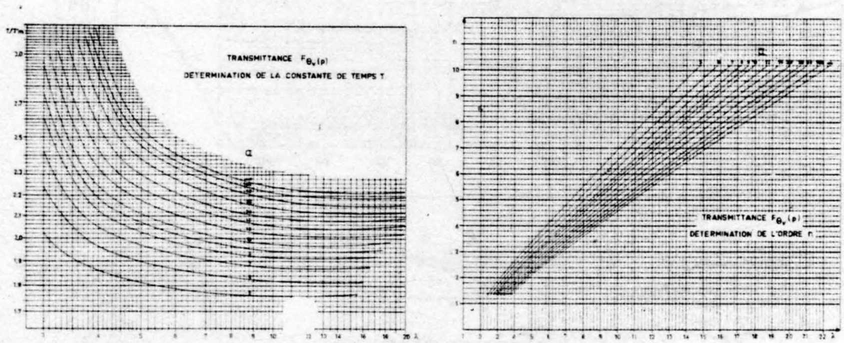

Figure 8

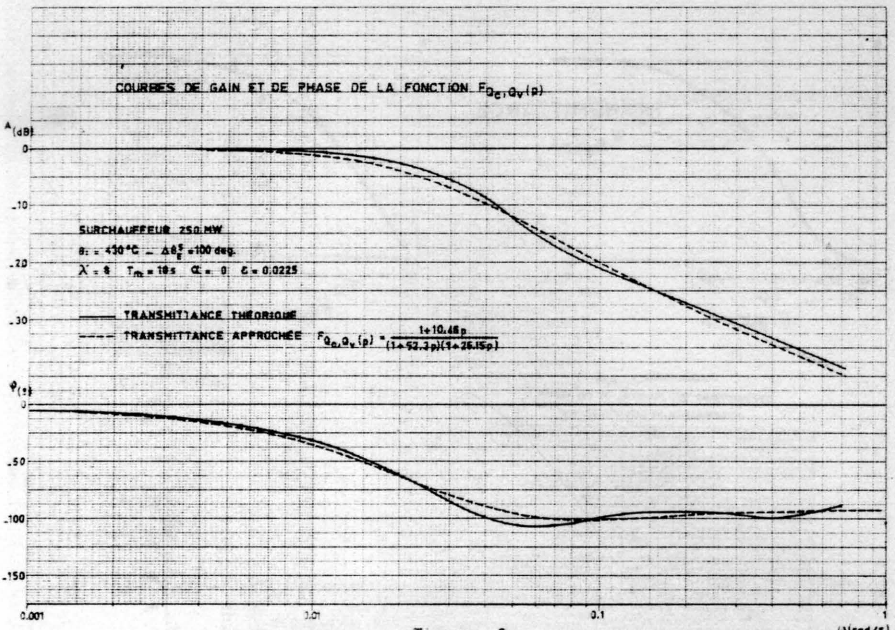

Figure 9

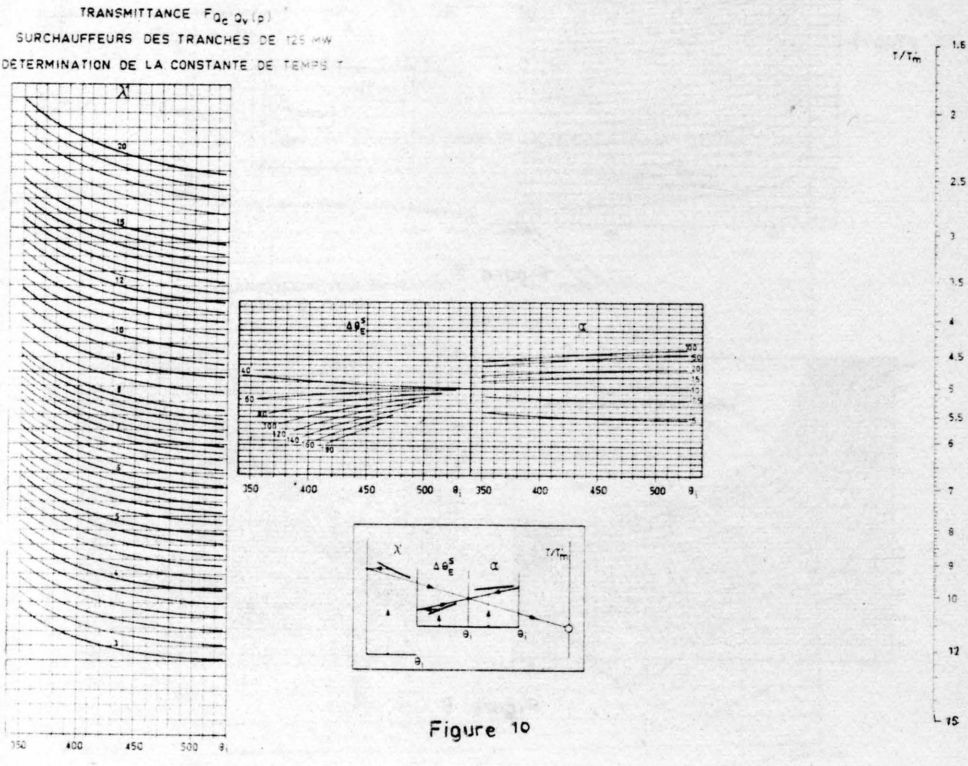

Figure 10

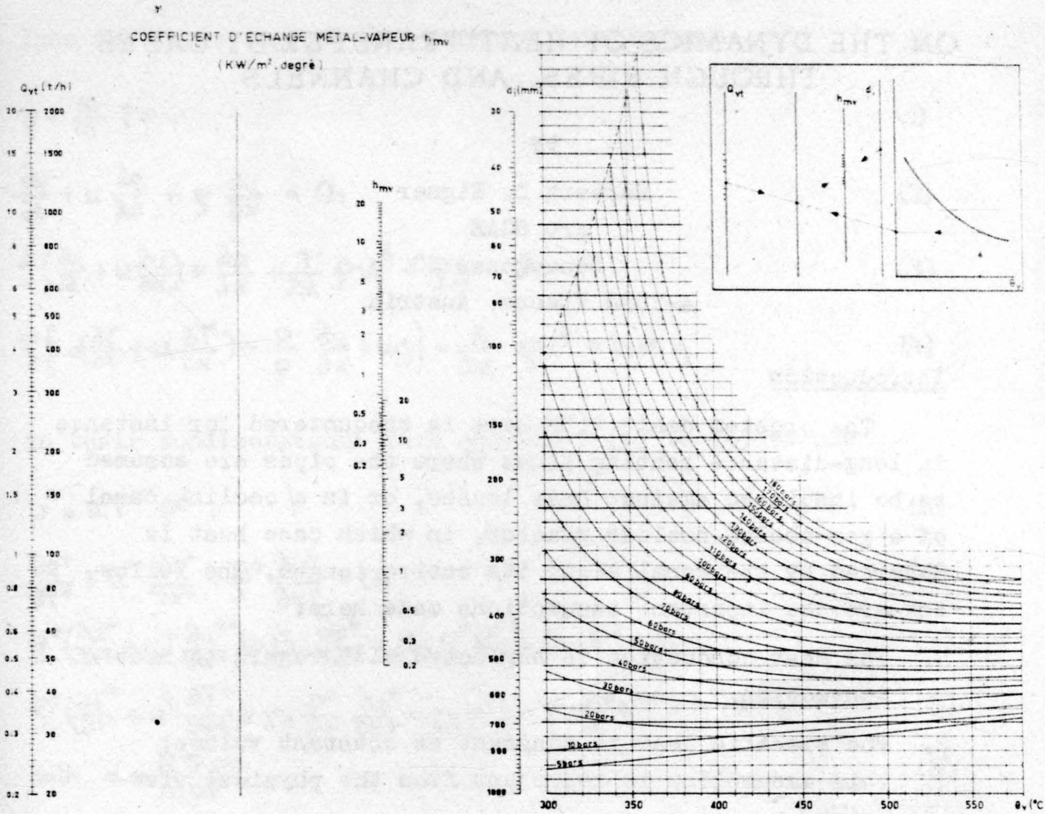

Figure 11

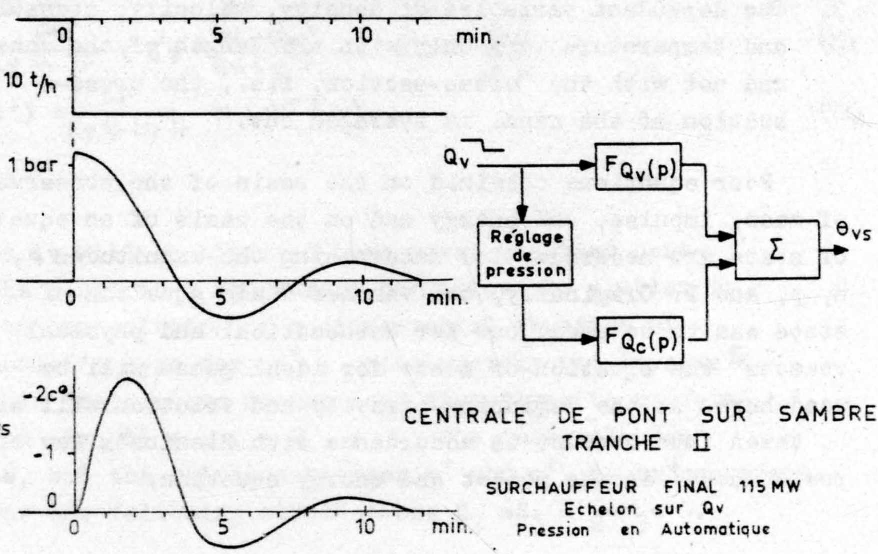

Figure 12

ON THE DYNAMICS OF HEAT TRANSFER BY GASES THROUGH PIPES AND CHANNELS

by

Herbert D. Eigner
c/o SGAE
Lenaugasse 10
A-1082 Vienna, Austria

Introduction

The problem dealt with here is encountered for instance in long-distance heating lines where the pipes are assumed to be insulated against heat losses, or in a cooling canal of a gas-cooled nuclear reactor, in which case heat is absorbed by the canal along its entire length. The following are the important assumptions made here:

1. The heat conduction is neglected with regard to heat convection.
2. The specific heat is constant at constant volume; this assumption is important from the physical viewpoint.[1]
3. The dependent variables of density, velocity, pressure, and temperature vary only with the length of the canal and not with the cross-section, i.e., the cross-section of the canal is averaged out.

Four equations obtained on the basis of the conservation of mass, impulse, and energy and on the basis of an equation of state are necessary for determining the magnitudes ρ, u, p, and T. Originally, the Van der Waals equation of state was to be used, but for mathematical and physical reasons[2] the equation of state for ideal gases will be used here. At the beginning, gravity and friction will also be taken into account in accordance with Blasius's law of resistance [3] in the moment and energy equation.

Thus the following set of equations is obtained:

$$p = \frac{R}{m} T \varrho , \tag{1}$$

$$\frac{\partial \varrho}{\partial t} + u \frac{\partial \varrho}{\partial x} + \varrho \frac{\partial u}{\partial x} = 0 , \tag{2}$$

$$\varrho \left(\frac{\partial u}{\partial t} + u \frac{\partial u}{\partial x} \right) + \frac{\partial p}{\partial x} + \frac{\lambda}{2d} \varrho u^2 + \varrho g = 0 , \tag{3}$$

$$\varrho \left[c_\varrho \left(\frac{\partial T}{\partial t} + u \frac{\partial T}{\partial x} \right) + \frac{p}{\varrho} \frac{\partial u}{\partial x} + u g \right] = \frac{\lambda}{2d} \varrho u^3 + h(x) ; \tag{4}$$

in their nondimensional form equations (1) to (4) become

$$p^+ = \alpha T^+ \varrho^+ , \tag{5}$$

$$\frac{\partial \varrho^+}{\partial t^+} + u^+ \frac{\partial \varrho^+}{\partial x^+} + \varrho^+ \frac{\partial u^+}{\partial x^+} = 0 , \tag{6}$$

$$\varrho^+ \left(\frac{\partial u^+}{\partial t^+} + u^+ \frac{\partial u^+}{\partial x^+} \right) + \beta_1 \frac{\partial p^+}{\partial x^+} + \beta_2 \varrho^+ u^{+2} + \beta_3 \varrho^+ = 0 , \tag{7}$$

$$\varrho^+ \left(\frac{\partial T^+}{\partial t^+} + u^+ \frac{\partial T^+}{\partial x^+} + \gamma_1 \frac{p^+}{\varrho^+} \frac{\partial u^+}{\partial x^+} + \gamma_3 u^+ \right) = \gamma_2 \varrho^+ u^{+3} + h^+(x^+) \tag{8}$$

$$\text{with } \alpha = \frac{R T_r \varrho_r}{m p_r} , \tag{9}$$

$$\beta_1 = \frac{p_r}{\varrho_r U_r^2} , \quad \beta_2 = \frac{\lambda L_r}{2d} , \quad \beta_3 = \frac{g L_r}{U_r^2} , \tag{10}$$

$$\gamma_1 = \frac{p_r}{c_\varrho \varrho_r T_r} , \quad \gamma_2 = \frac{\lambda L_r U_r^2}{2d \, c_\varrho T_r} , \quad \gamma_3 = \frac{g L_r}{c_\varrho T_r} , \tag{11}$$

$$h^+(x^+) = \frac{L_r}{c_\varrho \varrho_r U_r T_r} h(x^+ L_r) . \tag{12}$$

Thus it will be observed that given constant heating of the canal in a stationary condition the problem is reduced to the solution of a differential equation of the Bernoulli's type for u^+ ; unfortunately the integrals obtained in the process do not lend themselves to uniform evaluation for $\beta_2 = \gamma_2 = 0$ the integrals are evaluable, but the relation between x^+ and u^+ is transcendent. Throughout the following elucidations $\beta_2 = \beta_3 = {}_2 = {}_3 = 0$.

The Stationary Case with Arbitrary Heating

It follows from (6)

$$\rho^+ u^+ = A_1 , \tag{13}$$

from (7)

$$A_1 u^+ + \beta_1 p^+ = A_2 , \tag{14}$$

from (5)

$$\alpha \beta_1 A_1 T^+ = u^+ (A_2 - A_1 u^+) \tag{15}$$

and from (8)

$$u^{+2} - 2\delta_1 u^+ + \delta_2 = 0 , \tag{16}$$

$$_1u_2^+ = \delta_1 \pm \sqrt{\delta_1^2 - \delta_a} \tag{17}$$

with

$$\delta_1 = \frac{(1+\alpha\gamma_1^+) A_2}{(2+\alpha\gamma_1^+) A_1} , \tag{18}$$

$$\delta_2 = \frac{2\alpha\beta_1 (I + A_3)}{(2+\alpha\gamma_1^+) A_1} , \tag{19}$$

$$I = \int_0^{x^+} h^+ (x_0^+) d x_0^+ ; \tag{20}$$

(16) will be of the fourth order for a Van der Waals gas. The integration constants A_i (i = 1, 2, 3) are determined by means of the inlet magnitudes p_e^+, T_e^+, and w_e^+, they are

$$A_1 = w_e^+ , \tag{21}$$

$$A_2 = \frac{1}{p_e^+} (\alpha w_e^{+2} T_e^+ + \beta_1 p_e^{+2}) , \tag{22}$$

$$A_3 = w_e^+ T_e^+ \left[1 + \frac{\alpha\gamma_1^+}{2\beta_1} \frac{1}{p_e^{2+}} (\alpha w_e^{+2} T_e^+ + 2\beta_1 p_e^{+2})\right] ; \tag{23}$$

furthermore

$$c_\varrho = \frac{f}{2}\,\frac{R}{m}, \tag{24}$$

$$\alpha\gamma_1 = \frac{2}{f}, \tag{25}$$

f signifying the number of degrees of freedon of the gas molecules[5].

The Linearised Dynamic Case with Arbitrary Heating

The following linearised dynamic equations are derived from equations (5) to (8)

$$p_a^+ = \alpha(\varrho_a^+ T^+ + T_a^+ \varrho^+), \tag{26}$$

$$\frac{\partial \varrho_a^+}{\partial t^+} + u^+ \frac{\partial \varrho_a^+}{\partial x^+} + u_a^+ \frac{\partial \varrho^+}{\partial x^+} + \varrho_a^+ \frac{\partial u^+}{\partial x^+} + \varrho^+ \frac{\partial u_a^+}{\partial x^+} = 0, \tag{27}$$

$$\varrho^+\left(\frac{\partial u_a^+}{\partial t^+} + u^+ \frac{\partial u_a^+}{\partial x^+} + u_a^+ \frac{\partial u^+}{\partial x^+}\right) + u^+ \frac{\partial u^+}{\partial x^+}\varrho_a^+ + \beta_1 \frac{\partial p_a^+}{\partial x^+} = 0, \tag{28}$$

$$\varrho^+\left(\frac{\partial T_a^+}{\partial t^+} + u^+ \frac{\partial T_a^+}{\partial x^+} + u_a^+ \frac{\partial T^+}{\partial x^+}\right) + u^+ \frac{\partial T^+}{\partial x^+}\varrho_a^+ + \gamma_1\left(p^+ \frac{\partial u_a^+}{\partial x^+} + p_a^+ \frac{\partial u^+}{\partial x^+}\right) = h_a^+(x^+); \tag{29}$$

according to the Laplace transformation with regard to t^+ with

$$\mathcal{L}\varrho_a^+ = R^+, \tag{30}$$

$$\mathcal{L}u_a^+ = U^+, \tag{31}$$

$$\mathcal{L}p_a^+ = P^+, \tag{32}$$

$$\mathcal{L}T_a^+ = \vartheta^+, \tag{33}$$

$$\mathcal{L}h_a^+ = H^+ \tag{34}$$

from (26) to (29)

$$p^{+} = \alpha(T^{+}R^{+} + \varrho^{+}\vartheta^{+}) \,, \tag{35}$$

$$u^{+}R^{+\prime} + (u^{+\prime} + s)R^{+} + \varrho^{+}U^{+\prime} + \varrho^{+\prime}U^{+} = \varrho^{+}, \tag{36}$$

$$u^{+}u^{+\prime}R^{+} + A_1U^{+\prime} + \varrho^{+}(u^{+\prime} + s)U^{+} + \beta_1 p^{+\prime} = A_1, \tag{37}$$

$$u^{+}T^{+\prime}R^{+} + A_1\vartheta^{+\prime} + \varrho^{+}s\vartheta^{+} + \gamma_1 p^{+}U^{+\prime} + \varrho^{+}T^{+\prime}U^{+} + \gamma_1 u^{+\prime}P^{+} = \varrho^{+}T^{+} + H^{+} \tag{38}$$

with

$$\frac{\partial}{\partial x^{+}} =$$

By eliminating p^{+} from (37) and (38) by means of (35)

$$\alpha\beta_1(\varrho^{+} + \vartheta^{+\prime} + \varrho^{+\prime}\vartheta^{+}) = -\alpha\beta_1 T^{+}R^{+\prime} - (\alpha\beta_1 T^{+\prime} + u^{+}u^{+\prime})R^{+} - A_1U^{+\prime} - \varrho^{+}(u^{+\prime} + s)U^{+} + A_1, \tag{39}$$

$$A_1\vartheta^{+\prime} + \varrho^{+}(\alpha\gamma_1 u^{+\prime} + s)\vartheta = (\alpha\gamma_1 u^{+\prime}T^{+} + u^{+}T^{+\prime})R^{+} - \gamma_1 p^{+}U^{+\prime} - \varrho^{+}T^{+\prime}U^{+} + \varrho^{+}T^{+} + H^{+}; \tag{40}$$

from (39) and (40) we derive

$$\vartheta^{+\prime} = \frac{\Delta_1}{\Delta_0} \,, \tag{41}$$

$$\vartheta^{+} = \frac{\Delta_a}{\Delta_0} \tag{42}$$

with

$$\Delta_0 = \alpha\beta_1 A_1^2 \, \frac{u^{+\prime}(1 + \alpha\gamma_1) + s}{u^{+2}} \,, \tag{43}$$

$$\Delta_1 = -\frac{A_1}{u^{+}}\left(f_1 R^{+\prime} + f_2 R^{+} + f_3 U^{+\prime} + f_4 U^{+} + f_5\right), \tag{44}$$

$$\Delta_2 = -\left(g_1 R^{+\prime} + g_2 R^{+} + g_3 U^{+\prime} + g_4 U^{+} + g_5\right), \tag{45}$$

$$f_1 = \alpha\beta_1 T^{+}(\alpha\gamma_1 u^{+\prime} + s) \,, \tag{46}$$

$$f_2 = \frac{\alpha\beta_1}{A_1}\,\frac{u^{+\prime}}{u^{+}}\left[A_1 T^{+}(\alpha\gamma_1 u^{+\prime} + \ \ ) + h^{+}u^{+}\right], \tag{47}$$

$$f_3 = \frac{A_1}{u^{+2}}\left[u^{+2}(\alpha\gamma_1 u^{+\prime} + s) + \alpha^2\beta_1\gamma_1 u^{+\prime}T^{+}\right], \tag{48}$$

$$f_4 = \frac{A_1}{u^{+2}}\left[u^+(u^{+\prime}+s)(\alpha\gamma_1 u^{+\prime}+s)+\alpha\beta_1 u^{+\prime}T^{+\prime}\right], \tag{49}$$

$$f_5 = -A_1(\alpha\gamma_1 u^{+\prime}+s)-\alpha\beta_1\frac{u^{+\prime}}{u^{+2}}(A_1T^+ + u^+H^+), \tag{50}$$

$$g_1 = -\alpha\beta_1 A_1 T^+, \tag{51}$$

$$g_2 = \frac{\alpha\beta_1}{\varrho^+}(\varrho^+h^+ + A_1\varrho^{+\prime}T^+), \tag{52}$$

$$g_3 = \alpha^2\beta_1\gamma_1\varrho^{+2}T^+ - A_1^2, \tag{53}$$

$$g_4 = \varrho^+\left[\alpha\beta_1\varrho^+T^{+\prime} - A_1(u^{+\prime}+s)\right], \tag{54}$$

$$g_5 = -\alpha\beta_1\varrho^+(\varrho^+T^+ + H^+) + A_1^2; \tag{55}$$

from

$$\left(\frac{\Delta_2}{\Delta_0}\right)' = \frac{\Delta_1}{\Delta_0}$$

we obtain

$$k_1R^{+\prime\prime} + k_2R^{+\prime} + k_3R^+ = k_4U^{+\prime\prime} + k_5U^{+\prime} + k_6U^+ + k_7 \tag{56}$$

with

$$k_1 = -\alpha\beta_1A_1T^+\left[u^{+\prime}(1+\alpha\gamma_1)+s\right], \tag{57}$$

$$k_2 = \frac{\alpha\beta_1}{u^+}\left\{h^+u^+ - A_1T^+\left[u^{+\prime}(-1+\alpha\gamma_1)+s\right] - A_1u^+T^{+\prime}\right\}\left[u^{+\prime}(1+\alpha\gamma_1)+s\right] + \\ +\alpha\beta_1(1+\alpha\gamma_1)A_1T^+u^{+\prime\prime}, \tag{58}$$

$$k_3 = \frac{\alpha\beta_1}{u^{+2}}\left\{(h^{+\prime}u^+ + h^+u^{+\prime})u^+ - A_1(u^{+\prime}T^+ + u^{+\prime}T^{+\prime})u^+ - A_1T^+u^{+\prime}\left[u^{+\prime}(1+\alpha\gamma_1)+s\right]\right\}\cdot \\ \cdot\left[u^+(1+\alpha\gamma_1)+s\right] - \frac{\alpha\beta_1}{u^+}(h^+u^+ - A_1T^+u^{+\prime})(1+\alpha\gamma_1)u^{+\prime\prime}, \tag{59}$$

$$k_4 = \frac{A_1^2}{u^{+2}}(u^{+2} - \alpha^2\beta_1\gamma_1T^+)\left[u^{+\prime}(1+\alpha\gamma_1)+s\right], \tag{60}$$

$$k_5 = -\frac{A_1^2}{u^{+3}}\left\{\alpha\beta_1\left[(1+\alpha\gamma_1)u^+T^{+\prime} - \alpha\gamma_1u^{+\prime}T^+\right] - u^{+2}\left[u^{+\prime}(3+\alpha\gamma_1)+2s\right]\right\}\cdot \\ \cdot\left[u^{+\prime}(1+\alpha\gamma_1)+s\right] + (1+\alpha\gamma_1)A_1^2(\alpha^2\beta_1\gamma_1T^+ - u^{+2})\frac{u^{+\prime\prime}}{u^{+2}}, \tag{61}$$

$$k_6 = \frac{A_1^2}{u^{+3}}\left\{u^+(u^{+\prime}+s)\left[u^{+\prime}(1+\alpha\gamma_1)+s\right] + \alpha\beta_1(u^{+\prime}T^{+\prime} - u^+T^{+\prime\prime}) + u^{+2}u^{+\prime\prime}\right\}\cdot \\ \cdot\left[u^{+\prime}(1+\alpha\gamma_1)+s\right] + (1+\alpha\gamma_1)A_1^2\left[\alpha\beta_1T^{+\prime} - u^+(u^{+\prime}+s)\right]\frac{u^{+\prime\prime}}{u^{+2}}, \tag{62}$$

$$k_7 = \frac{A_1}{u^{+2}}\left\{-A_1u^+\left[u^{+\prime}(1+\alpha\gamma_1)+s\right] + \frac{\alpha\beta_1A_1}{u^+}(u^+T^{+\prime} - u^{+\prime}T^+) + \alpha\beta_1u^+H^{+\prime}\right\}\cdot \\ \cdot\left[u^{+\prime}(1+\alpha\gamma_1)+s\right] + (1+\alpha\gamma_1)A_1\left[A_1u^{+2} - \alpha\beta_1(A_1T^+ + u^+H^+)\right]\frac{u^{+\prime\prime}}{u^{+2}}; \tag{63}$$

from (56), (36) and its derivation to x^+ we obtain

$$R^{+} = \frac{\Delta_3^{I}}{\Delta_0^{I}}, \tag{64}$$

$$R^{+\prime} = \frac{\Delta_2^{I}}{\Delta_0^{I}}, \tag{65}$$

$$R^{+\prime\prime} = \frac{\Delta_1^{I}}{\Delta_0^{I}}$$

with

$$\Delta_3^{I} = l_1 U^{+\prime\prime} + l_2 U^{+\prime} + l_3 U^{+} + l_4 , \tag{66}$$

$$\Delta_2^{I} = n_1 U^{+\prime\prime} + n_2 U^{+\prime} + n_3 U^{+} + n_4 , \tag{67}$$

$$\Delta_0^{I} = k_1 \left[u^+ u^{+\prime\prime} - (u^{+\prime}+s)(2u^{+\prime}+s)\right] + u^+\left[k_2(u^{+\prime}+s) - k_3 u^+\right], \tag{68}$$

$$l_1 = -u^+(\varrho^+ k_1 + u^+ k_4), \tag{69}$$

$$l_2 = -u^+(2\varrho^+ k_1 + u^+ k_5) + \varrho^+(2u^{+\prime} + s - u^+ k_2), \tag{70}$$

$$l_3 = -u^+(\varrho^{+\prime\prime} k_1 + u^+ k_6) + \varrho^{+\prime}(2u^{+\prime} + s - u^+ k_2), \tag{71}$$

$$l_4 = +u^+(\varrho^{+\prime} k_1 - u^+ k_7) - \varrho^+(2u^{+\prime} + s - u^+ k_2), \tag{72}$$

$$n_1 = (u^+ k_4 + \varrho^+ k_1)(u^{+\prime} + s), \tag{73}$$

$$n_2 = (u^+ k_5 + 2\varrho^{+\prime} k_1)(u^{+\prime} + s) + \varrho^+(u^+ k_3 - u^{+\prime\prime} k_1), \tag{74}$$

$$n_3 = (u^+ k_6 + \varrho^{+\prime\prime} k_1)(u^{+\prime} + s) + \varrho^{+\prime}(u^+ k_3 - u^{+\prime\prime} k_1), \tag{75}$$

$$n_4 = (u^+ k_7 - \varrho^{+\prime} k_1)(u^{+\prime} + s) - \varrho^+(u^+ k_3 - u^{+\prime\prime} k_1); \tag{76}$$

from

$$\left(\frac{\Delta_3^{I}}{\Delta_0^{I}}\right)' = \frac{\Delta_2^{I}}{\Delta_0^{I}}$$

we finally obtain

$$U^{+'''} + v_1 U^{+''} + v_2 U^{+'} + v_3 U^{+} = v_4 \tag{77}$$

with

$$v_1 = \frac{l_1' + l_2 - n_1}{l_1} - \frac{\Delta_o^{I'}}{\Delta_o^{I}}, \tag{78}$$

$$v_2 = \frac{l_2' + l_3 - n_2}{l_1} - \frac{\Delta_o^{I'}}{\Delta_o^{I}} \frac{l_2}{l_1}, \tag{79}$$

$$v_3 = \frac{l_3' - n_3}{l_1} - \frac{\Delta_o^{I'}}{\Delta_o^{I}} \frac{l_3}{l_1}, \tag{80}$$

$$v_4 = \frac{-l_4' + n_4}{l_1} - \frac{\Delta_o^{I'}}{\Delta_o^{I}} \frac{l_4}{l_1}, \tag{81}$$

from (77), (64), (42), and (35) we obtain in that sequence U^+, R^+, ϑ^+, and p^+.

The Linearised Dynamic Case with Constant Heating

We have

$$h^{+'} = H^{+'} = 0; \tag{82}$$

we now introduce a new independent variable by means of

$$y^+ = x^+ + \delta_3, \quad z^{+2} = 2y^+ \tag{83}$$

and (17) acquires the form

$$u^+ = \delta_1 + \delta_4 z^+ \tag{84}$$

with

$$\delta_3 h^+ = A_3 - \frac{(2+\alpha\gamma_1)A_1\delta_1^2}{2\alpha\beta_1}\,, \tag{85}$$

$$\delta_4 = j\sqrt{\frac{\alpha\beta_1 h^+}{(2+\alpha\gamma_1)A_1}}\,. \tag{86}$$

Moreover, the reference length L_r in x^+ is chosen so that

$$|2(x^+ + \delta_3)| \leq 10^{-2} \tag{87}$$

and the calculation is continued as the first approximation for small z^+. We then obtain, since related back to (17), $\delta_4 z^+ < \delta_1$ - which is also binding

$$g_1 = \varepsilon_1 = \delta_1(A_1\delta_1 - A_2)\,, \tag{88}$$

$$g_2 = \frac{\varepsilon_2}{z^+}\,,\quad \varepsilon_2 = \delta_4(A_1\delta_1 - A_2)\,, \tag{89}$$

$$g_3 = \varepsilon_3 = \frac{A_1}{\delta_1}\left[\alpha\gamma_1 A_2 - (1+\alpha\gamma_1)A_1\delta_1\right], \tag{90}$$

$$g_4 = \frac{\varepsilon_4}{z^+}\,,\quad \varepsilon_4 = \frac{\delta_4}{\delta_1^2}(A_2 - 3A_1\delta_1)A_1\,, \tag{91}$$

$$g_5 = \varepsilon_5 = \frac{A_1}{\delta_1}(2A_1\delta_1 - A_2 - \alpha\beta_1 H^+)\,, \tag{92}$$

$$\Delta_0 = \frac{\varepsilon_6}{Z^+} , \quad \varepsilon_6 = \frac{\delta_4}{\delta_1^2} A_1^2 \alpha \beta_1 (1 + \alpha \gamma_1) , \tag{93}$$

$$\Delta_0^I = \frac{\varepsilon_9}{Z^{+4}} , \quad \varepsilon_9 = -2 \delta_1^3 \delta_4^2 A_1 , \tag{94}$$

$$L_1 = \frac{\vartheta_1}{Z^+} , \quad \vartheta_1 = -2 \delta_1^2 \delta_4 A_1^2 , \tag{95}$$

$$L_2 = \frac{\vartheta_2}{Z^{+2}} , \quad \vartheta_2 = (1+\alpha\gamma_1)(2+\alpha\gamma_1)\delta_4^2 (A_1 \delta_1 + 2 A_2) ,$$

$$L_3 = \frac{\vartheta_3}{Z^{+4}} , \quad \vartheta_3 = -2 \delta_1 \delta_4^2 A_1^2 , \tag{97}$$

$$L_4 = \frac{\vartheta_4}{Z^{+3}} , \quad \vartheta_4 = -(1+\alpha\gamma_1)\delta_1 \delta_4 (2A_2 - 3A_1\delta_1 + \alpha\beta_1 H^+) A_1 , \tag{98}$$

$$n_1 = \frac{\eta_1}{Z^{+2}} , \quad \eta_1 = -\vartheta_3 , \tag{99}$$

$$n_2 = \frac{\eta_2}{Z^{+4}} , \quad \eta_2 = \eta_1 , \tag{100}$$

$$n_3 = \frac{\eta_3}{Z^{+4}} , \quad \eta_3 = \delta_4^2 A_1^2 \left\{ \frac{\delta_4^2}{\delta_1} \left[(5+\alpha\gamma_1)(2+\alpha\gamma_1) - 4(1+\alpha\gamma_1) \right] + \alpha\gamma_1 \left[5 - (2+\alpha\gamma_1) \frac{\beta_1 h^+}{\gamma_1 A_2} \right] \right\} , \tag{101}$$

$$n_4 = \frac{\eta_4}{Z^{+4}} , \quad \eta_4 = -(1+\alpha\gamma_1)\delta_4^2 (A_1\delta_1 - \alpha\beta_1 H^+) A_1 , \tag{102}$$

$$\dddot{U}^+ + a_1 \ddot{U}^+ + a_2 \dot{U}^+ + a_3 U^+ = a_4 , \tag{103}$$

$$a_1 = V_1 Z^+ - V_1 + \frac{3}{Z^{+2}} = 0 , \tag{104}$$

$$a_2 = V_2 Z^{+2} - V_1 + \frac{3}{Z^{+2}} = 2 \frac{\vartheta_2 + \vartheta_3}{\vartheta_1} \frac{1}{Z^+} , \tag{105}$$

$$a_3 = V_3 Z^{+3} = 0 , \tag{106}$$

$$a_4 = V_4 Z^{+3} = - \frac{\vartheta_4}{\vartheta_1} \frac{1}{Z^+} \tag{107}$$

with

$$\frac{\partial}{\partial z^+} =$$

The solution of (103) to (107) is [6]

$$U^+ = z^+\left[B_1 J_2\left(2\sqrt{2\frac{\varphi_2+\varphi_3}{\varphi_1}}\sqrt{z^+}\right) + B_2 N_2\left(2\sqrt{2\frac{\varphi_3+\varphi_3}{\varphi_1}}\sqrt{z^+}\right) - \frac{\varphi_4}{2(\varphi_2+\varphi_3)} + B_3 \qquad (108)$$

with the integration constants B_i (i = 1, 2, 3). It is noteworthy that the Laplace argument s in (108) finds admission only via ξ_4. Moreover, we obtain from (64), (42) and (35) in that order

$$R^+ = \frac{1}{\varepsilon_q}\left(\varphi_1 z^+ \ddot{U}^+ + (\varphi_2 z^+ - \varphi_1)\dot{U}^+ + \varphi_3 U^+ + \varphi_4 z^+\right), \qquad (109)$$

$$\vartheta^+ = -\frac{1}{\varepsilon_6\,\varepsilon_q}\Big\{(\varepsilon_1\eta_1 + \varepsilon_2\varphi_1)z^+\ddot{U}^+ + \left[\varepsilon_2(\varphi_2 z^+ - \varphi_1) + \varepsilon_3\varepsilon_q\right]\dot{U}^+ +$$

$$+ (\varepsilon_1\eta_3 z^+ + \varepsilon_2\varphi_3 + \varepsilon_4\varepsilon_q)U^+ + (\varepsilon_1\eta_4 + \varepsilon_2\varphi_4 + \varepsilon_5\varepsilon_q)z^+\Big\} \qquad (110)$$

$$P^+ = \frac{1}{\beta_1 A_1}\left[-\varepsilon_1 + \delta_4(A_2 - 2A_1\delta_1)z^+\right]R^+ + \frac{A_1\alpha}{\delta_1}\left(1 - \frac{\delta_4}{\delta_1}z^+\right)\vartheta^+ \qquad (111)$$

with

$$\dot{U}^+ = \sqrt{2\frac{\varphi_2+\varphi_3}{\varphi_1}}\sqrt{z^+}\left[B_1 J_1\left(2\sqrt{2\frac{\varphi_2+\varphi_3}{\varphi_1}}\sqrt{z^+}\right) + B_2 N_1\left(2\sqrt{\frac{\varphi_2+\varphi_3}{\varphi_1}}\sqrt{z^+}\right)\right] - \frac{\varphi_4}{2(\varphi_2+\varphi_3)}, \qquad (112)$$

$$\ddot{U}^+ = 2\frac{\varphi_2+\varphi_3}{\varphi_1}\left[B_1 J_0\left(2\sqrt{2\frac{\varphi_2+\varphi_3}{\varphi_1}}\sqrt{z^+}\right) + B_2 N_0\left(2\sqrt{2\frac{\varphi_2+\varphi_3}{\varphi_1}}\sqrt{z^+}\right)\right]. \qquad (113)$$

The integration constants B_i (i=1, 2, 3) are generally determined from the input interferences P_e^+, ϑ_e^+ and W_e^+, where the definition equation

$$W^+ = \frac{A_1}{\delta_1}\left(1-\frac{\delta_4}{\delta_1} z^+\right)U^+ + (\delta_1+\delta_4 z^+)R^+ \tag{114}$$

is to be taken into account, we obtain

$$\Delta_o^{II} B_1 = (\varepsilon_7 P_e^+ - b_4)\Delta_{11} + (\varepsilon_6\varepsilon_7 \vartheta_e^+ + c_4)\Delta_{21} + (\varepsilon_7 W_e^+ - d_4)\Delta_{31}, \tag{115}$$

$$\Delta_o^{II} B_2 = -(\varepsilon_7 P_e^+ - b_4)\Delta_{12} - (\varepsilon_6\varepsilon_7 \vartheta_e^+ + c_4)\Delta_{22} - (\varepsilon_7 W_e^+ - d_4)\Delta_{32}, \tag{116}$$

$$\Delta_o^{II} B_3 = (\varepsilon_7 P_e^+ - b_4)\Delta_{13} + (\varepsilon_6\varepsilon_7 \vartheta_e^+ + c_4)\Delta_{23} + (\varepsilon_7 W_e^+ - d_4)\Delta_{33} \tag{117}$$

with

$$b_1 = \frac{\sqrt[4]{2\delta_3}}{\beta_1 A_1}\left[-\varepsilon_1 + \delta_4(A_2 - 2A_1\delta_1)\sqrt{2\delta_3}\right]\left[2(\varphi_2+\varphi_3)\sqrt[4]{2\delta_3}\, J_o^e + (\varphi_2\sqrt{2\delta_3} - \varphi_1) J_1^e \sqrt{2\frac{\varphi_2+\varphi_3}{\varphi_1}} + \right.$$
$$\left. + \varphi_3 \sqrt[4]{2\delta_3}\, J_2^e\right] - \frac{A_1 c_1 \alpha}{\varepsilon_6 \delta_1}\left(1 - \frac{\delta_4}{\delta_1}\sqrt{2\delta_3}\right), \tag{118}$$

$$b_2 = \frac{\sqrt[4]{2\delta_3}}{\beta_1 A_1}\left[-\varepsilon_1 + \delta_4(A_2 - 2A_1\delta_1)\sqrt{2\delta_3}\right]\left[2(\varphi_2+\varphi_3)\sqrt[4]{2\delta_3}\, N_o^e + (\varphi_2\sqrt{2\delta_3} - \varphi_1)\sqrt{2\frac{\varphi_2+\varphi_3}{\varphi_1}}\, N_1^e + \right.$$
$$\left. + \varphi_3 \sqrt[4]{2\delta_3}\, N_2^e\right] - \frac{A_1 c_2 \alpha}{\varepsilon_6 \delta_1}\left(1 - \frac{\delta_4}{\delta_1}\sqrt{2\delta_3}\right), \tag{119}$$

$$b_3 = \frac{1}{\beta_1 A_1}\left[-\varepsilon_1 + \delta_4(A_2 - 2A_1\delta_1)\sqrt{2\delta_3}\right]\varphi_3 - \frac{A_1 c_3 \alpha}{\varepsilon_6 \delta_1}\left(1 - \frac{\delta_4}{\delta_1}\sqrt{2\delta_3}\right), \tag{120}$$

$$b_4 = \frac{\varphi_4}{2\beta_1 A_1}\left[-\varepsilon_1 + \delta_4(A_2 - 2A_1\delta_1)\sqrt{2\delta_3}\right]\left(\sqrt{2\delta_3} + \frac{\varphi_1}{\varphi_2+\varphi_3}\right) - \frac{A_1 c_4 \alpha}{\varepsilon_6 \delta_1}\left(1 - \frac{\delta_4}{\delta_1}\sqrt{2\delta_3}\right), \tag{121}$$

$$c_1 = \sqrt[4]{2\delta_3}\left\{2\frac{\varphi_2+\varphi_3}{\varphi_1}\sqrt[4]{2\delta_3}(\varepsilon_1\eta_1 + \varepsilon_2\varphi_1) J_o^e + \left[\varepsilon_2(\varphi_2\sqrt{2\delta_3} - \varphi_1) + \varepsilon_8\varepsilon_7\right]\sqrt{2\frac{\varphi_2+\varphi_3}{\varphi_1}}\, J_1^e + \right.$$
$$\left. + c_3 \sqrt[4]{2\delta_3}\, J_2^e\right\}, \tag{122}$$

$$c_2 = \sqrt[4]{2\delta_3}\left\{2\frac{\varphi_2+\varphi_3}{\varphi_1}\sqrt[4]{2\delta_3}(\varepsilon_1\eta_1 + \varepsilon_2\varphi_1) N_o^e + \left[\varepsilon_2(\varphi_2\sqrt{2\delta_3} - \varphi_1) + \varepsilon_3\varepsilon_7\right]\sqrt{2\frac{\varphi_2+\varphi_3}{\varphi_1}}\, N_1^e + c_3\sqrt[4]{2\delta_3}\, N_2^e\right\}, \tag{123}$$

$$c_3 = \varepsilon_1\eta_3\sqrt{2\delta_3} + \varepsilon_2\varphi_3 + \varepsilon_4\varepsilon_7, \tag{124}$$

$$c_4 = (\varepsilon_1\eta_4 + \varepsilon_2\varphi_4 + \varepsilon_5\varepsilon_7)\sqrt{2\delta_3} - \varphi_4\frac{c_3\sqrt{2\delta_3} + \varepsilon_2(\varphi_2\sqrt{2\delta_3} - \varphi_1) + \varepsilon_3\varepsilon_7}{2(\varphi_2+\varphi_3)}, \tag{125}$$

$$d_1 = \frac{A_1\varepsilon_7}{\delta_1}\left(1 - \frac{\delta_4}{\delta_1}\sqrt{2\delta_3}\right)\sqrt{2\delta_3}\, J_2^e + (\delta_1 + \delta_4\sqrt{2\delta_3})\sqrt[4]{2\delta_3}\left[2(\varphi_2+\varphi_3)\sqrt[4]{2\delta_3}\, J_o^e + (\varphi_2\sqrt{2\delta_3} - \varphi_1)\sqrt{2\frac{\varphi_2+\varphi_3}{\varphi_1}}\, J_1^e + \right.$$

$$+ \varphi_3 \sqrt[4]{2\delta_3} \; J_2^e \Big), \tag{126}$$

$$d_2 = \sqrt[4]{2\delta_3} \left\{ \frac{A_1 \varepsilon_7}{\delta_1} \left(1 - \frac{\delta_4}{\delta_1} \sqrt{2\delta_3}\right) \sqrt[4]{2\delta_3}\, N_2^e + (\delta_1 + \delta_4 \sqrt{2\delta_3}) \Big[2(\varphi_2 + \varphi_3) \sqrt[4]{2\delta_3}\, N_0^e + (\varphi_2 \sqrt{2\delta_3} - \varphi_1) N_1^e \cdot \right.$$

$$\left. \cdot \sqrt{2 \frac{\varphi_2 + \varphi_3}{\varphi_1}} + \varphi_3 \sqrt[4]{2\delta_3}\, N_2^e \Big] \right\}, \tag{127}$$

$$d_3 = \frac{A_1 \varepsilon_7}{\delta_1} \left(1 - \frac{\delta_4}{\delta_1} \sqrt{2\delta_3}\right) + (\delta_1 + \delta_4 \sqrt{2\delta_3})\, \varphi_3, \tag{128}$$

$$d_4 = \frac{\varphi_4}{2(\varphi_2 + \varphi_3)} \left\{ (\delta_1 + \delta_4 \sqrt{2\delta_3}) \left[\sqrt{2\delta_3} (\varphi_2 + \varphi_3) + \varphi_1 \right] - \frac{A_1 \varepsilon_7}{\delta_1} \left(1 - \frac{\delta_4}{\delta_1} \sqrt{2\delta_3}\right) \sqrt{2\delta_3} \right\}, \tag{129}$$

$$J_i^e = J_i \left(2 \sqrt{2 \frac{\varphi_2 + \varphi_3}{\varphi_1}} \sqrt[4]{2\delta_3} \right),$$

$$N_i^e = N_i \left(2 \sqrt{2 \frac{\varphi_2 + \varphi_3}{\varphi_1}} \sqrt[4]{2\delta_3} \right),$$

$$i = 0, 1, 2,$$

ij being the complements of the elements in the section of the i-th line and the j-th column of

$$\Delta_0^{II} = \begin{vmatrix} b_1 & b_2 & b_3 \\ c_1 & c_2 & c_3 \\ d_1 & d_2 & d_3 \end{vmatrix} \tag{130}$$

Finally the following transfer functions result with (115) to (130) from (108) to (114)

$$P_a^+ - P_{ao}^+ = G_1(s)\, P_e^+ + G_2(s)\, \vartheta_e^+ + G_3(s)\, W_e^+, \tag{131}$$

$$\vartheta_a^+ - \vartheta_{ao}^+ = G_4(s)\, P_e^+ + G_5(s)\, \vartheta_e^+ + G_6(s)\, W_e^+, \tag{132}$$

$$W_a^+ - W_{ao}^+ = G_7(s)\, P_e^+ + G_8(s)\, \vartheta_e^+ + G_9(s)\, W_e^+ \tag{133}$$

with

$$G_1(S)=\frac{1}{\varepsilon_7\beta_1A_1}\left[-\varepsilon_1+\delta_4(A_2-2A_1\delta_1)z_a^+\right]\left[\varphi_1 z_a^+\psi_1+(\varphi_2 z_a^+-\varphi_1)\chi_1+\varphi_3\varphi_1\right]+$$
$$+\frac{A_1\alpha}{\delta_1}\left(1-\frac{\delta_4}{\delta_1}z_a^+\right)G_4(S), \tag{134}$$

$$G_2(S)=\frac{1}{\varepsilon_7\beta_1A_1}\left[-\varepsilon_1+\delta_4(A_2-2A_1\delta_1)z^+a\right]\left[\varphi_1 z_a^+\psi_2+(\varphi_2 z^+a-\varphi_1)\chi_1+\varphi_3\varphi_2\right]+$$
$$+\frac{A_1\alpha}{\delta_1}\left(1-\frac{\delta_4}{\delta_1}z_a^+\right)G_5(S), \tag{135}$$

$$G_3(S)=\frac{1}{\varepsilon_7\beta_1A_1}\left[-\varepsilon_1+\delta_4(A_2-2A_1\delta_1)z^+_a\right]\left[\varphi_1 z_a^+\psi_3+(\varphi_2 z_a^+-\varphi_1)\chi_3+\varphi_3\varphi_3\right]+$$
$$+\frac{A_1\alpha}{\delta_1}\left(1-\frac{\delta_4}{\delta_1}z_a^+\right)G_6(S), \tag{136}$$

$$G_4(S)=-\frac{1}{\varepsilon_6\varepsilon_7}\left\{(\varepsilon_1\eta_1+\varepsilon_2\varphi_1)z_a^+\psi_1+\left[\varepsilon_2(\varphi_2 z_a^+-\varphi_1)+\varepsilon_3\varepsilon_7\right]\chi_1+\right.$$
$$\left.+(\varepsilon_1\eta_3 z^+a+\varepsilon_2\varphi_3+\varepsilon_4\varepsilon_7)\varphi_1\right\}, \tag{137}$$

$$G_5(S)=-\frac{1}{\varepsilon_6\varepsilon_7}\left\{(\varepsilon_1\eta_1+\varepsilon_2\varphi_1)z_a^+\psi_2+\left[\varepsilon_2(\varphi_2 z_a^+-\varphi_1)+\varepsilon_3\varepsilon_7\right]\chi_2+\right.$$
$$\left.+(\varepsilon_1\eta_3 z^+a+\varepsilon_2\varphi_3+\varepsilon_4\varepsilon_7)\varphi_2\right\}, \tag{138}$$

$$G_6(S)=-\frac{1}{\varepsilon_6\varepsilon_7}\left\{(\varepsilon_1\eta_1+\varepsilon_2\varphi_1)z^+a\psi_3+\left[\varepsilon_2(\varphi_2 z^+a-\varphi_1)+\varepsilon_3\varepsilon_7\right]\chi_3+\right.$$
$$\left.+(\varepsilon_1\eta_3 z^+a+\varepsilon_a\varphi_3+\varepsilon_4\varepsilon_7)\varphi_3\right\}, \tag{139}$$

$$G_7(S)=\frac{A_1}{\delta_1}\left(1-\frac{\delta_4}{\delta_1}z^+_a\right)\varphi_1+\frac{1}{\varepsilon_7}(\delta_1+\delta_4 z^+a)\left[\varphi_1 z^+a\psi_1+(\varphi_2 z^+a-\varphi_1)\chi_1+\varphi_3\varphi_1\right], \tag{140}$$

$$G_8(S)=\frac{A_1}{\delta_1}\left(1-\frac{\delta_4}{\delta_1}z^+a\right)\varphi_2+\frac{1}{\varepsilon_7}(\delta_1+\delta_4 z^+a)\left[\varphi_1 z^+a\psi_2+(\varphi_2 z^+a-\varphi_1)\chi_2+\varphi_3\varphi_2\right], \tag{141}$$

$$G_9(S)=\frac{A_1}{\delta_1}\left(1-\frac{\delta_4}{\delta_1}z^+_a\right)\varphi_3+\frac{1}{\varepsilon_7}(\delta_1+\delta_4 z^+a)\left[\varphi_1 z^+a\psi_3+(\varphi_2 z^+a-\varphi_1)\chi_3+\varphi_3\varphi_3\right], \tag{142}$$

$$P^+_{ao}=\frac{1}{\varepsilon_7\beta_1A_1}\left[-\varepsilon_1+\delta_4(A_2-2A_1\delta_1)z_a^+\right]\left[\varphi_1 z_a^+\psi_4+(\varphi_2 z_a^+-\varphi_1)\chi_4+\varphi_3\varphi_4+\varphi_4 z^+_a\right]+$$
$$+\frac{A_1\alpha}{\delta_1}\left(1-\frac{\delta_4}{\delta_1}z_a^+\right)\vartheta^+_{ao}, \tag{143}$$

$$\vartheta^+_{ao}=-\frac{1}{\varepsilon_6\varepsilon_7}\left\{(\varepsilon_1\eta_1+\varepsilon_2\varphi_1)z^+_a\psi_4+\left[\varepsilon_2(\varphi_2 z_a^+-\varphi_1)+\varepsilon_3\varepsilon_7\right]\chi_4+\right.$$
$$\left.+(\varepsilon_1\eta_3 z^+a+\varepsilon_2\varphi_3+\varepsilon_4\varepsilon_7)\varphi_4+(\varepsilon_1\eta_4+\varepsilon_2\varphi_4+\varepsilon_5\varepsilon_7)z^+_a\right\}, \tag{144}$$

$$W^+_{ao}=\frac{A_1}{\delta_1}\left(1-\frac{\delta_4}{\delta_1}z^+a\right)\varphi_4+\frac{1}{\varepsilon_7}(\delta_1+\delta_4 z^+_a)\left[\varphi_1 z^+_a\psi_4+(\varphi_2 z^+_a-\varphi_1)\chi_4+\varphi_3\varphi_4+\varphi_4 z^+_a\right], \tag{145}$$

$$\Delta_o^{II}\varphi_1=\varepsilon_7\left[z^+a(J_2^a\Delta_{11}-N_2^a\Delta_{12})+\Delta_{13}\right], \tag{146}$$

$$\Delta_o^{I}\varphi_2=\varepsilon_6\varepsilon_7\left[z^+a(J_2^a\Delta_{21}-N_2^a\Delta_{22})+\Delta_{23}\right]; \tag{147}$$

$$\Delta_o^{I}\varphi_3=\varepsilon_7\left[z^+_a(J_2^a\Delta\quad-N_2^a\Delta_{32})+\Delta_{33}\right], \tag{148}$$

$$\Delta_o^{II}\varphi_4=z^+a\left[J_2^a(-b_4\Delta_{11}+c_4\Delta_{21}-d_4\Delta_{31})+N_2^a(b_4\Delta_{12}-c_4\Delta_{22}+\right.$$
$$\left.+d_4\Delta_{32})\right]-b_4\Delta_{13}+c_4\Delta_{23}-d_4\Delta_{33}-\frac{\varphi_4 z^+a\,\Delta_o^{II}}{2(\varphi_1+\varphi_2)}, \tag{149}$$

$$\Delta_o^{II} \chi_1 = \varepsilon_7 \sqrt{2\frac{\varphi_2+\varphi_3}{\varphi_1}} \sqrt{z_a^+} \; (J_1^a \Delta_{11} - N_1^a \Delta_{12}), \tag{150}$$

$$\Delta_o^{II} \chi_2 = \varepsilon_6 \varepsilon_7 \sqrt{2\frac{\varphi_2+\varphi_3}{\varphi_1}} \sqrt{z_a^+} \; (J_1^a \Delta_{21} - N_1^a \Delta_{22}), \tag{151}$$

$$\Delta_o^{II} \chi_3 = \varepsilon_7 \sqrt{2\frac{\varphi_2+\varphi_3}{\varphi_1}} \sqrt{z_a^+} \; (J_1^a \Delta_{31} - N_1^a \Delta_{32}), \tag{152}$$

$$\Delta_o^{II} \chi_4 = \sqrt{2\frac{\varphi_2+\varphi_3}{\varphi_1}} \sqrt{z_a^+} \left[J_1^a(-b_4\Delta_{11} + c_4\Delta_{21} - d_4\Delta_{31}) + N_1^a(b_4\Delta_{12} - c_4\Delta_{22} + d_4\Delta_{32})\right] - \frac{\varphi_4 \Delta_o^{II}}{2(\varphi_2+\varphi_3)}, \tag{153}$$

$$\Delta_o^{II} \psi_1 = 2\varepsilon_7 \frac{\varphi_2+\varphi_3}{\varphi_1} (J_o^a \Delta_{11} - N_o^a \Delta_{12}), \tag{154}$$

$$\Delta_o^{II} \psi_2 = 2\varepsilon_6\varepsilon_7 \frac{\varphi_2+\varphi_3}{\varphi_1} (J_o^a \Delta_{21} - N_o^a \Delta_{22}), \tag{155}$$

$$\Delta_o^{II} \psi_3 = 2\varepsilon_7 \frac{\varphi_2+\varphi_3}{\varphi_1} (J_o^a \Delta_{31} - N_o^a \Delta_{32}), \tag{156}$$

$$\Delta_o^{II} \psi_4 = 2\frac{\varphi_2+\varphi_3}{\varphi_1} \left[J_o^a(-b_4\Delta_{11} + c_4\Delta_{21} - d_4\Delta_{31}) + N_o^a(b_4\Delta_{12} - c_4\Delta_{22} + d_4\Delta_{32})\right], \tag{157}$$

$$J_i^a = J_i\left(2\sqrt{2\frac{\varphi_2+\varphi_3}{\varphi_1}} \sqrt{z_a^+}\right), \quad N_i^a = N_i\left(2\sqrt{2\frac{\varphi_2+\varphi_3}{\varphi_1}} \sqrt{z_a^+}\right), \quad i = 0, 1, 2,$$

we should like to point out once more that the Laplace argument s in (134) to (145) appears only via ε_5, ξ_4, η_3, η_4, and if there are no disturbances in the heating, even only via η_3. The latter expressions are after all also only a first approximation for small z^+. We shall now examine the physical significance of (87). For this purpose we shall take the input magnitudes as reference magnitudes:

$$u_e^+ = \rho_e^+ = p_e^+ = T_e^+ = w_e^+ = 1$$

given p_e^+, T_e^+ and w_e^+, we then obtain from (5) or (9)

$$\alpha = 1, \tag{158}$$

from (10)

$$\beta_1 = \frac{p_e^2 m}{w_e^2 T_e R}, \tag{159}$$

from (25) and (158)

$$\gamma_1 = \frac{2}{f}, \tag{160}$$

from (12) and (24)

$$h^{+} = \frac{2m}{f R\, We\, Te} Lrh \,, \tag{161}$$

from (21) to (23) with (158) to (160)

$$A_1 = 1 \,, \tag{162}$$

$$A_2 = 1 + \beta_1 \,, \tag{163}$$

$$A_3 = 1 + \frac{1}{f \beta_1}(1 + 2\beta_1) \,, \tag{164}$$

from (18), (158) to (160), (162) and (163)

$$\delta_1 = \frac{(f+2)(1+\beta_1)}{2(f+1)} \,, \tag{165}$$

from (85) with (158) to (165)

$$-\delta_3 h^{+} = \frac{f\beta_1}{4(f+1)} \left(\frac{1}{\beta_1} - \frac{f+2}{f}\right)^2 , \tag{166}$$

and from (86) with (158) to (162)

$$\delta_4 = j\sqrt{\frac{f\beta_1 \; h^{+}}{2(f+1)}} \,. \tag{167}$$

Combining (87), (161) and (166) we obtain

$$\left| La - \frac{f^2 pe^2}{8(f+1)\, We h} \left(\frac{1}{\beta_1} - \frac{f+2}{f}\right)^2 \right| \leqq 10^{-2} \frac{Lr}{2} \,; \tag{168}$$

The validity of

$$\left| \frac{\delta_4}{\delta_1} \right| = \sqrt{\frac{4(f+1) m \beta_1 Lrh}{R\, We\, Te}} \; \frac{1}{(f+2)(\beta_1+1)} < 1 \,. \tag{169}$$

also represents advantage for the quality of the approximation given here.

It also follows from the heat flow q of the heating at the surface of the cooling channel with the thermic diameter

$$h = \frac{4}{d} q. \tag{170}$$

If $B_1 > 10$, the approximations

$$\left| L_a - \frac{(f+2)^2 p_e^2}{8(f+1) w_e h} \right| \leqq 5.10^{-3} L_r \tag{171}$$

and

$$\left| \frac{\delta_4}{\delta_1} \right| = \frac{2}{(f+2) p_e} \sqrt{(f+1) w_e h L_r} < 1 \tag{172}$$

can be used for (168) and (169).

(171) and (172) contain a contradiction, thus the approximation given here is thus not very good for $B_1 > 10$.

The following approximate values are recorded in gas-cooled fast breeder reactors for helium ($m = 4 \cdot 10^{-3}$ kg/mol, $f = 3$):
$d = 2 \cdot 10^{-2}$m;
$q = 10^6$ Watt/m^2;
p_e= a0 at;
$T_e=10^3$ deg. K;
w_e=10 kg/m^{2}sec (corresponds to a throughput rate of approx. 1 % of the speed of sound at 10^3 deg. K);
thus according to (159)
$B = 4.63 \cdot 10^3$.
and according to (171)
$L_r = \frac{4}{5} \cdot 10^5$ m = 80 km
with
$d = 4 \cdot 10^{-2}$m;
$q = 10^4$ Watt/m^W

$p_e = 1$ atm.,
$T_e = 10^3$ deg. K
$w_e = 10^2 kg/m^2 sec$
becomes according to (159)
$\beta = 0.463$,
according to (168)
$L_r = \frac{7}{5} \cdot 10^3 m = 1.4$ km
and according to (169)

$$\left| \frac{\delta_4}{\delta_1} \right| = 0{,}96 < 1 \; ;$$

in this case the transfer functions developed here can be used and have a considerable degree of accuracy; however, due to the reality of $\delta_4 \, z_a^+$, L_a may not be longer than about 7 metres.

Nomenclature

Latin letters

c_p	specific heat at constant volume (Watt sec/kg deg.)
d	diameter (m)
g	9.81 m/sec^{+2}
h	Watt/m^3
J_n	Bessel function of the n-th order
j	$\sqrt{-1}$
L	length
m	molecular weight (kg/Mol)
N_n	Neumann's function of the n-th order
p	pressure (kg/m sec^2)

R	8.317 Wattsec/deg. Mol
s	Laplace argument
t	time (sec)
T	temperature (deg. K)
u	velocity (m/sec)
w	ρ u mass flow density (kg/m^2sec)
x	coordinate (m)

Greek letters

λ	coefficient of friction
ρ	density (kg/m^3)

Subscripts

a	on the output side
d	dynamic
e	on the input side
r	designates reference magnitudes

Superscripts

a	output side
e	input side
+	designates dimensionless magnitudes

Bibliography

1. Zierep, J.: Vorlesungen über theoretische Gasdynamik, Verlag G. Braun, Karlsruhe, 1963, S. 7.

2. Ref. 1, S. 2.

3. Schlichting, H.: Grenzschicht-Theorie, Verlag G. Braun, Karlsruhe, 1958, S. 465.

4. Eigner, H.D.: The Fundamentals of Heat Exchanger Dynamics With Special Attention to Double Tube Heat Exchangers. Proc. of the 3rd Int.Conf. of the Int.Fed. of Automatic Control, London, June 1966.

5. Ref. 1, S. 6.

6. Jahnke-Emde-Lösch: Tafeln höherer Funktionen. B.G. Teubner Verlagsgesellschaft, Stuttgart, 1960, S. 154-156.

7. Transactions of the ANS, Vol. 10, Nr. 2 (1967). S. 649-654.

DYNAMIC RESPONSE OF CROSSFLOW HEAT EXCHANGERS

MASAMI MASUBUCHI
YOKOHAMA NATIONAL UNIVERSITY
OHOKA-MACHI, MINAMI-KU
YOKOHAMA, JAPAN

1. Introduction

The research on the dynamics of heat exchangers has become increasingly active and important with the development of automatic control. Numerous papers on the dynamics and control of counter-and parallelflow and multi-pass heat exchangers have been published. The knowledge of dynamic response is not only indispensable to operate heat exchange processes satisfactorily by using automatic control, but also is necessary to effect a good design.

Meanwhile, crossflow heat exchanger has been used extensively in the fields of gas turbine and air conditioning processes and its static response has been known to us for many years [1-3], but, the dynamic analyses are very few [4-6].

In this paper, three patterns of crossflow heat exchanger which has series and side capacities are analyzed by frequency response method and some numerical examples for dimensionless parameters are compared.

2. Fundamental equations

The three patterns are shown in Fig.1. They are:

1) Both fluids unmixed case; There is a temperature distribution in both x- and y-directions in each fluid.

2) One fluid mixed, the other unmixed; The first fluid has temperature distribution in both directions, but the second fluid has temperature distribution in y-direction only.

3) Both fluid mixed case; The first fluid has temperature distribution in x-direction only and the second fluid in y-direction only.

Moreover, in the following analysis, it has been assumed that;

a) Fluid velocities, heat transfer coefficients are all constant and do not change with the temperature of fluid or heat exchange surfaces.

b) The fluid and wall capacitances are independent of temperature, time and position.

c) Longitudinal conduction in the fluids and in the walls is assumed to be zero.

d) There is no heat loss to outer circumferences.

The fundamental equations of dynamics can be obtained as follows:

Case 1)

In the first fluid, consider a fluid element $\frac{W_1}{y_0}\Delta y \Delta x$ with temperature θ_1 as shown in Fig.2(a). The heat balance through an infinitesimal area $\Delta x \Delta y$ in the first fluid gives

$$\frac{d}{dt}\left(\frac{W_1}{y_0}\Delta y \Delta x \cdot \theta_1\right) = K(\theta_2 - \theta_1)\cdot \Delta x \Delta y$$

From this

$$\frac{W_1}{y_0}\Delta y \Delta x \frac{\partial \theta_1}{\partial t} + \frac{W_1}{y_0}\Delta y \Delta x \frac{\partial \theta_1}{\partial x}\frac{dx}{dt} = K(\theta_2 - \theta_1)\Delta x \Delta y$$

So that finally

$$\frac{W_1}{y_0}\frac{\partial \theta_1}{\partial t} + \frac{W_1}{y_0} v_1 \frac{\partial \theta_1}{\partial x} = K(\theta_2 - \theta_1) \qquad (1)$$

Applying the same consideration to the second fluid gives the dynamic equation as

$$\frac{W_2}{x_0}\frac{\partial \theta_2}{\partial t} + \frac{W_2}{x_0} v_2 \frac{\partial \theta_2}{\partial y} = K(\theta_1 - \theta_2) \qquad (2)$$

Nomenclature

A=sectional area perpendicular to flow

$a_1=x_0 y_0 K/(W_1 v_1)$ dimensionless parameter

$a_2=x_0 y_0 K/(W_2 v_2)$ dl. parameter

$a_1'=x_0 y_0 \alpha_1/(W_1 v_1)$ dl. parameter

$a_2'=x_0 y_0 \alpha_2/(W_2 v_2)$ dl. parameter

$b_1=x_0 \alpha_{s1}/(C_1 v_1)$ dl. parameter

$b_2=x_0 \alpha_{s2}/(C_2 v_1)$ dl. parameter

$b=x_0 \alpha_1/(C v_1)$ dl. parameter

C=heat capacity of wall per unit length

C_1 for fluid 1, C_2 for fluid 2, C for series capacity

c=specific heat of fluid

K=over-all coefficient of heat transmission

$L_1=x_0/v_1$

$L_2=y_0/v_2$

p=Laplace transform operator for X or Y

$R=\alpha_{s1}/\alpha_1$, $R'=\alpha_{s2}/\alpha_2$

$r=L_2/L_1=v_1 y_0/(v_2 x_0)$ dl.

$r'=\alpha_2/\alpha_1$ dl.

s=Laplace transform operator for τ

t=time

v=fluid velocity

$W=A\gamma c$=heat capacity of fluid per unit length in the flow direction

$X=x/x_0$ dl. coordinate

$Y=y/y_0$ dl. coordinate

x_0=length of heat exchanger in x-direction

y_0=length of heat exchanger in y-direction

x=coordinate in the first flow

y=coordinate in the second flow

Case 2)

For the first fluid, the same relation as equ.(1) yields

$$\frac{\overline{W}_1}{y_0}\frac{\partial \theta_1}{\partial t} + \frac{\overline{W}_1}{y_0} v_1 \frac{\partial \theta_1}{\partial x} = K(\theta_2 - \theta_1) \tag{3}$$

For the second fluid, by the heat balance through an area $x_0 \Delta y$ for Δt, the following equation is obtained.

$$\overline{W}_2 \Delta y \Delta \theta_2 + \overline{W}_2 v_2 \Delta t \Delta y \frac{\partial \theta_2}{\partial y} = \int_0^{x_0} \Delta y \Delta t \cdot K(\theta_1 - \theta_2)\,dx$$

finally

$$\overline{W}_2 \frac{\partial \theta_2}{\partial t} + \overline{W}_2 v_2 \frac{\partial \theta_2}{\partial y} = K \int_0^{x_0} (\theta_1 - \theta_2)\,dx \tag{4}$$

where, θ_2 is a function of y.

Case 3)

For the first fluid, the similar relation as equ.(4) yields

$$\overline{W}_1 \frac{\partial \theta_1}{\partial t} + \overline{W}_1 v_1 \frac{\partial \theta_1}{\partial x} = K \int_0^{y_0} (\theta_2 - \theta_1)\,dy \tag{5}$$

where, θ_1 is a function of x.

and for the second fluid

$$\overline{W}_2 \frac{\partial \theta_2}{\partial t} + \overline{W}_2 v_2 \frac{\partial \theta_2}{\partial y} = K \int_0^{x_0} (\theta_1 - \theta_2)\,dx \tag{6}$$

where, θ_2 is a function of y.

In the above basic equations, heat capacities of all walls are neglected.

α_1 =coefficient of heat transfer between the first fluid and series capacity

α_2 =coefficient of heat transfer between the second fluid and series capacity

α_{s1} =coefficient of heat transfer between the first fluid and side capacity

α_{s2} =coefficient of heat transfer between the second fluid and side capacity

θ = temperature

$\Theta = \int_0^{\infty} \theta e^{-s\tau} d\tau$

$\overline{\Theta} = \int_0^{\infty} \Theta e^{-pX} dX$ or $\int_0^{\infty} \Theta e^{-pY} dY$

γ =density of fluid

τ =t/L_1 dimensionless time

Sufix: 1,2 for fluid 1 and 2 respectively, i for inlet, o for outlet, s for wall capacity

Now, by using the non-dimensional parameters τ, X, Y, a_1, a_2 and r, following fundamental equations are obtained.

From equ.(1) and (2)

$$\left.\begin{aligned} \frac{\partial \theta_1}{\partial X} + \frac{\partial \theta_1}{\partial \tau} &= a_1(\theta_2 - \theta_1) \\ \frac{\partial \theta_2}{\partial Y} + r\frac{\partial \theta_2}{\partial \tau} &= a_2(\theta_1 - \theta_2) \end{aligned}\right\} \tag{7}$$

From equ.(3) and (4)

$$\left.\begin{aligned} \frac{\partial \theta_1}{\partial X} + \frac{\partial \theta_1}{\partial \tau} &= a_1(\theta_2 - \theta_1) \\ \frac{\partial \theta_2}{\partial Y} + r\frac{\partial \theta_2}{\partial \tau} &= a_2\int_0^1(\theta_1 - \theta_2)dX \end{aligned}\right\} \tag{8}$$

From equ.(5) and (6)

$$\left.\begin{aligned} \frac{\partial \theta_1}{\partial X} + \frac{\partial \theta_1}{\partial \tau} &= a_1\int_0^1(\theta_2 - \theta_1)dY \\ \frac{\partial \theta_2}{\partial Y} + r\frac{\partial \theta_2}{\partial \tau} &= a_2\int_0^1(\theta_1 - \theta_2)dX \end{aligned}\right\} \tag{9}$$

3. Transfer functions

Case 1)

i) Assume the boundary conditions are $\begin{cases} \Theta_1 = \Theta_{1i} & \text{for } X=0 \\ \Theta_2 = 0 & \text{for } Y=0 \end{cases}$

where, Θ_{1i} is a function of s only.

This means that the input signal Θ_{1i} is a temperature variation and that there is no temperature variation at the inlet of the second fluid. When the corresponding output Θ_{1o} is taken, the transfer function is defined as

$$G_1(s,Y) = \frac{\Theta_{1o}}{\Theta_{1i}}$$

ii) Second boundary conditions are $\begin{cases} \Theta_2 = \Theta_{2i} & \text{for } Y=0 \\ \Theta_1 = 0 & \text{for } X=0 \end{cases}$

where, Θ_{2i} is a function of s only.

The second transfer function is

$$G_2(s,Y) = \frac{\Theta_{1o}}{\Theta_{2i}}$$

Now, consider the transfer function G_1 as an example. The Laplace transform of equ.(7) for τ yield

$$\frac{\partial \Theta_1}{\partial X} + (s + a_1)\Theta_1 = a_1 \Theta_2$$

$$\frac{\partial \Theta_2}{\partial Y} + (rs + a_2)\Theta_2 = a_2 \Theta_1$$

By the second Laplace transform of the above equations for Y, and by putting $s + a_1 = \lambda_1$, $rs + a_2 = \lambda_2$, following result yieldd

$$\frac{\partial \bar{\Theta}_1}{\partial X} + \lambda_1 \bar{\Theta}_1 = a_1 \bar{\Theta}_2$$

and from the boundary condition $\Theta_{2i} = 0$

$$p\bar{\Theta}_2 + \lambda_2 \bar{\Theta}_2 = a_2 \bar{\Theta}_1$$

From these two equations

$$\frac{\partial \bar{\Theta}_1}{\partial X} + \left(\lambda_1 - \frac{a_1 a_2}{p + \lambda_2}\right)\bar{\Theta}_1 = 0$$

is given, and the solution is obtained as

$$\bar{\Theta}_1 = C \exp\left\{-\left(\lambda_1 - \frac{a_1 a_2}{p + \lambda_2}\right)X\right\} \qquad C = \text{const.}$$

In the boundary conditions, $\Theta_1 = \Theta_{1i}$ for X= 0, and Θ_{1i} is a function of s only, that is, Θ_{1i} is not a function of Y, then

$$\bar{\Theta}_1 = \mathcal{L}\left[\Theta_{1i}\right] = \frac{\Theta_{1i}}{p} \qquad \text{for} \quad X = 0$$

Therefore

$$C = \frac{\Theta_{1i}}{p}$$

At X = 1, the solution is

$$\bar{\Theta}_1\Big|_{X=1} = \frac{\Theta_{1i}}{p} \exp\left\{-\left(\lambda_1 - \frac{a_1 a_2}{p+\lambda_2}\right)\right\} = \frac{\Theta_{1i}}{p}\,\frac{p+\lambda_2}{p+\lambda_2}\, e^{-\left(\lambda_1 - \frac{a_1 a_2}{p+\lambda_2}\right)}$$

$$= \Theta_{1i}\, e^{-\lambda_1}\left(1 + \frac{\lambda_2}{p}\right)\left\{\frac{e^{\frac{a_1 a_2}{p+\lambda_2}}}{p+\lambda_2}\right\}$$

Inverse Laplace transform p → Y of this relation yields

$$\left[\Theta_1\right]_{X=1} = \Theta_{10} = \Theta_{1i} e^{-\lambda_1}\left[e^{-\lambda_2 Y} I_0\left(2\sqrt{a_1 a_2 Y}\right) + \lambda_2 \int_0^Y e^{-\lambda_2 y} I_0\left(2\sqrt{a_1 a_2 y}\right) dy\right]$$

where, $I_0\left(2\sqrt{a_1 a_2 y}\right) = \sum_n^\infty \frac{(a_1 a_2 y)^n}{(n!)^2}$

and, $\int_0^Y y^n e^{-\lambda_2 y} dy = \frac{n!}{\lambda_2^{n+1}} - e^{-\lambda_2 Y} \sum_{k=0}^{n} \frac{Y^k n!}{\lambda_2^{n-k+1} k!}$

The transfer function is thus determined as

$$G_1 = \frac{\Theta_{10}}{\Theta_{1i}} = e^{-\lambda_1 - \lambda_2 Y} \sum_{n=0}^{\infty} \frac{(a_1 a_2 Y)^n}{(n!)^2} + e^{-\lambda_1} \sum_{n=0}^{\infty} (a_1 a_2)^n \frac{1}{n!\,\lambda_2^n} - e^{-\lambda_1 - \lambda_2 Y} \sum_{n=0}^{\infty}\sum_{k=0}^{n} \frac{(a_1 a_2)^n Y^k}{\lambda_2^{n-k} k!\, n!}$$

But, the third term with n = k can be cancelled by the first term in this equation, so the result is reduced to

$$G_1(s,Y)=\frac{\Theta_{1o}}{\Theta_{1i}}=e^{-\lambda_1}\sum_{n=0}^{\infty}(a_1a_2)^n\frac{1}{n!\lambda_2^n}-e^{-\lambda_1-\lambda_2Y}\sum_{n=0}^{\infty}\sum_{k=0}^{n-1}(a_1a_2)^n\frac{Y^k}{n!k!\lambda_2^{n-k}} \quad (10)$$

By the similar manipulations, the second transfer function is given

$$G_2(s,Y)=\frac{\Theta_{1o}}{\Theta_{2i}}=a_1e^{-\lambda_2Y}\sum_{n=0}^{\infty}(a_1a_2Y)^n\frac{1}{n!\lambda_1^{n+1}}-a_1e^{-\lambda_1-\lambda_2Y}\sum_{n=0}^{\infty}\sum_{k=0}^{n}(a_1a_2)^n\frac{Y^n}{n!k!\lambda_1^{n-k+1}} \quad (11)$$

For cases 2) and 3), the similar mathematical analysis gives the transfer functions and the result is shown on Table 1.

4. With heat capacities

Consider the cases with three kinds of heat capacities of the walls. They are one series capacity and two side capacities as shown in Fig.2(b). All heat capacities of the walls are assumed lumped.

Case 1)

Wall I

$$C_1\frac{\partial\theta_{s1}}{\partial t}=\alpha_{s1}(\theta_1-\theta_{s1})$$

Wall II

$$C_2\frac{\partial\theta_{s2}}{\partial t}=\alpha_{s2}(\theta_2-\theta_{s2})$$

Wall III

$$C\frac{\partial\theta}{\partial t}=\alpha_1(\theta_1-\theta)+\alpha_2(\theta_2-\theta)$$

For the first fluid

$$W_1\frac{\partial\theta_1}{\partial t}+W_1v_1\frac{\partial\theta_1}{\partial x}=y_0\alpha_1(\theta-\theta_1)+y_0\alpha_{s1}(\theta_{s1}-\theta_1)$$

For the second fluid

$$W_2\frac{\partial\theta_2}{\partial t}+W_2v_2\frac{\partial\theta_2}{\partial y}=x_0\alpha_2(\theta-\theta_2)+x_0\alpha_{s2}(\theta_{s2}-\theta_2)$$

These equations can be modified by using dimensionless parameters as

$$\left\{\begin{aligned}
&\frac{\partial\theta_{s1}}{\partial\tau}=b_1(\theta_1-\theta_{s1})\\
&\frac{\partial\theta_{s2}}{\partial\tau}=b_2(\theta_2-\theta_{s2})\\
&\frac{\partial\theta}{\partial\tau}=b(\theta_1-\theta)+r'b(\theta_2-\theta)\\
&\frac{\partial\theta_1}{\partial\tau}+\frac{\partial\theta_1}{\partial X}=a_1(\theta-\theta_1)+Ra_1'(\theta_{s1}-\theta_1)\\
&r\frac{\partial\theta_2}{\partial\tau}+\frac{\partial\theta_2}{\partial Y}=a_2'(\theta-\theta_2)+R'a_2'(\theta_{s2}-\theta_2)
\end{aligned}\right. \quad (12)$$

Case 2)

Wall I

$$C_1 \frac{\partial \theta_{s1}}{\partial t} = \alpha_{s1}(\theta_1 - \theta_{s1})$$

Wall II

$$C_2 \frac{\partial \theta_{s2}}{\partial t} = \alpha_{s2}(\theta_2 - \theta_{s2})$$

Wall III

$$C \frac{\partial \theta}{\partial t} = \alpha_1(\theta_1 - \theta) + \alpha_2(\theta_2 - \theta)$$

First fluid

$$W_1 \frac{\partial \theta_1}{\partial t} + W_1 v_1 \frac{\partial \theta_1}{\partial x} = y_0 \alpha_{s1}(\theta_{s1} - \theta_1) + y_0 \alpha_1(\theta - \theta_1)$$

Second fluid

$$W_2 \frac{\partial \theta_2}{\partial t} + W_2 v_2 \frac{\partial \theta_2}{\partial y} = \alpha_2 \int_0^{x_0} (\theta - \theta_2) dx + x_0 \alpha_{s2}(\theta_{s2} - \theta_2)$$

Fundamental equations with dimensionless parameters are:

$$\left\{ \begin{aligned} &\frac{\partial \theta_{s1}}{\partial \tau} = b_1(\theta_1 - \theta_{s1}) \\ &\frac{\partial \theta_{s2}}{\partial \tau} = b_2(\theta_2 - \theta_{s2}) \\ &\frac{\partial \theta}{\partial \tau} = b(\theta_1 - \theta) + br'(\theta_2 - \theta) \\ &\frac{\partial \theta_1}{\partial \tau} + \frac{\partial \theta_1}{\partial X} = a_1'(\theta - \theta_1) + Ra_1'(\theta_{s1} - \theta_1) \\ &r\frac{\partial \theta_2}{\partial \tau} + \frac{\partial \theta_2}{\partial Y} = a_2' \int_0^1 (\theta - \theta_2) dX + R'a_2'(\theta_{s2} - \theta_2) \end{aligned} \right. \tag{13}$$

Case 3)

Wall I

$$C_1 \frac{\partial \theta_{s1}}{\partial t} = \alpha_{s1}(\theta_1 - \theta_{s1})$$

Wall II

$$C_2 \frac{\partial \theta_{s2}}{\partial t} = \alpha_{s2}(\theta_2 - \theta_{s2})$$

Wall III

$$C \frac{\partial \theta}{\partial t} = \alpha_1(\theta_1 - \theta) + \alpha_2(\theta_2 - \theta)$$

First fluid

$$W_1 \frac{\partial \theta_1}{\partial t} + W_1 v_1 \frac{\partial \theta_1}{\partial x} = y_0 \alpha_{s1}(\theta_{s1} - \theta_1) + \alpha_1 \int_0^{y_0} (\theta - \theta_1) dy$$

Second fluid

$$W_2 \frac{\partial \theta_2}{\partial t} + W_2 v_2 \frac{\partial \theta_2}{\partial y} = x_0 \alpha_{s2}(\theta_{s2} - \theta_2) + \alpha_2 \int_0^{x_0} (\theta - \theta_2) dx$$

These are reduced to the following equations:

$$
\begin{cases}
\dfrac{\partial\theta_{s1}}{\partial\tau} = b_1(\theta_1 - \theta_{s1}) \\
\dfrac{\partial\theta_{s2}}{\partial\tau} = b_2(\theta_2 - \theta_{s2}) \\
\dfrac{\partial\theta}{\partial\tau} = b(\theta_1 - \theta) + br'(\theta_2 - \theta) \\
\dfrac{\partial\theta_1}{\partial\tau} + \dfrac{\partial\theta_1}{\partial X} = a_1'\displaystyle\int_0^1 (\theta - \theta_1)dY + Ra_1'(\theta_{s1} - \theta_1) \\
r\dfrac{\partial\theta_2}{\partial\tau} + \dfrac{\partial\theta_2}{\partial Y} = a_2'\displaystyle\int_0^1 (\theta - \theta_2)dX + R'a_2'(\theta_{s2} - \theta_2)
\end{cases}
\tag{14}
$$

The transfer functions from these equs.(12),(13) and (14) are shown on the Table 2.

5. Numerical examples of frequency response

As is well known, frequency response can be obtained from transfer function by putting $s = j\omega$.

The dimensionless parameters used are:

$a_1 = 1$	$R = R' = 1$
$a_2 = 1$	$r = r' = 1$
$a_1' = 2$	$b = b_1 = b_2 = 1$, 10 and 20
$a_2' = 2$	

Figs.3 and 4 are for case 3) and Fig.5 is for case 2). These figures show the effects of series and side capacities.

Fig.6 shows that the frequency response may vary according to the position of the detecting means. This suggests some possibility of detecting phase advance.

Acknowledgements

The author is grateful to Mr. K.Yoneyama and S.Kaneko, graduate students of Yokohama National University, for their numerical calculations and also is grateful to Mr.S.Maki for his earnest assistance for digital computation and to Mr. Y.Kawashima for his drawing of several figures.

Bibliograghy

(1) W.Nusselt; Der Wärmeübergang im Kreuzstrom, Zeitshrift des VDI, Bd.55, Nr.48, 1911, p.2021

(2) D.M.Smith; Mean Temperature Difference in Cross Flow, Engg., 138,Nov.2, 1934, pp.479-481

(3) Y.Takahashi; Mean Temperature Difference in Two-pass Crossflow Heat Exchanger, Trans JSME,vol.9, no.36,II-85, 1943

(4) K.Okamura; Dynamics of Crossflow Heat Exchangers, Preprint for the 122nd Automatic Control Symposium, The Soc. of Automatic Control, Japan, 1960

(5) G.M.Dusinberre; Calculations of Transients in a Crossflow Heat Exchangers, J. of Heat Transfer, Trans ASME, Series C, vol.81, 1959, p.61

(6) G.M.Myers, J.W.Mitchell, R.F.Norman; The Transient Response of Crossflow Heat Exchangers, Evaporators, and Condensers, J. of Heat Transfer, Trans ASME, Feb. 1967, pp.75-80

Table 1

Case	output / input	Transfer function
1	$\frac{\Theta_{1o}}{\Theta_{1i}}$	$e^{-\lambda_1}\sum_{n=0}^{\infty}(a_1a_2)^n\frac{1}{n!\lambda_2^n} - e^{-\lambda_1-\lambda_2 r}\sum_{n=0}^{\infty}\sum_{k=0}^{n-1}(a_1a_2)^n\frac{r^k}{n!k!\lambda_2^{n-k}}$
	$\frac{\Theta_{1o}}{\Theta_{2i}}$	$a_1e^{-\lambda_2 r}\sum_{n=0}^{\infty}(a_1a_2r)^n\frac{1}{n!\lambda_1^{n+1}} - a_1e^{-\lambda_1-\lambda_2 r}\sum_{n=0}^{\infty}\sum_{k=0}^{n}(a_1a_2)^n\frac{r^n}{n!k!\lambda_1^{n-k+1}}$
2	$\frac{\Theta_{1o}}{\Theta_{1i}}$	$e^{-\lambda_1}+\frac{\frac{1}{\lambda_1^2}a_1a_2(1-e^{-\lambda_1})^2}{\lambda_2-\frac{a_1a_2}{\lambda_1}+\frac{a_1a_2}{\lambda_1^2}(1-e^{-\lambda_1})}\left[1-e^{-\{\lambda_2-\frac{a_1a_2}{\lambda_1}+\frac{a_1a_2}{\lambda_1^2}(1-e^{-\lambda_1})\}r}\right]$
	$\frac{\Theta_{1o}}{\Theta_{2i}}$	$\frac{a_1(1-e^{-\lambda_1})}{\lambda_1}e^{-\{\lambda_2-\frac{a_1a_2}{\lambda_1}+\frac{a_1a_2}{\lambda_1^2}(1-e^{-\lambda_1})\}r}$
3	$\frac{\Theta_{1o}}{\Theta_{1i}}$	$\frac{a_1a_2(1-e^{-\lambda_1})^2(\lambda_2+e^{-\lambda_2}-1)}{\lambda_1^2\lambda_2^2-a_1a_2(\lambda_2+e^{-\lambda_2}-1)(\lambda_1+e^{-\lambda_1}-1)}+e^{-\lambda_1}$
	$\frac{\Theta_{1o}}{\Theta_{2i}}$	$\frac{a_1\lambda_1\lambda_2(1-e^{-\lambda_1})(1-e^{-\lambda_2})}{\lambda_1^2\lambda_2^2-a_1a_2(\lambda_2+e^{-\lambda_2}-1)(\lambda_1+e^{-\lambda_1}-1)}$

where, $\lambda_1 = s + a_1$, $\lambda_2 = rs + a_2$

Table 2

Case	output / input	Transfer function
1	$\frac{\Theta_{1o}}{\Theta_{1i}}$	$e^{-\lambda_1}\sum_{n=0}^{\infty}\frac{\mu^n}{n!\lambda_2^n} - e^{-\lambda_1-\lambda_2\Upsilon}\sum_{n=0}^{\infty}\sum_{k=0}^{n-1}\frac{\mu^n\Upsilon^k}{n!k!\lambda_2^{n-k}}$
	$\frac{\Theta_{1o}}{\Theta_{2i}}$	$\frac{a_1' b e^{-\lambda_2\Upsilon}}{s+b+r'b}\left[\sum_{n=0}^{\infty}\frac{(\mu\Upsilon)^n}{n!\lambda_1^{n+1}} - e^{-\lambda_1}\sum_{n=0}^{\infty}\sum_{k=0}^{n}\frac{(\mu\Upsilon)^n}{n!k!\lambda_1^{n-k+1}}\right]$
2	$\frac{\Theta_{1o}}{\Theta_{1i}}$	$e^{-\lambda_1}+\frac{a_1'a_2'b^2r'(1-e^{-\lambda_1})^2(1-e^{-\lambda_2'\Upsilon})}{\lambda_1^2(s+b+br')^2\lambda_2'}$
	$\frac{\Theta_{1o}}{\Theta_{2i}}$	$\frac{a_1'br'(1-e^{-\lambda_1})}{\lambda_1(s+b+r'b)}e^{-\lambda_2'\Upsilon}$
3	$\frac{\Theta_{1o}}{\Theta_{1i}}$	$e^{-\lambda_1}+\frac{a_1'a_2'b^2r'\left(1-\frac{1-e^{-\lambda_2}}{\lambda_2}\right)\frac{(1-e^{-\lambda_1})^2}{\lambda_1}}{\lambda_1\lambda_2(s+b+r'b)^2-a_1'a_2'b^2r'\left(1-\frac{1-e^{-\lambda_1}}{\lambda_1}\right)\left(1-\frac{1-e^{-\lambda_2}}{\lambda_2}\right)}$
	$\frac{\Theta_{2o}}{\Theta_{1i}}$	$\frac{a_2'b(s+b+r'b)(1-e^{-\lambda_1})(1-e^{-\lambda_2})}{\lambda_1\lambda_2(s+b+r'b)^2-a_1'a_2'b^2r'\left(1-\frac{1-e^{-\lambda_1}}{\lambda_1}\right)\left(1-\frac{1-e^{-\lambda_2}}{\lambda_2}\right)}$

where,

$$\lambda_1 = s + a_1' + a_1'R - \frac{a_1'b_1R}{s+b_1} - \frac{a_1'b}{s+b+br'}$$

$$\lambda_2 = rs + a_2' + a_2'R' - \frac{a_2'b_2R'}{s+b_2} - \frac{a_2'r'b}{s+b+br'}$$

$$\lambda_2' = \lambda_2 + \frac{a_1'a_2'b^2r'}{\lambda_2(s+b+r'b)^2}\left(\frac{1-e^{-\lambda_1}}{\lambda_1}-1\right)$$

$$\mu = \frac{a_1'a_2'b^2r'}{(s+b+r'b)^2}$$

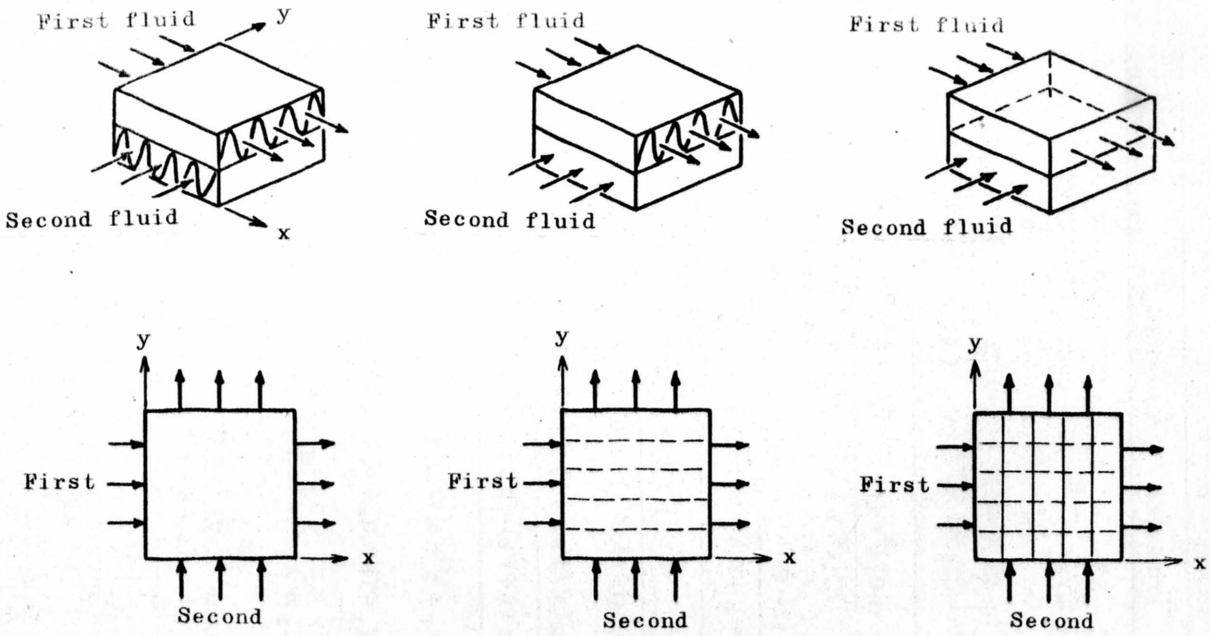

1)Both fluids unmixed case

2)One fluid is mixed, the other is unmixed

3)Both fluids mixed case

Fig.1 Crossflow Heat Exchanger

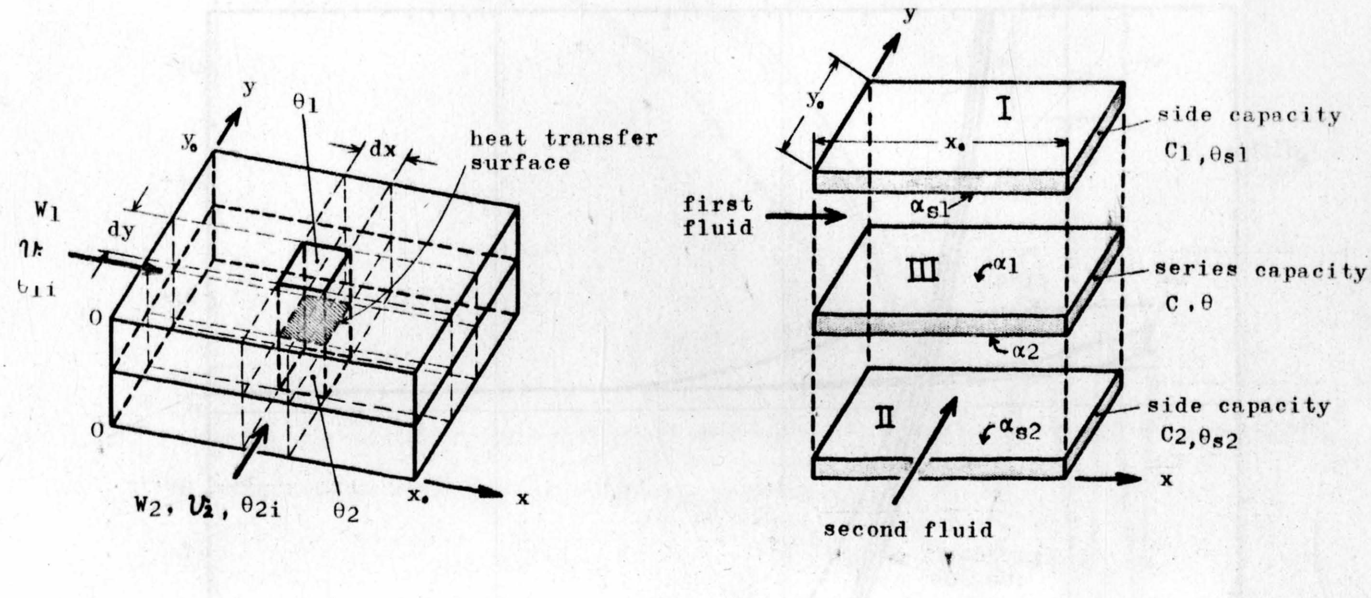

a) Without solid capacities

b) With series and side capacities

Fig.2 Fluid Element in the First and Second Fluid

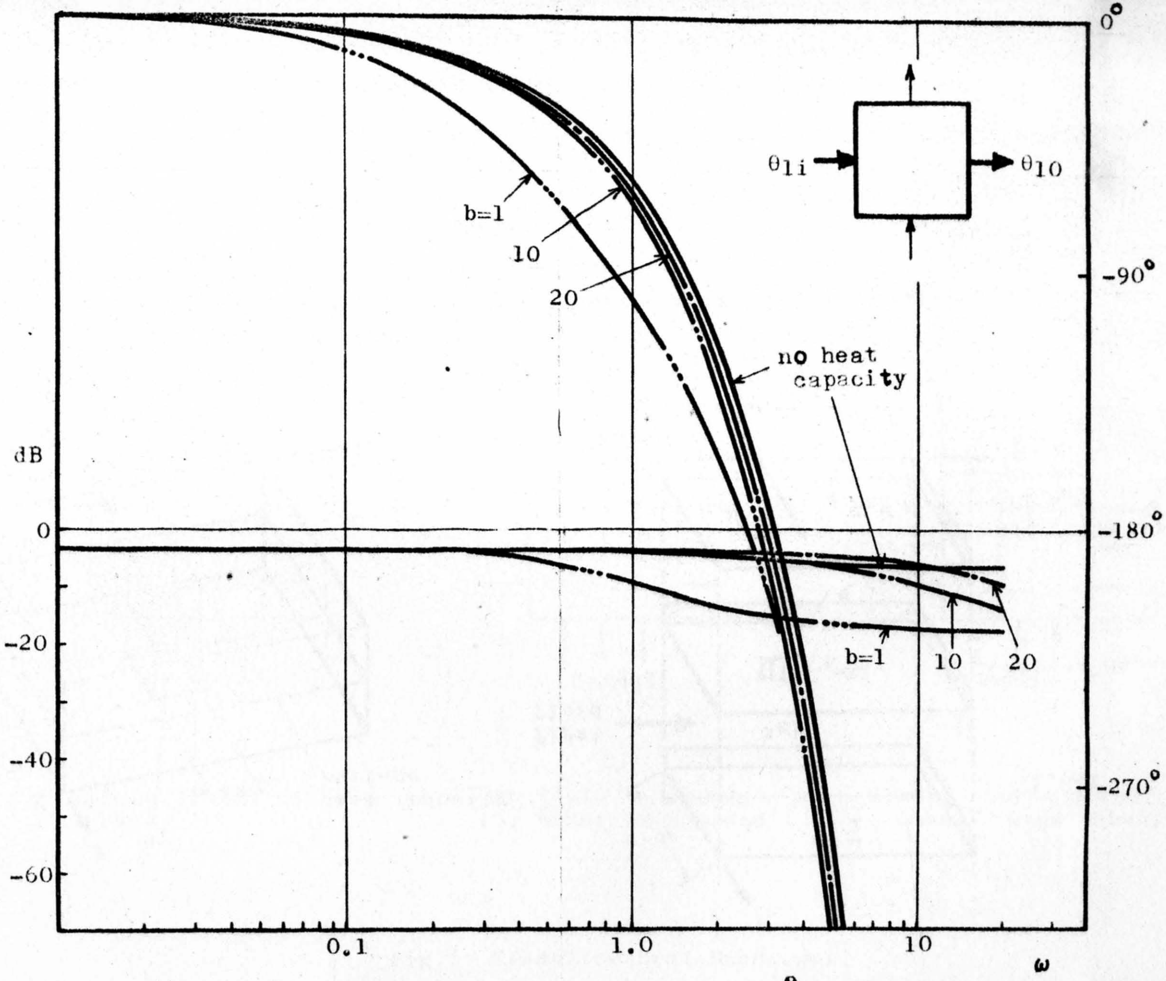

Fig.3 Frequency Response of $\frac{\theta_{10}}{\theta_{1i}}$

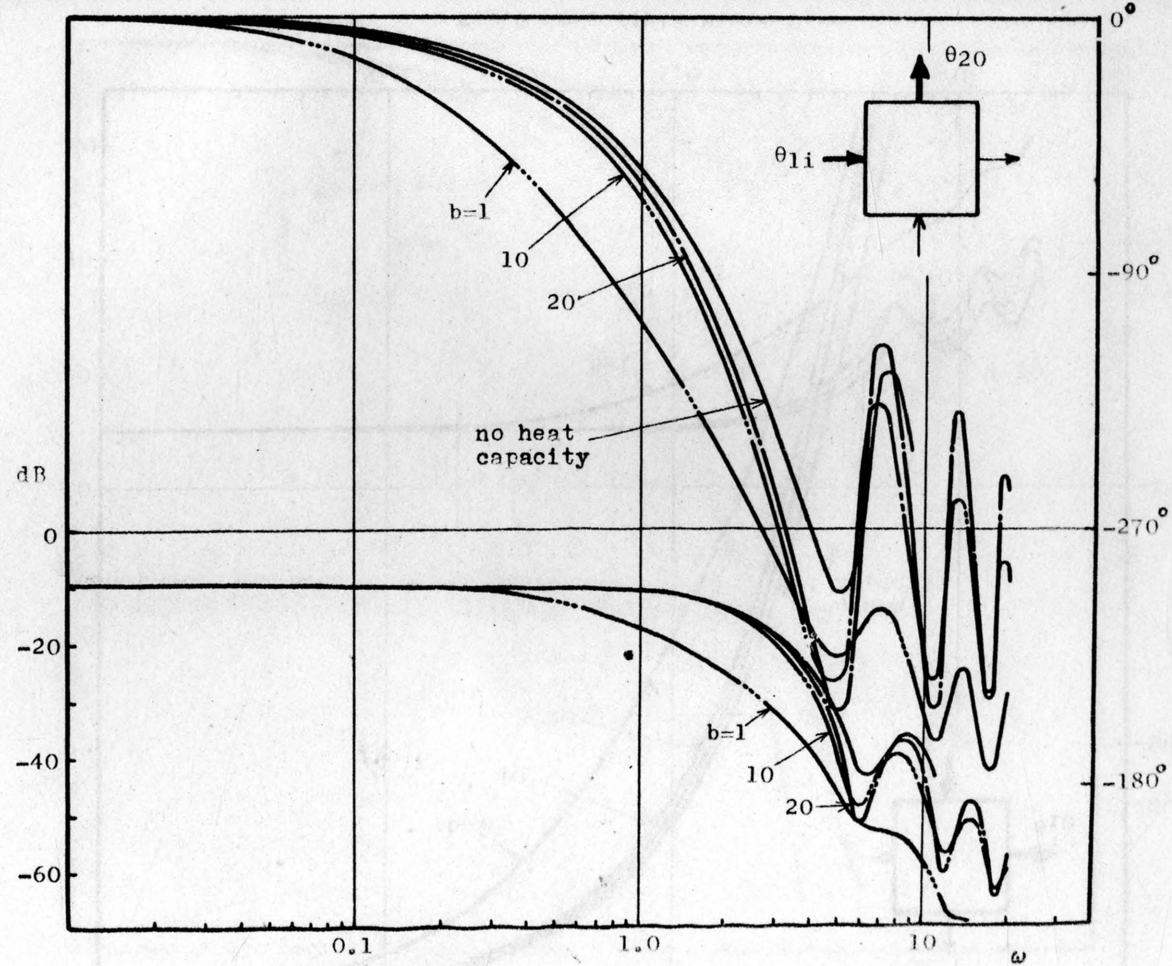

Fig.4 Frequency Response of $\frac{\theta_{20}}{\theta_{1i}}$

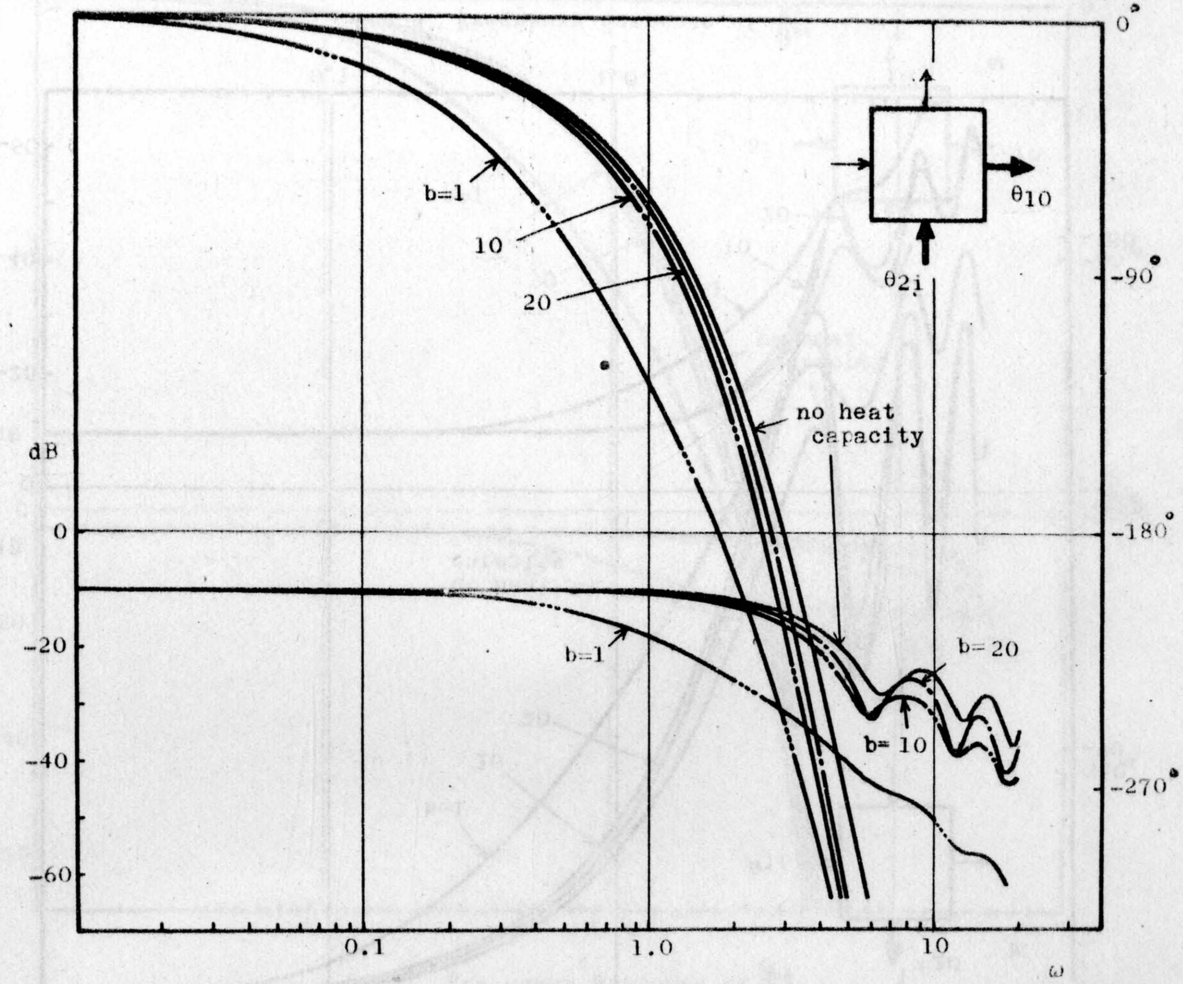

Fig.5 One Fluid Mixed Case

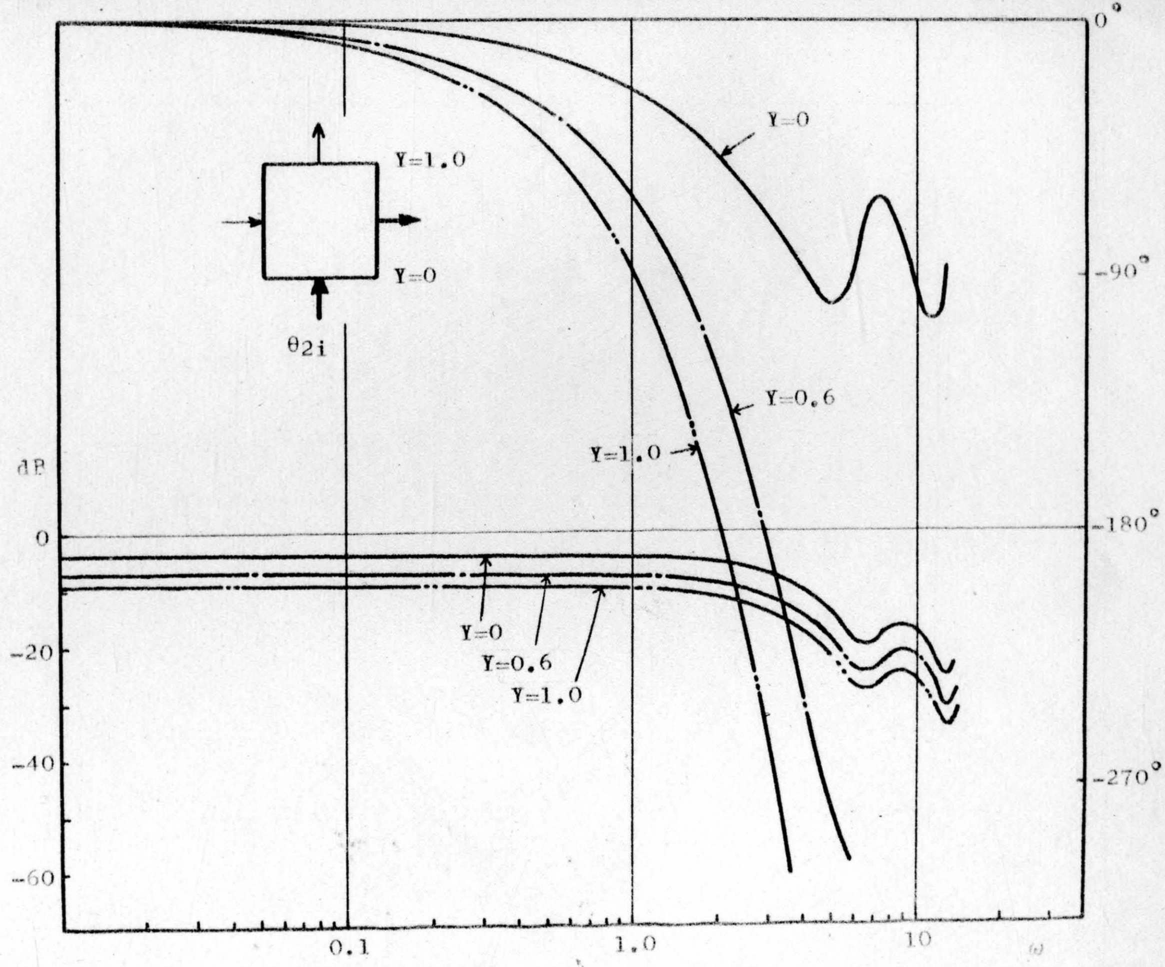

Fig.6 Effect of Position Y